Using VR Headsets for Helicopter Simulations

Analysing How Field-of-View In VR Headsets Affects Helicopter Pilot Performance

Sheharyar Ali

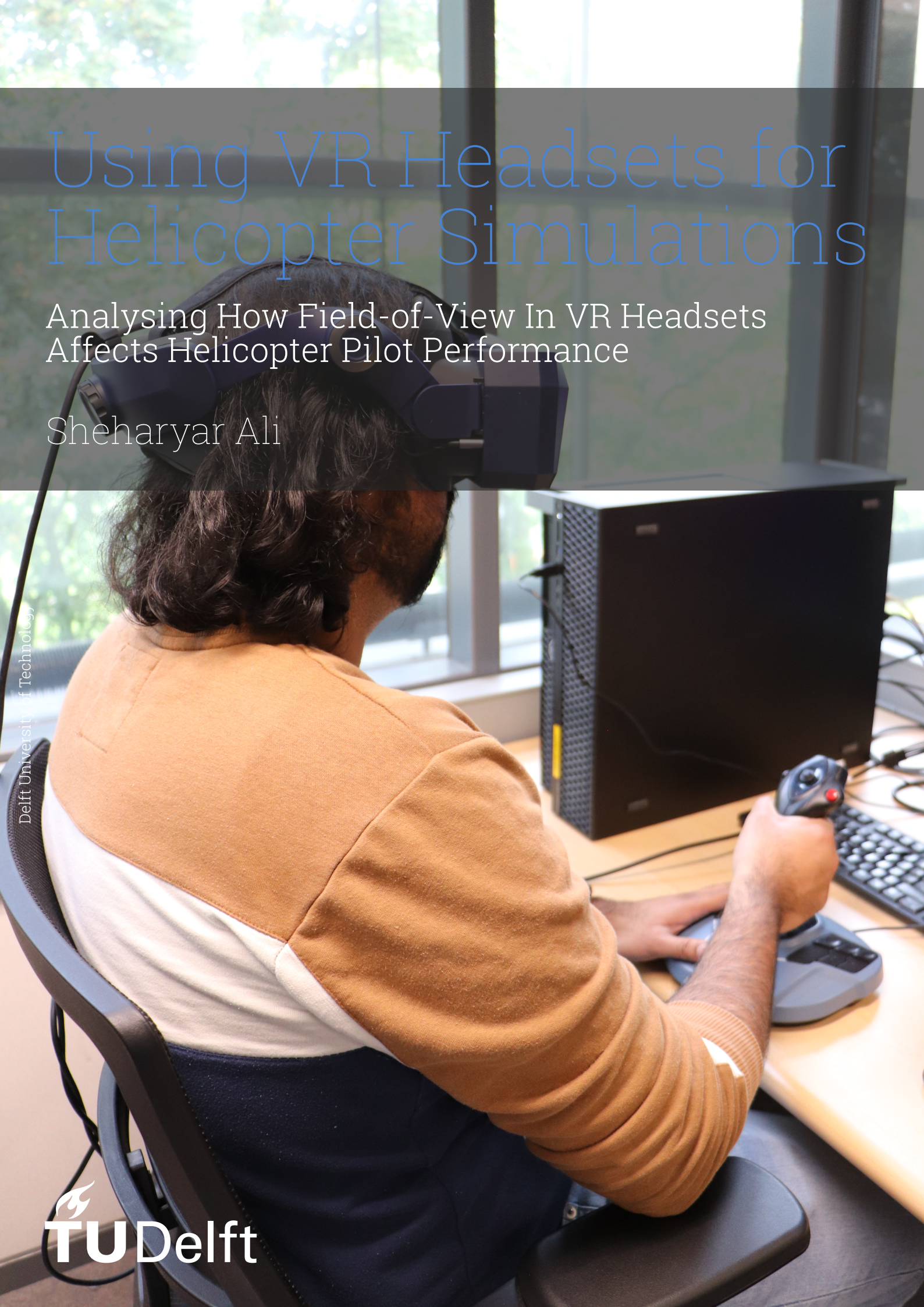

Delft University of Technology

TU Delft

This page is intentionally left blank.

Using VR Headsets for Helicopter Simulations

Analysing How Field-of-View In VR Headsets Affects Helicopter Pilot Performance

by

Sheharyar Ali

to obtain the degree of Master of Science
at the Delft University of Technology,
to be defended publicly on Wednesday October 30, 2024 at 1:00 PM.

Student number:	4798791	
Project duration:	February 5, 2024 – October 30, 2024	
Thesis committee:	Prof. Dr. Ir. M. Mulder,	TU Delft, supervisor
	Ir. O. Stroosma,	TU Delft, supervisor
	Dr. Ir. M.M. van Paassen,	TU Delft, supervisor

This thesis is under embargo until December 31, 2025.

Cover:	Participant doing Control Experiment with a VR headset
Style:	TU Delft Report Style, with modifications by Daan Zwaneveld

An electronic version of this thesis is available at `http://repository.tudelft.nl/`.

TU Delft

This page is intentionally left blank.

Preface

This thesis is a culmination of a long and arduous journey to get to a point where I can call myself an Aerospace Engineer. I am eternally grateful for the support of my family, without whom, I would not have had the strength to carry on. I am also grateful to my friends who have made Delft seem like my home away from home. Lastly, my gratitude goes out to my supervisors who have guided me through the many uncertain stages of this long, but fulfilling project.

I hope you find the report interesting.

Sheharyar Ali
Delft, October 2024

Summary

The role of flight simulators in replacing traditional helicopter flight testing has been well documented and can not be understated. Since they offer a cheaper and safer alternative to real life flight testing, the focus is always being put on making them of a high enough fidelity to ensure that they can be used to train helicopter pilots. One aspect that affects this fidelity is the visual cueing system used. With standard projection systems exhibiting issues such as a restricted Field of View (FoV) , there is demand to find alternatives that can mitigate these issues without completely breaking the bank. This is of great importance since having a restricted FoV means that the pilot is receiving less information in their peripheral vision which can lead to a worsening performance. An alternative to using standard projection systems is to use Virtual Reality (VR) headsets since the 360 [$^\circ$] Field of Regard they offer, may mitigate the problems associated with a restricted FoV. While some research has been done into how pilot performance is affected when using VR headsets for this purpose, there is a significant research gap when it comes to explaining exactly why these effects occur.
To this end, the goal of this thesis is to create a visual model which can be used to explain why a pilot's perception is affected when aspects of the visual cues are changed in a VR headset, and use this to try and rationalise why the change in performance happens. The research objective for this thesis is **How does using VR headsets to perform visual cueing affect the performance of Pilots flying a Helicopter Simulation**. The relevant research questions are:

1. **What manoeuvre is most impacted by changing Field of View (FoV)?**
2. **What is the predicted pilot behaviour for the critical manoeuvre with changing FoV?**
3. **What is the actual pilot behaviour for the critical manoeuvre with changing FoV?**
4. **What is the overall effect of changing FoV on pilot performance?**
5. **What strategies do pilots employ to overcome adverse effects of changing FoV?**

The literature study showed that restricting FoV removes feedback that the pilots get from their peripheral vision, and this affects their perception of velocity and motion. This information was used to create a visual model which sought to calculate how the azimuth and elevation angles of visible points in space changed as the helicopter moved through the world. This was done in an effort to find the most salient point, i.e. the point that would give the most amount of feedback to the pilot. It was found that, for a helicopter with only pitch and surge as its degrees-of-freedom, the most salient point for pitch feedback would be found right in front of the pilot, i.e. at a horizontal viewing angle of 0 [$^\circ$]. For velocity, this would be found at a horizontal viewing angle of ± 45 [$^\circ$].
To validate these findings, a human-in-the-loop experiment was conducted where participants had to control a two degree-of-freedom helicopter system and do two disturbance rejection tasks; one for pitch and one for velocity. These would be done for various FoVs to test if there was a trend emerging between the performance and the FoV. The hypothesis was that there should not be a significant change in performance for the pitch disturbance rejection task across the different FoVs. For the velocity disturbance rejection task, the performance should improve significantly as the FoV was increased from 20 [$^\circ$] to 90 [$^\circ$] and, beyond an FoV of 90 [$^\circ$], there should not be a significant change in performance. Thirteen participants in total did the experiments and the results showed that there was no significant trend in performance across the different FoVs for either of the disturbance rejection tasks.
Based on the subjective comments of the participants, an analysis of the azimuth and elevation angles of an example run, and an analysis of the visual flow seen by the participants throughout their run, it was concluded that the participant got more pitch feedback than velocity feedback. This meant that the participants were looking at the centre of the screen, as to get the most amount of pitch feedback, regardless of the FoV. All they needed was any small piece of the terrain to be visible to get enough velocity feedback to adequately complete the task.
While these results were not as expected, they provided an opportunity to gain insights into the problem and come up with recommendations for future research. Chief among them is the recommendation to analyse and test a system with more than two degrees-of-freedom as this would require pilots to use

their peripheral vision to decouple the different types of motion during a flight. Additionally, the use of full head-tracking of the VR set-up was omitted for the experiments for this thesis, but is recommended to be used by future researchers. This is because allowing for head tracking can lead to a more comfortable experience for the participants and would offer interesting insight into pilot behaviour. Lastly, the visual model created here focused on analysing the points that gave the most amount of visual feedback, but did not account for any additional effects that the less salient points might have on the observer. Since a larger FoV means that the pilot is getting non-zero feedback from a larger number of points, future visual models should try and analyse if the number of visible points has any impact on pilot performance.

This page is intentionally left blank.

Contents

Preface i

Summary ii

Nomenclature viii

1 Introduction 1

2 Background 3
2.1 Impact of Field of View (FoV) . . . 3
2.2 Experimental Methods . . . 10
2.3 Pilot Models . . . 11
2.4 Helicopter Model . . . 17
2.5 Conclusion . . . 19

3 Visual model 21

4 Experiment Methodology 31
4.1 Experiment Basics . . . 31
4.2 Model structure . . . 32
4.3 Forcing Function . . . 35
4.4 Experimental setup . . . 37

5 Results and Discussion 41
5.1 Subjective Results . . . 41
5.2 Objective Results . . . 41
5.3 Discussion . . . 42
5.4 Recommendations . . . 46

6 Conclusion 49

References 52

A Alternate Visual Model 55
A.1 Background . . . 55
A.2 Results . . . 59
A.2.1 Constant κ . . . 60
A.2.2 Variable κ . . . 62
A.3 Sensitivity Analysis . . . 66
A.4 Discussion . . . 68

B Flow Visualisation 70

C Experiment Procedure 75
C.1 General Procedure . . . 75
C.2 Terminating Experiment Due To Motion Sickness . . . 76

D Experiment Matrix 77

E Human Research Ethics Committee Documents 78

List of Figures

2.1 Figure showing the FoV provided by the N-Cab simulator [9] . . . 6
2.2 Figure showing the FoV provided by the F-Cab simulator [9] . . . 6
2.3 Figure showing the FoV of the actual UH-60A helicopter [9] . . . 7
2.4 Figure showing the procedure for the two FoV experiments done by Pretto et al [11] . . 9
2.5 Figure showing the (a) Full FoV Condition, (b) the Central FoV condition, with FoV changing from 10 [°] (top) to 60 [°] (bottom) and (c) the Peripheral FoV condition, with FoV changing from 10 [°] (top) to 60 [°] (bottom) [11] . . . 9
2.6 Figure showing the feedback loop for a simple compensatory tracking task [18] . . . 11
2.7 Figure showing the multi-modal cybernetic pilot model [23] . . . 12
2.8 Figure showing an example model for a human controlling the lateral position of a car [25] 13
2.9 Figure showing the model that would be applicable for a human controlling the lateral position of a car with the heading angle and lateral position as feedback [25] . . . 13
2.10 Figure showing the Cooper-Harper Handling Qualities Rating Scale [26] . . . 14
2.11 Figure showing the Bedford rating scale [27] . . . 15
2.12 Figure showing the VCR scale [6] . . . 15
2.13 Figure showing the combined average VCRs for the different testing conditions in research done by Podzus et al [6] . . . 16
2.14 Figure showing the helicopter dynamics model for [18] . . . 17

3.1 Figure showing the projection of point P onto the spherical retina . . . 22
3.2 Figure showing the motion used for the analysis . . . 23
3.3 Figure showing the flow for the example movement . . . 23
3.4 Figure showing the variation of the partial derivatives of the Azimuth and Elevation angles with x and y-coordinates . . . 25
3.5 Figure showing the variation of the partial derivatives of the Azimuth and the Elevation angles with FoV . . . 26
3.6 Figure showing the behaviour of the partial derivatives with respect to FoV . . . 27
3.7 Figure showing the variation of the highest value of partial derivatives of the Azimuth angle for the different FoVs . . . 28
3.8 Figure showing the variation of the highest value of partial derivatives of the Elevation angle for the different FoVs . . . 29

4.1 Figure showing the proposed structure for the Velocity Disturbance Rejection Task . . . 32
4.2 Figure showing the DRA (RAE) research Lynx Helicopter [31] . . . 34
4.3 Figure showing the proposed structure for the Pitch Disturbance Rejection Task . . . 35
4.4 Figure showing the Velocity and Pitch Forcing Functions . . . 37
4.5 Figure showing two screenshots from the simulation; one for and FoV of 140 [°] and one for an FoV of [°] . . . 37
4.6 Figure showing the pitch indicator reticle and the horizon line used for the pitch disturbance rejection task . . . 38
4.7 Figure showing the Pimax 8KX VR headset and the accompanying base station . . . 38
4.8 Figure showing the MISC scale as the participants would have seen it in the simulation [37] . . . 39

5.1 Figure showing the boxplots for the Pitch and velocity disturbance rejection tasks . . . 42
5.2 Figure showing the variation of the participant's pitch angle and velocity for the chosen run 43
5.3 Figure showing the flow for the participant's run . . . 44
5.4 Figure showing the value of the partial derivative of the Azimuth and Elevation angles w.r.t θ and (udt) at an angle of 45 [°] . . . 44

5.5 Figure showing the value of the partial derivative of the Azimuth and Elevation angles w.r.t θ and (udt) at an angle of 7.5 [°] . . . 45
5.6 Figure showing the run order data and the boxplot for this run order data for all the participants . . . 46

A.1 Figure showing the perspective projection method [38] . . . 55
A.2 Figure showing the difference in projection effects and no projection effects on the view 58
A.3 Figure showing the viewing angle for the optimal positions and the max Δ for each FoV for Case 1 . . . 60
A.4 Figure showing the viewing angle for the optimal positions and the max Δ for each FoV for Case 2 . . . 61
A.5 Figure showing the viewing angle for the optimal positions and the max Δ for each FoV for Case 3 . . . 62
A.6 Figure showing the viewing angle for the optimal positions and the max Δ for each FoV for Case 4 . . . 63
A.7 Figure showing the change in κ for changing FoVs . . . 64
A.8 Figure showing the viewing angle for the optimal positions and the max Δ for each FoV for Case 5 . . . 65
A.9 Figure showing the viewing angle for the optimal positions and the max Δ for each FoV for Case 6 . . . 66
A.10 Figure showing the optimal horizontal viewing angle for all six Cases . . . 67
A.11 Figure showing the optimal vertical viewing angle for all six Cases . . . 67
A.12 Figure showing the maximum value of Δ for all six Cases . . . 68

B.1 Figure showing the flow at t = 0.5 [s], u = 0.2 [m/s], θ = -5 [°] and $\dot{\theta}$ = -1.25 [°/s] . . . 70
B.2 Figure showing the flow at t = 1.0 [s], u = 0.69 [m/s], θ = -2.8 [°] and $\dot{\theta}$ = 1.43 [°/s] . . . 71
B.3 Figure showing the flow at t = 1.5 [s], u = 0.77 [m/s], θ = -1.1 [°] and $\dot{\theta}$ = -0.78 [°/s] . . . 71
B.4 Figure showing the flow at t = 2.5 [s], u = 1.49 [m/s], θ = -1.1 [°] and $\dot{\theta}$ = 1.25 [°/s] . . . 72
B.5 Figure showing the flow at t = 3.5 [s], u = 2.03 [m/s], θ = -5 [°] and $\dot{\theta}$ = 0.77 [°/s] . . . 72
B.6 Figure showing the flow at t = 4 [s], u = 2.21 [m/s], θ = 0 [°] and $\dot{\theta}$ = 0.34 [°/s] . . . 73
B.7 Figure showing the flow for the participant's run at t = 35 [s], u = 2.64 [m/s], θ = -11 [°] and $\dot{\theta}$ = 9.1 [°/s] . . . 73
B.8 Figure showing the flow for the participant's run at t = 35 [s], u = 0.0 [m/s], θ = -11 [°] and $\dot{\theta}$ = 9.1 [°/s] . . . 74
B.9 Figure showing the flow for the participant's run at t = 35 [s], u = 2.64 [m/s], θ = 0 [°] and $\dot{\theta}$ = 0 [°/s] . . . 74

List of Tables

2.1 Table showing the simulator settings used throughout the two campaigns [6] 4
2.2 Table showing the performance tolerances used for the objective analysis [6] 4

3.1 Table showing the number of points tested for each FoV 28

4.1 Table showing the parameters of the helicopter model 35
4.2 Table showing the values of the parameters for the velocity forcing function 36
4.3 Table showing the values of the parameters for the pitch forcing function 36

5.1 Table showing the results of the one-way ANOVA analysis for the two disturbance rejection tasks 42

A.1 Table showing the six cases to analyse 58
A.2 Table showing the number of positions to analyse for each FoV 59
A.3 Table showing the values of the parameters used for each Case 59
A.4 Table showing the optimal position, the horizontal and vertical viewing angle of this position and the value of Δ for each FoV for Case 1 60
A.5 Table showing the optimal position, the horizontal and vertical viewing angle of this position and the value of Δ for each FoV for Case 2 61
A.6 Table showing the optimal position, the horizontal and vertical viewing angle of this position and the value of Δ for each FoV for Case 3 62
A.7 Table showing the optimal position, the horizontal and vertical viewing angle of this position and the value of Δ for each FoV for Case 4 63
A.8 Table showing the values of κ as FoV increases 64
A.9 Table showing the optimal position, the horizontal and vertical viewing angle of this position and the value of Δ for each FoV for Case 5 65
A.10 Table showing the optimal position, the horizontal and vertical viewing angle of this position and the value of Δ for each FoV for Case 6 66
A.11 Table showing the Percentage decrease for all six Cases 69

C.1 Table showing the commands and the associated keybinds for the simulation 76

D.1 Table showing the Experiment Matrix used to determine the order in which the participants do the experiments 77

Nomenclature

Abbreviations

Abbreviation	Definition
ANOVA	Analysis of Variance
AVES	Air Vehicle Simulator
DLR	German Aerospace Center
FFS	Full Flight Simulator Level
FoR	Field of Regard
FoV	Field of View
GS	Glide-slope
HPS	Helicopter Pilot Station
HQR	Handling Qualities Rating
HREC	Human Research Ethics Committee
HUD	Heads-Up Display
MISC	MIsery SCale
MLE	Maximum Likelihood Estimator
NLR	Netherlands Aerospace Center
NASA	National Aeronautics and Space Administration
NVD	Night Vision Devices
RAF	British Royal Airforce
RMSE	Root-Mean Squared Error
ROC	Rate of Climb
ROD	Rate of Descent
RoCS	Rotorcraft Certification by Simulation
RTO	Rejected Take-off
TDP	Take-off Decision Point
VCR	Visual Cue Rating
VR	Virtual Reality

Symbols

Symbol	Definition	Unit
$A_t(k)$	Forcing Function component amplitude	[m/s] or [°]
Az	Azimuth Angle	[°]
dt	Change in time	[s]
Ele	Elevation Angle	[°]
FoV	Field of View	[°]
K_m	Motion Gain	[-]
K_v	Visual Gain	[-]
M_q	Moment Derivative with respect to pitch rate	[1/s]
$M_{\theta_{1s}}$	Moment Derivative with respect to longitudinal cyclic input	$[1/s^2]$
P	3D Vector of a point in space	[m,m,m]
P'	3D Vector of a translated point in space	[m,m,m]
p	Angular velocity around the body-fixed x-axis	[rad/s]
Q	3D Vector of a point projected on a sphere	[m,m,m]

Symbol	Definition	Unit
Q'	3D Vector of a translated point projected on a sphere	[m,m,m]
q	Angular velocity around the body-fixed y-axis	[rad/s]
r	Angular velocity around the body-fixed z-axis	[rad/s]
R_y	Orthogonal Rotational matrix	[-]
s	Laplace variable	[-]
T_I	Visual Lag Constant	[s]
T_L	Visual lead Constant	[s]
T_m	Measurement Time	[s]
t	Time	[s]
u	Horizontal velocity component in the body-fixed x-direction	[m/s]
v	Horizontal velocity component in the body-fixed y-direction	[m/s]
w	Vertical velocity component in the body-fixed z-direction	[m/s]
X_u	Force Derivative with respect to forward velocity	[1/s]
$X_{\theta_{1s}}$	Force Derivative with respect to longitudinal cyclic input	$[m/s^2 rad]$
x	Horizontal position in the body-fixed x-direction	[m]
y	Horizontal position in the body-fixed y-direction	[m]
z	Horizontal position in the body-fixed z-direction	[m]
δ_c	Control input representing collective pitch angle	[rad]
δ_{lat}	Control input representing lateral control	[rad]
δ_{lon}	Control input representing longitudinal control	[rad]
δ_p	Control input representing tail rotor pitch angle	[rad]
θ	Pitch angle	[rad]
θ_0	Collective pitch angle	[rad]
θ_{1s}	Swashplate servo pitch angle	[rad]
θ_{1c}	Swashplate servo roll angle	[rad]
θ_{0T}	Tail rotor collective pitch angle	[rad]
ψ	Yaw angle	[rad]
ϕ	Roll angle	[rad]
$\phi_t(k)$	Forcing Function component phase shift	[rad]
τ_m	Motion Perception Delay	[1/s]
τ_v	Visual Perception Delay	[1/s]
ω_c	Crossover Frequency	[rad/s]
ω_m	Measurement Time Base Frequency	[rad/s]
$\omega_t(k)$	Forcing Function Component Frequency	[rad/s]
ω_{nm}	Neuromuscular Frequency	[rad/s]
ζ_{nm}	Neuromuscular Damping	[-]
$\frac{\partial Az}{\partial(udt)}$	Partial Derivative of the Azimuth angle with respect to distance moved	[rad/m]
$\frac{\partial Az}{\partial\theta}$	Partial Derivative of the Azimuth angle with respect to pitch angle	[-]
$\frac{\partial Ele}{\partial(udt)}$	Partial Derivative of the Elevation angle with respect to distance moved	[rad/m]
$\frac{\partial Ele}{\partial\theta}$	Partial Derivative of the Elevation angle with respect to pitch angle	[-]

1

Introduction

Flight simulators play a crucial role in providing a cheaper and safer alternative to real-world flight testing. Helicopter flight tests often involve pilots having to perform manoeuvres in extreme conditions and often requiring the pilot to test the limits of the helicopter flight envelope [1]. This necessitates the use of very well trained pilots and top-of-the line equipment, and carries severe risks to pilot and equipment safety. Pilot-in-the-loop flight simulations offer a viable alternative to real-world flight testing by taking out the risk of pilot and equipment damage, while also being cheaper and being able to encompass a larger flight envelope [2]. They also reduce the environmental and noise impact of such testing, and can circumvent the logistics of setting up flight testing in a given airspace [1]. With a high enough fidelity, flight simulators can be used to certify helicopters and train pilots in such a way that the pilots can successfully transfer their training of flying a simulator into flying a real helicopter [3].

To achieve such goals however, requires the use of systems of a very high fidelity [1]. One example of such systems that hold incredible importance in a simulator, is the visual cueing system. Pilots rely extensively on the visual cues provided by the simulators to perform any basic manoeuvre, and the importance of providing high quality visual cues is imperative if any extreme manoeuvres need to be done in the simulator [4]. Traditionally, the visual cueing system of a flight simulator consists of a series of projectors projecting the out-of-window scene on a large screen. These methods, while effective, can often have limitations on aspects such as their Field of View (FoV), Resolution, Depth perception etc which can significantly lower the visual fidelity. A restricted FoV in particular can be detrimental as it hinders any activity occurring in an observer's peripheral vision, leading to degraded performance [5]. These problems can be solved using higher quality equipment, but that adds extra costs and complexity to the whole mix [5]. A viable alternative to this, is the use of Virtual Reality (VR) headsets to replace the traditional projection systems. VR headsets allows a pilot to feel more immersed in the virtual world, and offers cheaper fixes to some of the aforementioned problems [1]. The biggest advantage of VR over the traditional systems is the 360 [$^\circ$] Field of Regard that is offered by the VR headsets. The Field of View determines the instantaneous view that a pilot can see at any time, while the Field of Regard determines the total view a pilot can see if they were able to move their head and the view moved along with them. In traditional systems, the Field of Regard is equal to the Field of View but in VR headsets, the pilots can easily move their head around and the view would move with them giving them a full 360 [$^\circ$] Field of Regard. This can help to raise the visual fidelity greatly for simulators. While VR technology has improved significantly in recent years, there is still very little research being done into using VR headsets as an alternative to current-gen projection systems [1].

The current research surrounding the use of VR headsets in the context of flight simulators has been squarely focused on understanding what effects it has on a pilot's ability to fly. This involves documenting the adverse effects of using VR headsets, such as motion sickness, and how to mitigate them, as well seeing how pilot performance changes overall [1][6]. While this does provide useful insights into positive and negative aspects of using VR headsets in this context, there is a clear gap in knowledge about why such performance changes can occur. As such, this study aims to understand and analyse how using VR headsets for visual cueing would affect pilot performance and why these changes are

specifically happening. The goal is to create a visual model which can be used to explain why a pilot's perception is affected when aspects of the visual cues are changed in a VR headset, and use this to try and rationalise why the change in performance happens. To this end, the research objective for the thesis is: **How does using VR headsets to perform visual cueing affect the performance of Pilots flying a Helicopter Simulation**. To facilitate this objective, the focus was put on seeing what impact the Field of View has on pilot performance, when using VR headsets. The following research questions have been created to help achieve the research objective:

1. **What manoeuvre is most impacted by changing Field of View (FoV)?**
2. **What is the predicted pilot behaviour for the critical manoeuvre with changing FoV?**
3. **What is the actual pilot behaviour for the critical manoeuvre with changing FoV?**
4. **What is the overall effect of changing FoV on pilot performance?**
5. **What strategies do pilots employ to overcome adverse effects of changing FoV?**

2 Background

This chapter details the literature study done to try and make a start on completing the research objective. Information about the impact of FoV on pilot behaviour, based on previous literature is shown in section 2.1. Information about the experimental methods used by other researchers is detailed in section 2.2, while information about the pilot models that can be created from said experimentation methods is outlined in section 2.3. Information about creating a dynamic helicopter model is given in section 2.4 and finally, the main conclusions of this chapter are presented in section 2.5.

2.1. Impact of Field of View (FoV)

In any system where the goal is to create a simulation of a real-world vehicle, the importance of visual cues can not be understated. These cues can determine how realistic the simulation looks to the pilot and can determine how well they perform any given manoeuvres in the simulator. This is because the visual cues provide the pilots with feedback on various aspects of flight, such as their position and velocity, and having high quality visual cues means that the pilot gets more accurate feedback on these aspects. This means that visual cues play a big part in determining the fidelity of a simulator and this fidelity dictates how useful a simulator is for a given purpose [7]. Examples of important visual cues include:

- **Field of View (FoV):** This dictates how much of the scene the pilot can see at any given time [6] [8]
- **Resolution:** This dictates how clearly any object can be seen in the scene [6] [7]
- **Update rate:** This dictates the rate of change of the scene for any given movement within it [7].
- **Scene content:** This determines what there is to see in the scene and what forms of visual feedback the pilot can receive [7]

While all of these cues are important, the focus of this thesis is on the impact of the FoV only. The reason for this is because, in simulators that rely on projectors to project the view onto a fixed screen, the FoV is linked and restricted to the size of the screen and the settings used. This means that, if a pilot wishes to change the view envelope, they can only do so by translating or rotating the vehicle they are controlling. This essentially can lock pilots into the view envelope afforded to them by the limitations of the projection system and the FoV it can provide, i.e. they have a limited Field of Regard (FoR). The FoR is the total area that the pilot can see if the display system was able to move. In traditional flight simulators, this can only be done if high-resolution, expensive moving projectors are used and so, for most traditional simulators, their FoV = FoR [6]. In VR headsets however, this is not the case. Using VR headsets, a pilot can simply move their head around and the projected scenery will match. This means that VR headsets can allow pilots to mitigate issues with having a restricted FoV. The question then becomes whether or not having a restricted FoV would impact pilot performance in any way. If so, then VR headsets offer a better alternative to traditional projection systems in this regard. That is why the focus of this thesis is on evaluating how changes in FoV can impact pilot performance when using VR headsets, as this allows one to determine if the aforementioned benefit VR headsets have

over traditional systems has any impact on how well a pilot does.

Previous research, done by Podzus et al, has already sought to investigate this to a certain extent. In this research, the focus was on trying to determine if the current technology for visual cueing used in flight simulators is good enough to replace traditional compliance demonstration methods used to certify rotorcraft [6]. Traditional compliance demonstration procedures require large amounts of flight testing which can be dangerous and costly, especially for high risk manoeuvres. Thus, Podzus et al set about to find out if current-gen flight simulators are of a high enough fidelity to replace this flight testing, specifically for a category-A rejected take-off (CAT-A RTO). This manoeuvre involved the pilot taking-off as normal and then maintaining a pre-determined glideslope as they ascend backwards to a pre-determined Take-off Decision Point (TDP) height. Once this is achieved, the pilot must decide if they wish to reject take-off or continue take-off, based on whether or not an engine failure was triggered in the simulation. After the pilot has made a decision, they must then perform the required flight manoeuvre for that decision, as dictated by their training.
To test the cueing fidelity of modern simulators, this manoeuvre was carried out by trained pilots in two separate testing campaigns. The first campaign involved making use of the Air Vehicle Simulator (AVES) at the German Aerospace Center (DLR). For this campaign, the setup of AVES was altered to perform the test with four FoV conditions. The second campaign was carried out at the Helicopter Pilot Station (HPS) at the Royal Netherlands Aerospace Center (NLR) and involved the use of two VR headsets, instead of the standard projection methods. The two headsets were the Varjo XR-3 and the Pimax 8K-X. The FoVs tested for each campaign are outlined in Table 2.1

Table 2.1: Table showing the simulator settings used throughout the two campaigns [6]

Setting	**Horizontal FoV [°]**	**Vertical FoV [°] (up/down)**
AVES [DLR Campaign]	240	93 (+35 [°] / -58 [°])
Rotorcraft Certification by Simulation (RoCS) Sim [DLR Campaign]	220	78 (+20 [°] / -58 [°])
Full Flight Simulator Level D (FFS-D) [DLR Campaign]	180	60 (+24 [°] / -36 [°])
Full Flight Simulator Level C (FFS-C) [DLR Campaign]	150	40 (+13 [°] / -27 [°])
Varjo XR-3 [NLR Campaign]	88	65
Pimax 8K-X [NLR Campaign]	140	90

The RoCS Sim setting is the FoV used by the engineering simulator made by the RoCS project, while the FFS settings represent the minimum FoV needed to achieve the level D and level C certification for a flight simulator.
To analyse how pilots performed with the different testing conditions, the researchers made us of both objective and subjective rating techniques to measure performance. The subjective methods involved the pilots giving comments on how they feel like they did with the different FoVs, and what specific issues they encountered with the each of the tested setups. The objective analysis was done by looking at the simulator data and evaluating it against certain criteria imposed on different parts of the flight. These are shown in Table 2.2:

	Desired	**Adequate**
Take-Off Rate Of Climb (ROC)	350$\pm$50 ft/min	350$\pm$100 ft/min
Take-Off Glide-slope (GS)	4-5 knots	3-6 knots
Touchdown Rate Of Descent (ROD)	<400 ft/min	<500 ft/min
Touchdown GS	<5 knots	<10 knots
Touchdown Point	On X (32x32 ft)	On concrete (43x43 ft)

Table 2.2: Table showing the performance tolerances used for the objective analysis [6]

The DLR test campaign provided some interesting results with regards to the FoV needed to adequately perform the tasks. The subjective results showed that significantly lowering the FoV did indeed

hinder the participants. The pilots did find FoVs lower than 220 [°] to be objectionable as, according to their comments, the lower FoVs did not allow pilots to accurately estimate their flight path. The pilots claim that, for the FFS Level D and Level C settings, they were not able to maintain sight of the helipad for their entire flight and thus, had to use their instruments to complete the manoeuvre. This made the pilots feel uncomfortable and insecure while flying backwards. This is also somewhat echoed in the objective results where there were minor performance differences between the AVES, FFS Level D and RoCS Sim settings. However, for the FFS Level C setting, none of the pilots were able to meet the GS and ROC 'adequate' targets, as outlined in Table 2.2. The researchers compiled the objective and subjective results from the DLR test campaign and concluded that a minimum horizontal FoV of 190 [°] must be provided for the pilots to accurately perform the CAT-A RTO manoeuvre. This is because this FoV ensures that the pilots' peripheral vision is not obstructed and thus, the pilots are not distracted.
For the NLR test campaign, the pilots preferred the VR projection systems over the standard ones. The pilots claimed that the larger view provided by the VR headsets allowed them to always maintain sight of the helipad. Additionally, the pilots preferred the Pimax headset over the Varjo since the Pimax offered a larger FoV in general. This is despite the fact that the boundaries of the FoV were blurry in the Pimax but regardless, having a larger FoV made the pilots feel more comfortable. In terms of objective results of the campaign, the performance data for the pilots across the different projection system could not really be compared against one another. This is due to the fact that the different projection systems were used with different parameter settings, tolerances and procedures, which were all iterated and refined for different pilots. This is why the researchers used the objective results of one pilot's performance to draw their conclusions. They claim that the performance across the projection systems was relatively similar for this pilot, with the exception of the pilot's GS during descent. The researchers observed that the pilot had a much shallower approach when they were using the Varjo headset, which they claim is due to the fact that the pilot struggled to see the forward movement and height ground cues. The researchers theorise that this could be a result of the limited FoV offered by the Varjo since the pilots' GS using all other projection systems was in the adequate region of the tolerances. Regardless, the researchers' main conclusion is the fact that the **VR headsets are indeed a superior projection method** compared to the standard one, and that, despite the Varjo having a higher resolution, **the Pimax was the superior headset due to its higher FoV.**

Another research project that wanted to see how changing FoV affects the fidelity of flight simulators, is that done by Atencio Jr. In this research, Atencio Jr sought to evaluate how NASA's Ames Vertical Simulator compared to the real world case of a UH-60 A helicopter in flight [9]. The research revolved around asking pilots to perform certain tasks in both an actual UH-60A helicopter and in the simulator and see how their performance compared for both. Due to logistical reasons, two different types of simulators were used for this project, which are referred here and in the original paper as the F-Cab and the N-Cab. The main difference, of relevance to this project, between the F-Cab and the N-Cab is the fact that the N-Cab has a higher horizontal FoV than the F-Cab. The Horizontal FoV of the N-Cab is 140 [°] as compared to the 120 [°] in the F-Cab. The Hammer plots, which show how the out-of-window view is distributed for each configuration, are shown in Figure 2.1 and Figure 2.2, respectively:

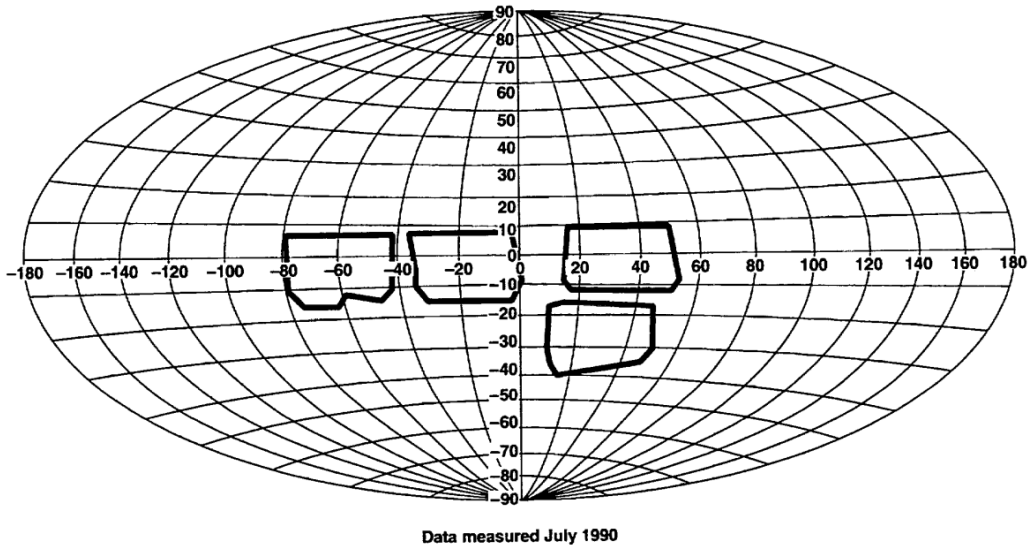

Figure 2.1: Figure showing the FoV provided by the N-Cab simulator [9]

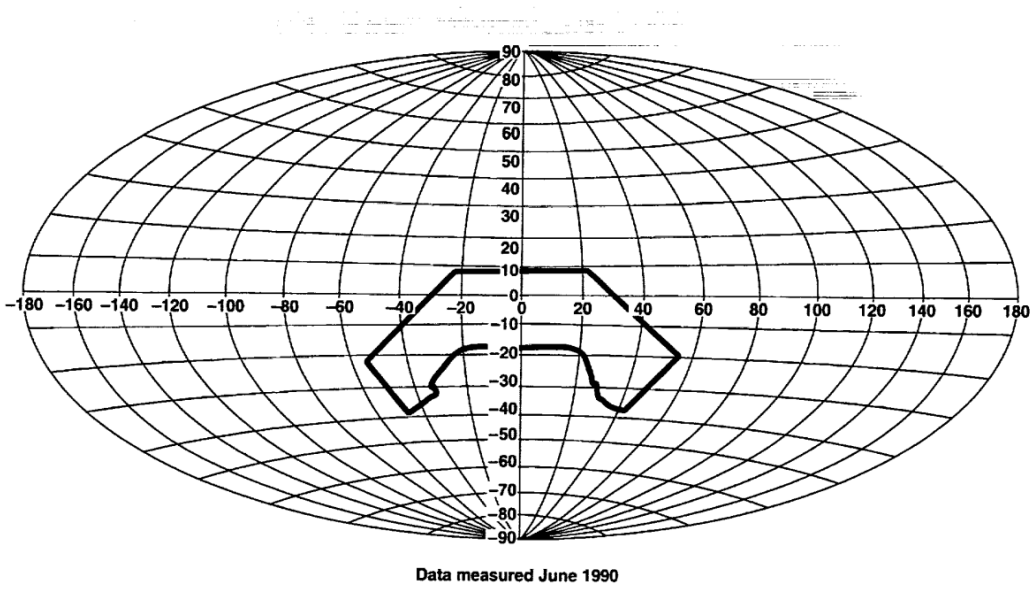

Figure 2.2: Figure showing the FoV provided by the F-Cab simulator [9]

If one compares this to the Hammer plot of the actual helicopter, pictured in Figure 2.3, it is clear that the simulators have a lower overall FoV than the actual helicopter.

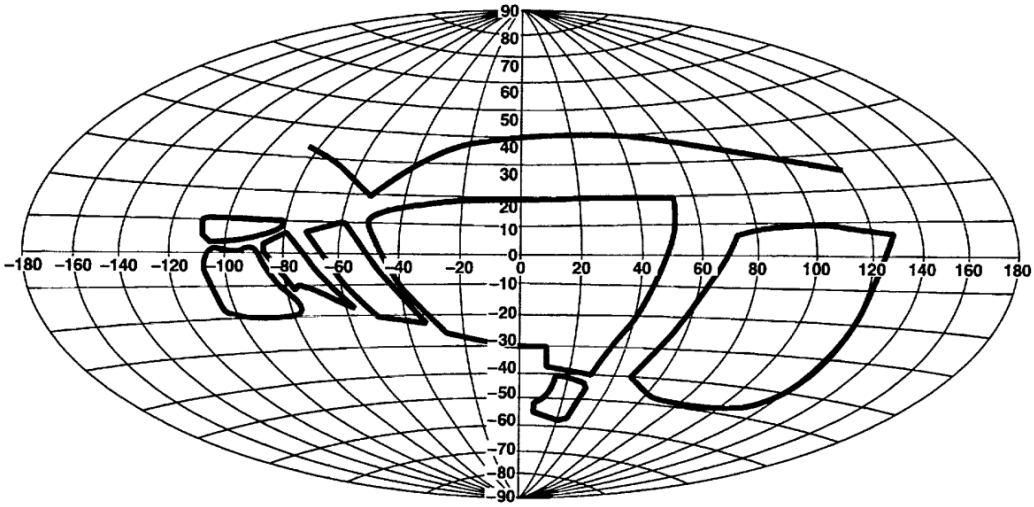

Figure 2.3: Figure showing the FoV of the actual UH-60A helicopter [9]

Some of the main differences between the simulators and the actual helicopter are:

1. The actual helicopter has an approximately 10 [°] larger up-view and about 15-20 [°] larger down-view as compared to the F-Cab
2. The F-cab does not have the chin window, right-side window and left-side window that the actual helicopter does
3. There is a gap of approximately 15 [°] between the centre and right-windows of the N-Cab, which does not exist in the actual helicopter
4. The actual helicopter has an approximately 10 [°] larger up-view and about 15 [°] larger down-view as compared to the N-Cab
5. The N-Cab lacks the chin window, right-side window and the overhead window that the actual helicopter has.

Because of these deficiencies, one can analyse the pilot comments regarding their performance in both the actual helicopter and the simulators to see what effect a degraded FoV has. The pilots were asked to perform three different tasks in the simulators and the helicopter, which are detailed below:

1. **Bob-up manoeuvre:** The pilot has to start from a hover and quickly ”bob-up” 40 [ft] to the target, and then stabilise. After a 5 [s] delay, the pilot has to descend back down to the original position and stabilise.
2. **Side-Step manoeuvre:** The pilot has to start from a hover and quickly translate 40 [ft] to the right and stabilise. This is followed by translating back to the original position and stabilising.
3. **Dash/Quick-Stop manoeuvre:** The pilot starts from a hover and quickly accelerates to 60 [kts]. This is followed by a rapid deceleration back to a hover.

The restricted FoVs of the simulators meant that the pilots encountered much difficulty during their runs. For the first task, the pilots had trouble seeing or anticipating the lower hover targets when they were at the top target. This meant that they often overshot the targets and/or had to make more abrupt movements to try and stop. This often affected their ability to stabilise at the end of the manoeuvre. This problem was also encountered for the side-step manoeuvre where pilots could not effectively see their stopping points. For the third task, the pilots could not see the references for spatial position when they pitched up or down due to the restrictive FoVs. This meant that they had to use the radar altimeter to find out what their height was, instead of using out-of-window visual cues, and only used the visual

cues to confirm if the manoeuvre had been completed successfully. This converted the task from a visual-reference task, as it would be in real-life, to an instrument-monitoring task. This is similar to the conclusions reached by Podzus et al whereby it was apparent that pilots had to rely heavily on their instruments. In both cases, the pilots had to go against their instincts to use out-of-window visual cues which raised their overall workload and lowered performance.
Similar work was done by Chung et al, whereby their goal was to evaluate the effect of three visual parameters of simulators, namely the FoV, Colimnation and Resolution [7]. The experiment setup made use of the R-Cab and N-Cab simulator setups mentioned previously. To see the effect of FoV, the researchers used a wide and a narrow FoV to test the participants. To create equivalent FoVs in each Cab, and to change the FoV from a wide to a narrow one, they made use of masks to block off certain windows in the Cabs. The experiment involved participants controlling a four degree-of-freedom simulation of a UH-60A helicopter and trying to keep their longitudinal and lateral position constant, in the face of a disturbance. Data was then collected on their position error. The results showed that the wider FoV resulted in better velocity control and thus, smaller position errors. The researchers link this to the idea that the improved velocity control performance provided by the wider FoV increases damping in the closed loop system. They theorise, that this is a result of the improved peripheral vision one gets from a wider FoV. Additionally, when the pilots were asked which FoV they preferred, the pilots chose the wider FoV as their perception of roll attitude control and longitudinal velocity control was much better.
The idea that roll control may be affected by the FoV was also tested in the research done by Kenyon et al [10]. They did a variety of experiments but the most relevant experiment to this project is the critical tracking experiment, where the objective was to keep the visual scene at a roll angle of 0 [°]. This had to be done for FoVs of 10 [°], 20 [°], 40 [°], 80 [°] and 120 [°]. The researchers measured the effective time delay of all the participants and used that as a metric to draw up their conclusions. The researchers found that the decrease in effective time delay was exponential as FoV was increased, with most participants reaching their minimum value with an FoV of 20 [°], and the rest reaching it with an FoV of 40 [°]. They theorise that an FoV of 40 [°] already contains enough of a ”peripheral view” to do the experiment effectively. For a roll tracking task, they theorise that most of the work is done by the participants’ central view and the peripheral view only enhances the performance slightly. Regardless, they also suggest that an FoV of something as small as 10 [°] is wholly insufficient to do such a task, as some peripheral vision is still needed. These results can be useful in coming up with FoVs that can be tested in the experiment phase of this project.

The last two research projects are a departure from the analysis of FoV for the use of simulators, but nonetheless they provide key insights into what happens when FoV changes. These concern research projects done by Pretto et al and Duh et al [11] [12]. The goal of the research by Pretto et al is to see how changing FoV affects (i) perceived amplitude of rotations about the body vertical axis, and (ii) the perceived speed of forward translations. To test the first condition, the experiment conducted by the researcher was as follows. Participants were seated in front of a large panoramic screen and were shown a cross right in the front of the screen. They were instructed to keep their eye on the cross at all times. They were then shown a pattern of white dots scattered around the screen and a target circle, located 5 [°] left of the cross. When the experiment starts, the red dot disappears and the white dots rotate with a given amplitude, depending on the testing condition, and the participants job is to determine how far they think the red dot has moved, depending on the flow presented by the white dots. This is repeated for a multitude of different rotation speeds and three different FoVs; namely 30 [°], 60 [°] and 230 [°]. The second experiment involved a random scattering of white dots on the same screen setup. These dots provided two stimuli; the first one was the standard stimulus which moved the dots towards the participants at a speed of 5 [m/s], and the second stimulus moved the dots towards the participants at a speed that varied with the experimental condition tested. The participants had to tell the researchers which stimulus was the faster one. A visual representation of the two experiments is presented in Figure 2.4

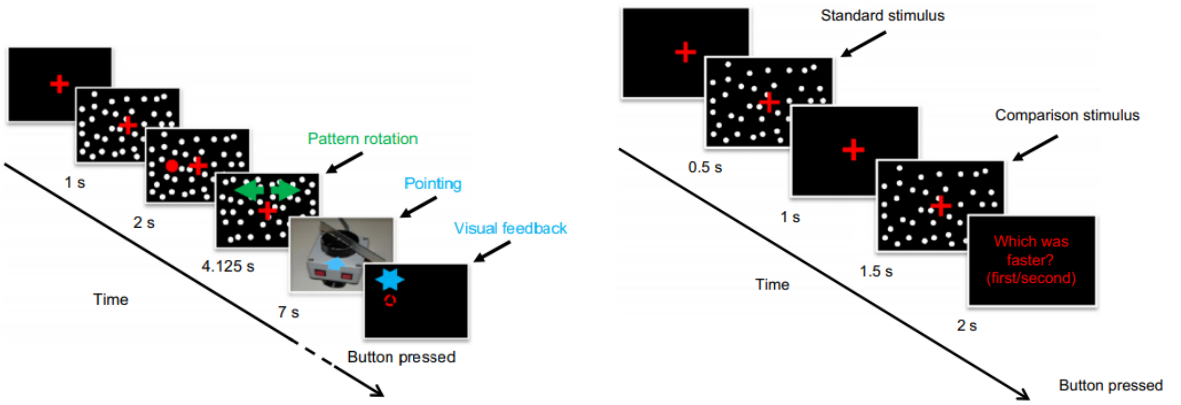

(a) Figure showing the procedure for the first FoV experiment done by Pretto et al [11]

(b) Figure showing the procedure for the second FoV experiment done by Pretto et al [11]

Figure 2.4: Figure showing the procedure for the two FoV experiments done by Pretto et al [11]

This experiment was done with two types of FoV conditions. The first one was a central FoV condition whereby the peripheral parts of the screen were occluded and no dots were shown there. The second was the peripheral FoV condition whereby the central part of the screen is occluded and dots were only shown in the peripheries. The difference between the conditions can be seen in Figure 2.5

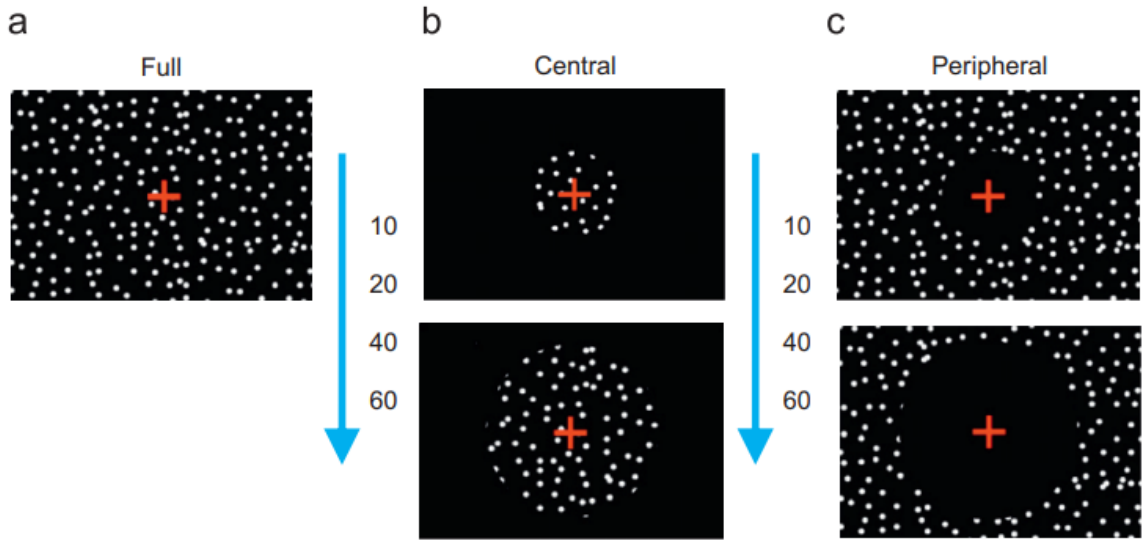

Figure 2.5: Figure showing the (a) Full FoV Condition, (b) the Central FoV condition, with FoV changing from 10 [°] (top) to 60 [°] (bottom) and (c) the Peripheral FoV condition, with FoV changing from 10 [°] (top) to 60 [°] (bottom) [11]

The results of the first experiment led the researchers to the conclusion that increasing the FoV beyond 30 [°] does not impact the average performance of the participants. However, it does decrease the variance of the results slightly. The results of the second experiment seem to show that, for central FoVs smaller than 60 [°], the participants underestimate the visual speed. If the participants were only using their peripheral vision, the participants tended to overestimate the visual speed.
The goal of the research, by Duh et al, was to investigate the relationship between FoV and scene content on the postural stability of participants [12]. The study revolves around the fact that the more immersed a participant is in the scene, the easier it is to induce vection. Vection is when a person believes that they are moving, even though they are not. Duh et al sought to investigate if changing the FoV and the scene content of a simulation where the participant is shown to be rotating, can affect a participant's postural stability. To this end, the participants were shown two separate scenes, one a city scene and one a simple radial pattern, and the scenes were changed such that the participant felt

like they were rotating around in the scene. The participant's job was to try and maintain their stance throughout the simulation and data was collected on how long it took for the participants' stance to break and how hard the participants found it maintain their stance. The working theory here is that the more immersed a participant is in the scene, the more likely they are to experience vection, which would cause them to lose their balance. The scenes were presented at six different FoVs and it was found that the participants showed more dispersion and found it harder to keep balance as FoV increased. The researchers concluded that by receiving more information in their peripheral vision, the participants had greater self-motion perception.

Based on all this research, some key conclusions can be reached about the impact of FoV on pilot control. Due to a lack of motion cues received in the peripheral region of the retina (caused by a narrow FoV), the pilot feels less immersed and tends to underestimate their own speed [11] [12] . It is also worth noting that if motion is solely perceived using one's peripheral vision, i.e they only have their peripheral vision and nothing else, then they generally tend to significantly overestimate their speed [11]. Conversely, if the FoV is smaller than 60 [$^\circ$], the pilot will underestimate their speed [11]. If pilots incorrectly estimate their velocities in such tasks, their damping in the closed loop system is lowered and their positional control becomes worse [7]. Additionally, while the crossover frequency of the pilot does not change due to a reduced FoV, their effective time delay increases and their phase margin decreases [10]. Degraded out-of-window visual cues can cause a lot of problems in a scenario where a pilot needs to accurately and precisely judge their position and velocity. The manoeuvre that would be most impacted by degradation of out-of-window cues would be a near-ground hover since pilots use their surroundings to provide them with cues pertaining to their velocity and position. Therefore, it is wise to assess the impact of FoV on pilot behaviour in the case of a pilot performing some sort of manoeuvre close to the ground, while hovering.
While the research done does a good job in pointing out what happens when FoV degrades, there is a significant gap in knowledge about why this ends up happening. The general consensus is that a lack of activity in the peripheral region of a pilot's vision leads to worse performance, but nothing has as-of-yet sought to explain why that is. The key piece missing, which this thesis aims to provide, is what information is being lost in the peripheral vision of a pilot as their FoV degrades, and how that can be modelled and used to predict pilot performance. Having reached a good understanding of the theory to test and develop, three key things are still missing. These are, namely, knowledge on how to set up and carry out an experiment to test any hypotheses developed, knowledge on how to create a working simulation of a helicopter to do the experiments in and, knowledge on how the outputs of the experiments can be analysed and linked to a pilot model. These aspects are discussed in full, in the proceeding sections

2.2. Experimental Methods

As one would expect, the methods used in the experimentation stage of the research depended heavily on what the goal of the research was. For research that was focused on evaluating impacts of visual cues in a realistic setting, the emphasis was on having an experiment setup of the highest possible fidelity. This means that the experiment would be done in either an actual helicopter, as was the case in research done by Baron et al [8] and Hoh et al [13], or by having a highly detailed simulation, as was the case in research done by Podzus et al [6], [2], Baker [14], Iseler [15] and Erazo et al [16]. For the simulations, the fidelity of the different aspects of the simulation varied depending on what the overall goal of the research is. For research projects which revolve around testing the fidelity of the simulators, as compared to the real-world case, particular attention is paid to ensure that the experience of the simulation is almost identical to a real world scenario. This involves factors such as:

- Using a highly detailed (six or four degrees-of-freedom) helicopter model to simulate the dynamics [6] [8]
- Ensuring that the layout of the various instruments and Heads-Up Display (HUD) elements resemble those of an actual helicopter [14]
- Using highly trained participants such as trained helicopter or aircraft pilots [6][8][14]
- Testing participants in tasks that they would perform in their normal routine in a real-life helicopter (such as a CAT-A RTO). [6]

Most experiments relevant to this topic, focus solely on the impact of specific visual cues on the pilot, instead of comparing the visual cues of simulators with a real-world example. Such research will often involve either augmenting or degrading visual cues and evaluating how pilot performance changes [10] [11] [17] [18] [19] . The experiment tasks that the participants have to perform are limited to simple disturbance rejection tasks or velocity (or position) tracking tasks. A disturbance rejection task involves the pilot trying to negate a perturbing forcing function, such that they keep velocity, or position constant. The tracking tasks involve the participants trying to match their velocity or position with that of a particular target signal. The researchers will then make use of the time traces of the participants' output signals to see how their performance changes over time. This performance can then be compared against the different testing conditions, such that the researchers can get a basic understanding of how the participants were affected by the testing conditions. How this data is analysed, or indeed what type of data is even collected, depends heavily on the type of pilot model the researchers want to create. This elaborated upon in section 2.3.

2.3. Pilot Models

One of the most widely used pilot models for such investigations is the Crossover Model created by McRuer and Krendel [20]. This model suggests that that human pilots follow a set of adjustment rules for compensatory tracking tasks. Such tracking tasks involve pilots trying to minimise the error between a controlled element and a reference signal. The feedback loop for such a task is shown in Figure 2.6:

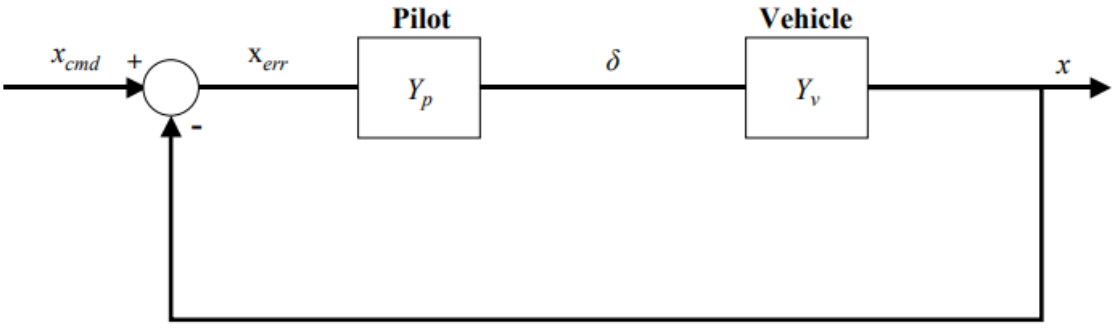

Figure 2.6: Figure showing the feedback loop for a simple compensatory tracking task [18]

The Crossover Model states that a pilot will change their dynamics, Y_p, such that the open loop dynamics, Y_pY_v, resemble Equation 2.1:

$$Y_PY_V = \frac{\omega_c e^{-\tau s}}{s} \tag{2.1}$$

where ω_c is the crossover frequency and τ is the pilot delay. The crossover frequency represents the transition frequency beyond which, the pilot is unable to effectively perform closed loop tracking and the system acts as open loop. The pilot delay is there to represent delays caused by pilot perception, interpretation and neuromuscular actuation. To achieve the open loop dynamics of Equation 2.1, the pilot dynamics, Y_p will take the form of:

$$Y_p(s) = K_p \frac{(1 + T_L s)}{(1 + T_I s)} e^{-\tau s} \tag{2.2}$$

where K_p is the pilot gain, T_L is the lead constant and T_I is the lag constant . The lag and lead constants are thus chosen to provide the open loop dynamics depending on the dynamics of the controlled elements. The goal would then be to calculate these pilot parameters for the different testing conditions in an experiment to see how pilot behaviour and dynamics change.

While this model is widely used, it does have a very simplistic representation of the pilot's dynamics [21]. Thus, one can supplement the Crossover model with more realistic representation of pilots' sen-

sory and neuromuscular aspects, as is done in the Cybernetic model [22][23]. A visual representation of this model is given in Figure 2.7:

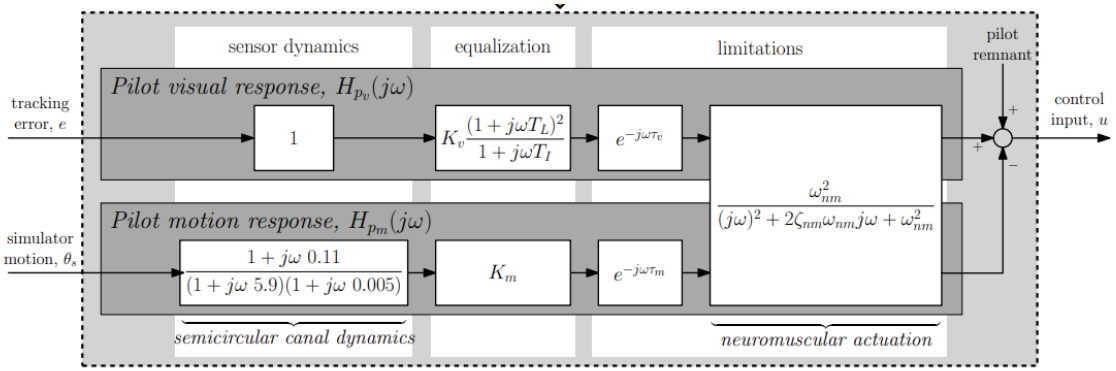

Figure 2.7: Figure showing the multi-modal cybernetic pilot model [23]

As can be seen in Figure 2.7, the pilot model is now split into two distinct modes; the visual (top) and the vestibular/motion (bottom) mode. For both modes, the entire model is split into sensor dynamics, equalisation terms and pilot limitations. The limitations part now contains the delays associated with both modes of perception as well as the term for neuromuscular limitations, given by H_{nm} in Figure 2.7. For the visual model, the sensor dynamics are usually modeled as a Unity gain [23]. Additionally, the equalisation dynamics of the visual response of the system shown in Figure 2.7 are different from the dynamics of Equation 2.2 because the equalisation dynamics represent the control strategy that the pilot uses. This means that the dynamics are dependant on the controlled aircraft dynamics. The dynamics shown in Figure 2.7 are typical for a system where the pilot needs to control an aircraft's pitch attitude [23]. The sensor dynamics for the vestibular mode, H_{sc} correspond to the dynamics of the semicircular canals found in human ears which are used for velocity perception [22] [23]. The main free parameters for this model are the equalization parameters (visual gain K_v, visual lead constant T_L, visual lag constant T_I and the motion gain K_m) and the visual and motion perception delays τ_v and τ_m, respectively. [22]. The free parameters can be calculated using various parameter estimation techniques, such as Fourier transforms, and the parameters obtained are in the frequency domain. Frequency domain parameter estimation models have the issue that they are a two-step process; the first step involves obtaining a non-parametric pilot describing functions in the frequency domain and the second step involves optimising the parameters. This is an issue because there are biases involved in both steps and they compound to have a major effect on the final result [24]. To alleviate this, one may need to use more complex techniques, like a Maximum Likelihood Estimator (MLE), which may make the final analysis of the result much harder. Another issue stems from the fact that a human controllers' remnant means that all signals in the loop are stochastic, and have power in all frequencies. Therefore, the forcing function has to be designed such that it has a signal-to-noise ratio over certain frequencies that the researcher wants to test. The problem however, is that the Crossover model is only applicable over a certain range of frequencies, called the crossover region, so the forcing function can not be made up of frequencies beyond this region. Additionally, if one wishes to use the multi-modal cybernetic model, multiple forcing functions are needed such that one can quantify the participants' responses to the visual and motion cue separately [23]. That means that the forcing functions and the cues have to be significantly different from one another.

One of the biggest challenges with the model however, is ensuring that the cues a participant receives, match up with the model design. As an example, take a situation where a human has to control the lateral position of a car on a straight road and one wishes to fit the model shown in Figure 2.8 to the human:

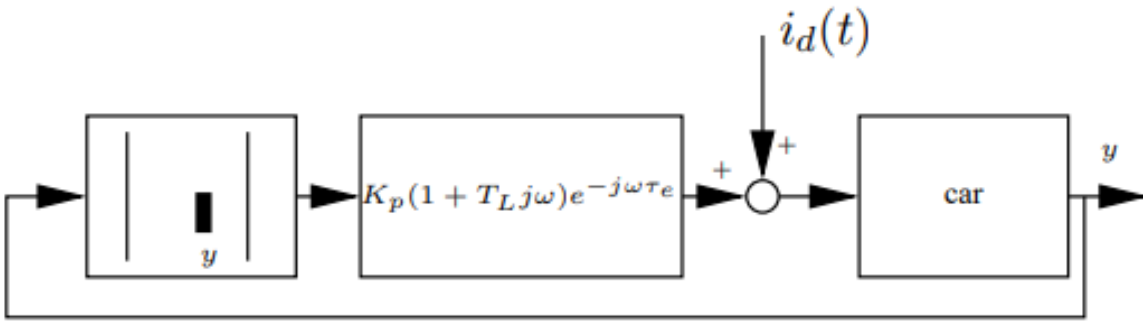

Figure 2.8: Figure showing an example model for a human controlling the lateral position of a car [25]

Here, the human gets the lateral position of the car as the only feedback (i.e. the first block) and then, based on the dynamics of the car (i.e. the third block), applies the proper equalisation (i.e. the second block). However, if the human is able to see the heading of the car, as they would in a realistic environment, then the control becomes a closure of two loops. This means that the model of Figure 2.8 is no longer applicable to the situation and instead, one has to use the model shown in Figure 2.9

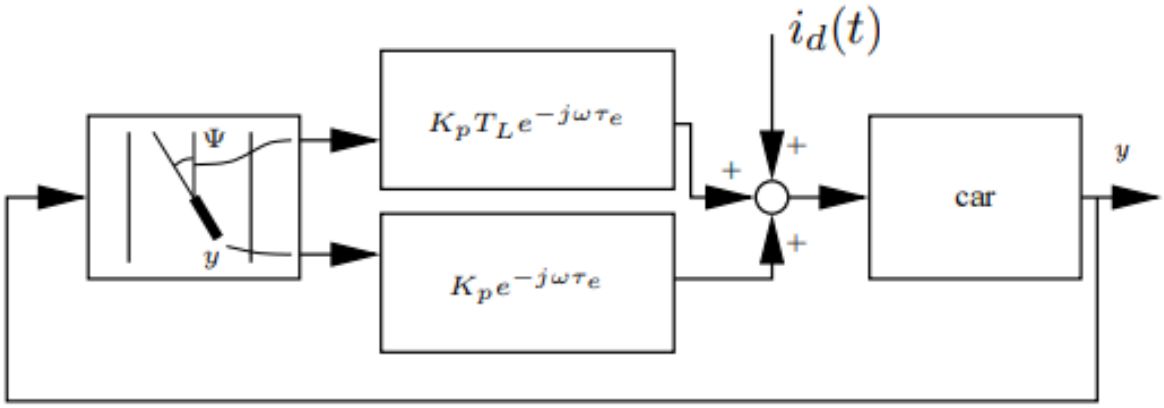

Figure 2.9: Figure showing the model that would be applicable for a human controlling the lateral position of a car with the heading angle and lateral position as feedback [25]

This highlights the inherent issue with trying to apply a cybernetic model to a realistic simulation; the fact that the researcher has to meticulously design the simulation such that the pilot only receives cues that the researcher wants them to. This can become difficult in highly detailed simulations since a pilot can just pick any emergent or invariant feature in the view and use that as a basis for their control inputs. This can result in the applicable cybernetic model, for this particular participant, having multiple loops and feedback channels that the researcher did not anticipate [25]. This is why, while this is a widely popular method of creating a pilot model in Human Machine Systems, the experiment design and analysis techniques required to create it can often be too complicated for what the research requires.

That is why a simpler technique often involves using the output data of the experiment directly and doing some kind of statistical test on it to determine how the pilot performance changes with respect to the experiment design. An example of this can be seen in the performance metrics used by Baron et al and by Podzus et al, which are shown in Table 2.2 [6] [8] . In these examples, the output data from the experiments is simply compared against each other rather than being used to build up a complex pilot model. This can often be supplemented by techniques like the Analysis of Variance (ANOVA)

test which aims to see if there was any significant trend emerging in the data for the different testing conditions [24].
One disadvantage of such methods, as compared to the Cybernetic model, is the fact that it does not give much insight into why the pilot behaviour changes; these methods merely point out how the performance changes. One method to remedy this is by using subjective methods to see how the pilots believe the conditions have changed and how they adapted to them. Three of the most widely used subjective assessment techniques are the Cooper-Harper Handling Qualities Rating Scale (HQR), the Bedford Rating Scale and the Visual Cue Rating (VCR) scale. The HQR is shown in Figure 2.10:

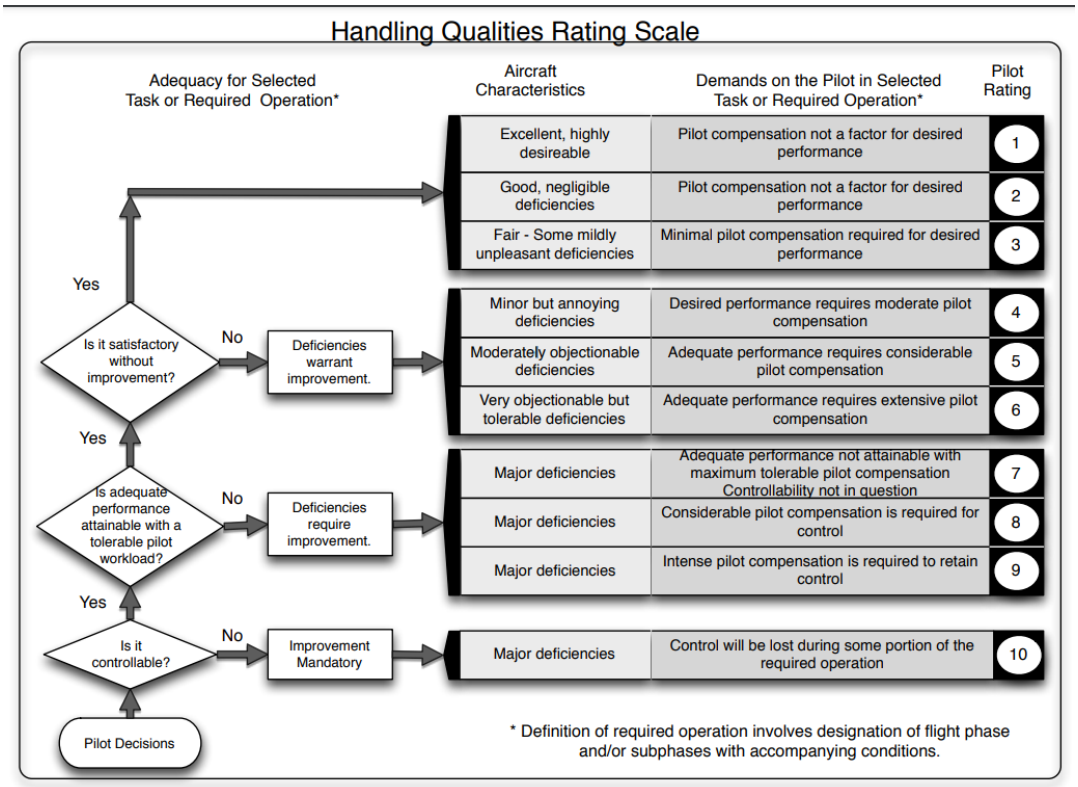

Figure 2.10: Figure showing the Cooper-Harper Handling Qualities Rating Scale [26]

The main use-case for this scale is when one needs to evaluate the additional effort a pilot needs to make (above the nominal task workload) to achieve a given level of performance, in the face of some sort of control augmentation [19] [26] . This scale is widely used in research in which the participants are trained pilots, since they can easily judge if the workload they are experiencing is something they would normally experience, or if it is due to the experimental condition being tested [7] [9] . The Bedford Rating scale, shown in Figure 2.11, has the same working principle as the HQR.

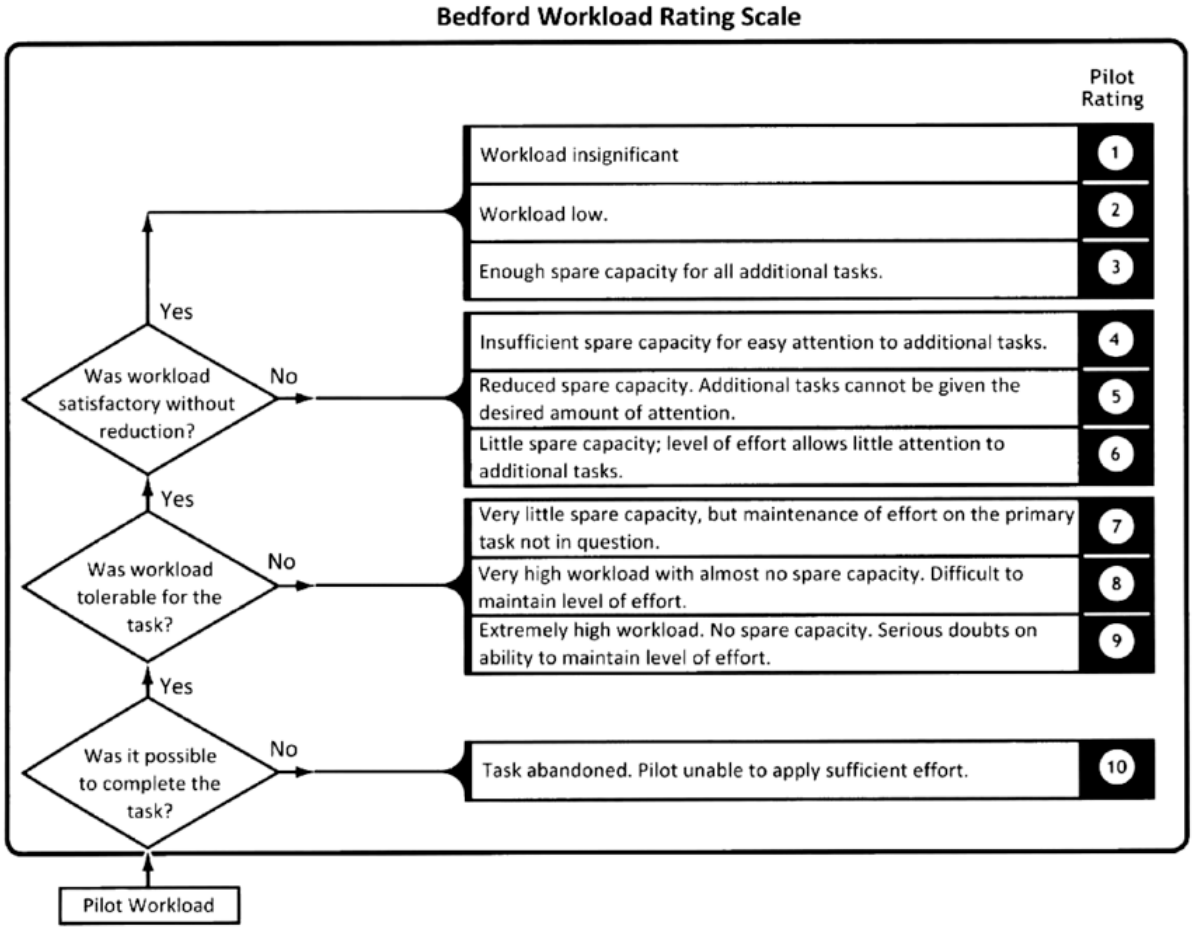

Figure 2.11: Figure showing the Bedford rating scale [27]

The final subjective assessment method worth discussing is the Visual Cue Rating Scale (VCR). Using a VCR scale involves the pilot giving a score of 1-5 based on how precise and aggressive they could be when controlling attitude and translational rates of a vehicle. The scale itself can be seen in Figure 2.12

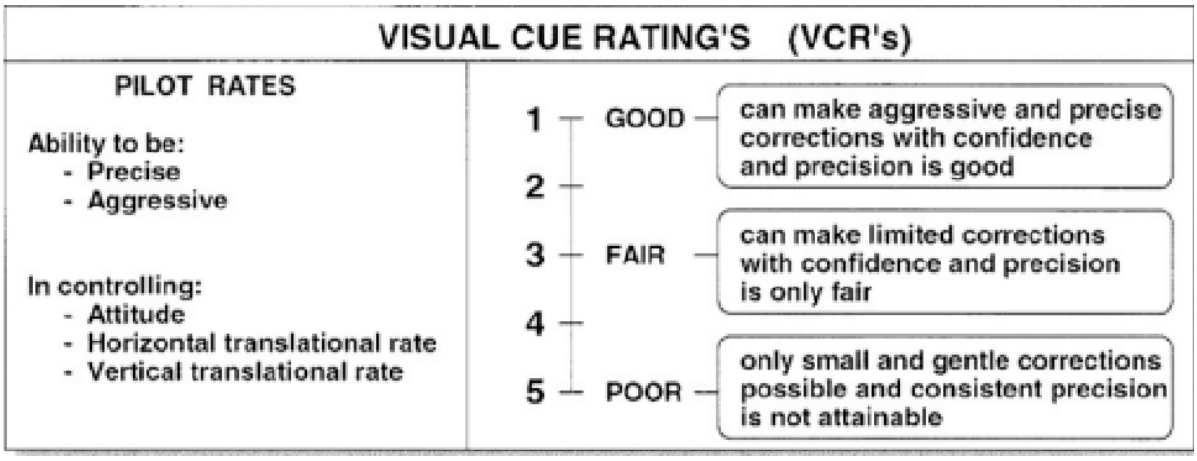

Figure 2.12: Figure showing the VCR scale [6]

In the research done by Podzus et al, the participants gave VCR scores for the translational rate and attitude, and this was then plotted together to give an intuitive visualisation of visual fidelity. The

combined average VCRs for all the conditions tested in this research (shown in Table 2.1) are shown in Figure 2.13

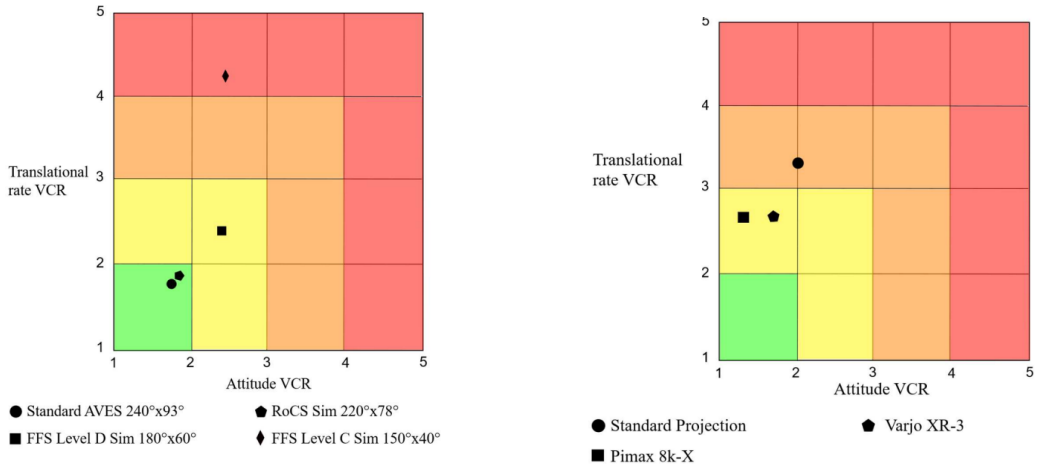

(a) Figure showing the combined average VCRs for translational rate and attitude for the DLR test campaign [6]

(b) Figure showing the combined average VCRs for translational rate and attitude for the NLR test campaign [6]

Figure 2.13: Figure showing the combined average VCRs for the different testing conditions in research done by Podzus et al [6]

As can be seen from the figures above, the combined VCR scale provides an intuitive way of comparing the different conditions against each other. However, this also highlights the issues with using such subjective rating scales; the training required to do so. Indeed, the reason why studies that choose to use such scales use trained pilots as test subjects is because those pilots have been trained in the nuances of using such subjective methods. As an example, take Pilot Rating 5 and 6 on the HQR in Figure 2.10. An average person would not be able to figure out the difference between a system that has ”moderately objectionable differences” and one that has ”very objectionable but tolerable differences”. This knowledge comes with training and experience that only pilots will likely have. Therefore, if the researcher expects to not have access to a lot of trained pilots for their experiments, as is the case for this thesis project, then the use of such scales can make the subjective results unreliable and inaccurate. In such a case, the researcher is better off asking more general and open-ended questions to gather subjective results. This means that one should not hope to use these subjective comments to create objective scores (like the Pilot Ratings).

The main conclusion that can be drawn for this part is the fact that the pilot model one uses depends heavily on what type of experimentation will be carried out. Detailed and complex models, like the Cybernetic model, can offer a lot of objective insight into how pilot performance and behaviour change, but require complex analysis techniques and precise experiment design. Additionally, if the structure of the model contains multiple control loops, then the analysis becomes more complicated in order to decouple the results of the multiple loops. This, of course, means that the experiment design and the experiment outputs must also be designed in such a way that enough information is available to decouple the results for the control loops. Simple models which compare variances in the objective pilot performance can easily quantify and explain what change occurs in pilot performance, but struggle to explain why the changes in pilot behaviour occur. These can be supplemented with subjective ratings, like the HQR or the Bedford Scale, but those have their own disadvantages. The biggest disadvantage is the fact that they require a lot of training for participants to efficiently use as an untrained participant will not know how to effectively discern the subtleties between the different ratings. Ultimately, what this research shows, is that one needs to ensure that they have a good understanding of what type of participants will do the experiment, and what the experiment will look like, before they choose to apply a pilot model to the results. The time-frame of this thesis means that it is not reasonable to expect that enough trained pilots will be available to do the experiments. This means that the use of the complex subjective rating scales is unlikely. Additionally, the results of the visual model developed will dictate what the experiment will need to look like. This will then influence what type of pilot model can be created.

2.4. Helicopter Model

The fidelity of the helicopter dynamics model depends heavily on the research being done. As an example, for the research done by Bachelder, the goal was to investigate how Night-Vision Devices (NVD) can be used to give the pilot of a rotor-craft some synthetic cues, and how their perception is affected [18]. This means that, for the purposes of the research, the helicopter model used in the experiments did not need to have a very high fidelity since the focus was on more on the cueing of the NVD and on pilot behaviour. This is why, Bachelder used a simple model, shown in Figure 2.14:

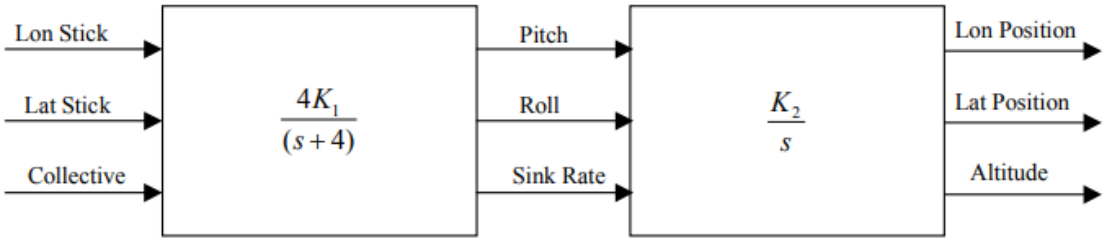

Figure 2.14: Figure showing the helicopter dynamics model for [18]

As can be seen from Figure 2.14, the dynamics consist of a simple integrator with lag to go from the control input to the attitude angles and a simple integrator to go from the attitude to position. Generally, however, the dynamics model used is derived from a six degrees-of-freedom model, whose state space representation is outlined as such [14] [17] [28]:

$$\dot{x}(t) = A\mathbf{x}(t) + B\mathbf{u}(t) \tag{2.3}$$

where

$$\begin{aligned} \mathbf{x} &= \{u, w, q, \theta, v, p, \phi, r, \psi\} \\ \mathbf{u} &= \{\theta_0, \theta_{1s}, \theta_{1c}, \theta_{0T}\} \end{aligned} \tag{2.4}$$

The components of the state vector, x(t) in Equation 2.4 are [28]:

- u: Horizontal velocity component in the body-fixed x-direction [m/s].
- w: Vertical velocity component in the body-fixed z-direction [m/s].
- q: Angular velocity around the body-fixed y-axis [rad/s].
- θ: Pitch angle [rad].
- v: Horizontal velocity component in the body-fixed y-direction [m/s].
- p: Angular velocity around the body-fixed x-axis [rad/s].
- ϕ: Roll angle [rad].
- r: Angular velocity around the body-fixed z-axis [rad/s].
- ψ: Yaw angle [rad].

and the components of the input vector, u(t) are [28]:

- θ_0: Collective pitch angle [rad].
- θ_{1s}: Swashplate servo pitch angle [rad].
- θ_{1c}: Swashplate servo roll angle [rad].
- θ_{0T}: Tail rotor collective pitch angle [rad].

For the system given by Equation 2.3 and Equation 2.4, the A and B matrices for the linearised system are given by:

$$\mathbf{A} = \begin{bmatrix} X_u & X_w - Q_e & X_q - W_e & -g\cos\Theta_e & X_v + R_e & X_p & 0 & X_r + V_e \\ Z_u + Q_e & Z_w & Z_q + U_e & -g\cos\Phi_e\sin\Theta_e & Z_v - P_e & Z_p - V_e & -g\sin\Phi_e\cos\Theta_e & Z_r \\ M_u & M_w & M_q & 0 & M_v & \begin{matrix} M_p - 2P_e I_{xz} I_{yy} \\ -R_e\left(I_{xx} - I_{zz}\right) I_{yy} \end{matrix} & 0 & \begin{matrix} M_r + 2R_e I_{xz} I_{yy} \\ -P_e\left(I_{xx} - I_{zz}\right) I_{yy} \end{matrix} \\ 0 & 0 & \cos\Phi_e & 0 & 0 & 0 & -\Omega_a\cos\Theta_e & \sin\Phi_e \\ Y_u - R_e & Y_w + P_e & Y_q & -g\sin\Phi_e\sin\Theta_e & Y_v & Y_p + W_e & -g\cos\Phi_e\cos\Theta_e & Y_r + U_e \\ L'_u & L'_w & L'_q + k_1 P_e - k_2 R_e & 0 & L'_v & L'_p + k_1 Q_e & 0 & L'_r + k_2 Q_e \\ 0 & 0 & \sin\Phi_e\tan\Theta_e & \Omega_a\sec\Theta_e & 0 & 1 & 0 & \cos\Phi_e\tan\Theta_e \\ N'_u & N'_w & N'_q - k_1 R_e - k_3 P_e & 0 & N'_v & N'_p + k_3 Q_e & 0 & N'_r + k_1 Q_e \end{bmatrix} \tag{2.5}$$

$$\mathbf{B} = \begin{bmatrix} X_{\theta_0} & X_{\theta_{1s}} & X_{\theta_{1c}} & X_{\theta_{0T}} \\ Z_{\theta_0} & Z_{\theta_{1s}} & Z_{\theta_{1c}} & Z_{\theta_{0T}} \\ M_{\theta_0} & M_{\theta_{1s}} & M_{\theta_{1c}} & M_{\theta_{0T}} \\ 0 & 0 & 0 & 0 \\ Y_{\theta_0} & Y_{\theta_{1s}} & Y_{\theta_{1c}} & Y_{\theta_{0T}} \\ L'_{\theta_0} & L'_{\theta_{1s}} & L'_{\theta_{1c}} & L'_{\theta_{0T}} \\ 0 & 0 & 0 & 0 \\ N'_{\theta_0} & N_{\theta_{1s}} & N'_{\theta_{1c}} & N'_{\theta_{0T}} \end{bmatrix} \tag{2.6}$$

where terms like X_u and X_{θ_0} are the various stability derivatives, U_e, V_e and W_e are the velocity components, P_e, Q_e and R_e are the angular rates and Θ_e, Φ_e and Ψ_e are the attitude angles [28]. Keen readers will notice that the A matrix in Equation 2.5 is an 8x8 matrix while the state vector, x has a size of nine. For the A matrix, the yaw angle, ψ has been omitted since the yaw angle has no effect on the aerodynamic or dynamic forces and moments [28]. Therefore, that would mean the last column was a column of zeros and that has been omitted such that the rest of the equation was readable on the page This particular model is also a more simplified version of the actual helicopter dynamics since it neglects the coupling between the rotor and the fuselage, but this is still an excellent representation of the helicopter dynamics [17] [28]. It is worth noting that the input vector, u(t), can be changed to suit the experiment being done. As an example, in the research done by Moon et al, the input vector consists of pilot inputs instead of attitude angles [17]:

$$u(t) = \begin{bmatrix} \delta_c & \delta_{\text{lon}} & \delta_{\text{lat}} & \delta_p \end{bmatrix} \tag{2.7}$$

where:

- δ_c: Control input representing collective pitch angle.
- δ_{lon}: Control input representing longitudinal control.
- δ_{lat}: Control input representing lateral control.
- δ_p: Control input representing tail rotor pitch angle.

Here the pilot inputs are mapped onto the attitude angles (much like the left block in Figure 2.14) using the following transfer function:

$$G_{act}(s) = \frac{30^2}{s^2 + 2(0.75)30s + 30^2} \tag{2.8}$$

This means that the rate commanded dynamics are, again, identical in all axis.

In conclusion, the best way to model the helicopter dynamics for this research would be to start with the six degrees-of-freedom system given in Equation 2.3 and Equation 2.4. Then, one needs to simplify it by removing all degrees-of-freedom which will not be used for the experiment and deciding what the input to the system will be. If the inputs are control inputs, then there needs to be a transformation block that converts those to attitude angles which can then be used to calculate the associated translations and rotations.

2.5. Conclusion

The goal of this literature study was to create research questions that complete the research objective: ”How does using VR headsets, to perform visual cueing, affect the performance of Pilots flying a Helicopter Simulation”. As such, the literature reviewed focused on finding out the answer to three main aspects of the research objective, namely:

1. What kinds of visual cues are crucial for pilots in helicopter flight?
2. What goes into creating a pilot and helicopter model that can be used in simulation and experiments?
3. How is pilot performance tested and evaluated?

The reviewed research revealed that the most important visual cues for pilots vary depending on what task they are performing. The most important task in a normal flight envelope would be a near-ground hover since it requires very precise velocity and position control. As such, for this manoeuvre, the most important visual cues are the Field of View (FoV) provided by the visual cueing system. Since the FoV of the view dictates how well the pilot can see all other visual cues, it can be deemed to be of the highest importance. If the FoV degrades significantly, the pilot will start to underestimate or overestimate how fast they are flying and will be prone to errors in maintaining their position. For a near-ground manoeuvre, this can be extremely dangerous, thus, maintaining a proper FoV is crucial for such a flight case. Additionally, the pilots will need to rely more on their instruments instead of the out-of-window cues which goes against their instincts, and that raises their workload.
Research into the types of pilot and helicopter models, as well as the experimental methods, used in literature also revealed some interesting results. The highest fidelity pilot model one can create is the Cybernetic model, which allows one to calculate pilot model parameters like the crossover frequency and effective time delay of the pilot. However, to build up such a model, the experimental methods one needs to use are quite extensive. One needs to ensure that the pilot receives proper visual (and if applicable, vestibular) cues in the actual experiment, the forcing function is designed such that the required system identification techniques can be applied effectively and, in case of a multi-loop model, the experiment itself has the correct outputs such that the multiple loops can be disentangled. The system identification techniques themselves can get extremely complicated, especially if non-linearities are present. Often times, this is far beyond the scope of the researchers' objectives and that is why they tend to use significantly simpler analysis methods. These involve asking the participants to do simple control tasks and just running an error analysis on the time traces of their outputs. This can be supplemented with subjective results which involve asking pilots to rate their performance and/or workload on a widely used scale, such as the HQR or the Bedford-Rating Scale. The use of such scales however, needs the participants to be experienced with the control tasks and with using the scales. The last part of the literature study to discuss is the type of helicopter dynamics model used. In general, previous researchers use a six degree-of-freedom model, whose states include three velocity components (u,v,w), three attitude angles (θ,ϕ,ψ) and three attitude rates (p,q,r). This model can then be simplified based on however degrees-of-freedom the researchers want the participants to have for the experiment.

Based on this research, the following research questions can be formulated:

1. **What manoeuvre is most impacted by changing Field of View (FoV)?**
2. **What is the predicted pilot behaviour for the critical manoeuvre with changing FoV?**
3. **What is the actual pilot behaviour for the critical manoeuvre with changing FoV?**
4. **What is the overall effect of changing FoV on pilot performance?**
5. **What strategies do pilots employ to overcome adverse effects of changing FoV?**

It is worth noting that the first research question has already been answered. The manoeuvre most impacted by the changing FoV is the near-ground hover with disturbances. The answers to the rest of the questions will be found using the visual model built, and the practical experiments.

This page is intentionally left blank.

3

Visual model

The goal of this chapter is to develop a visual model that can explain the nature of the information one loses when peripheral vision is obstructed. It is assumed that, in the visual field of the pilot, there exists a point that can offer the maximum amount of feedback for a given manoeuvre. It is assumed that, if such a point exists and is independent of the FoV, then when the FoV is lowered, this point would get clipped out of the view. This means that the pilot would no longer see the most salient point of the environment and would need to shift their gaze to the next-most salient point. Presumably, this would result in the velocity feedback that the pilot gets being much smaller and could be the reason for why people tend to underestimate their velocity as FoV shrinks, as per the findings of the literature study in section 2.1. Additionally, as shown in Chapter 2, the performance of the pilot degrades the most as FoV changes for forward translational motion. As such, it is worth analysing cases where the helicopter would move forward and backwards to see if the point of maximum feedback does exist. However, since helicopters must change their pitch to change their forward velocity, the motion of the pitch must also be considered. It was thus decided to limit the analysis to only these two degrees-of-freedom.

To do this, one needs to look at what type of flow is generated during motion. This flow can then be analysed to see how the human eye would see it and how this would affect their perception. Initially, an analysis was done that, among other things, focused on quantifying how this (3D) flow would look like when it was projected onto a 2D screen. This analysis did not yield tangible or useful results and thus, it was decided to ignore the effects of projecting the 3D motion onto a 2D screen. This means that the screen of the VR headset is just assumed to act as a ”window to the real world” (much like the human eye) and the only projection effects that will be considered, are those that are related to projecting objects onto the curved retina of human eyes. The alternate analysis is presented in Appendix A for the interested reader
To start the analysis, one considers there to be a point, P in space with the coordinates [x,y,z], i.e:

$$P = [x, y, z] \tag{3.1}$$

this point will be projected onto the surface of the observer’s retina at point Q as per Figure 3.1

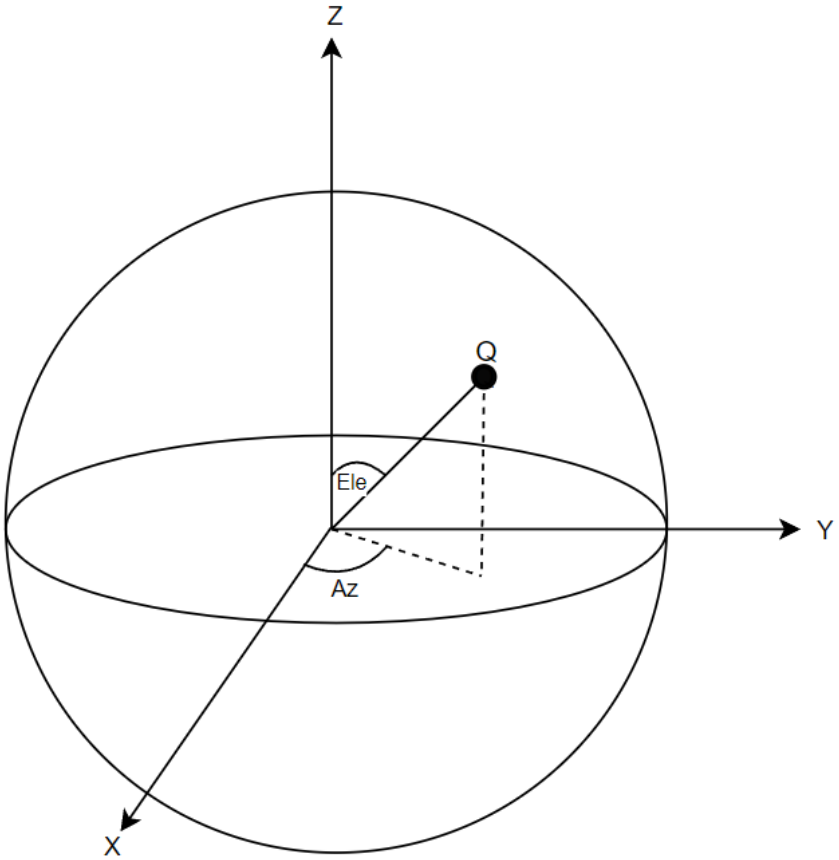

Figure 3.1: Figure showing the projection of point P onto the spherical retina

Here, **Az** and **Ele** refer to the azimuth and elevation angles of the point Q. To convert point P to point Q, Equation 3.2 can be used:

$$Q = (\frac{r}{|P|})P \tag{3.2}$$

where r is the radius of the sphere and $|P|$ is the magnitude of the vector P i.e.

$$|P| = \sqrt{x^2 + y^2 + z^2} \tag{3.3}$$

Assuming again that the helicopter has only two Degrees-Of-Freedom, pitching and forward translation, the new position of P, P', can be calculated using:

$$P' = R_Y(\theta)P - [u * dt, 0, 0] \tag{3.4}$$

where $R_Y(\theta)$ is the orthogonal rotational matrix and dt is a small time-step. $R_Y(\theta)$ is given by Equation 3.5:

$$R_Y(\theta) = \begin{bmatrix} \cos\theta & 0 & \sin\theta \\ 0 & 1 & 0 \\ -\sin\theta & 0 & \cos\theta \end{bmatrix} \tag{3.5}$$

Once P' is calculated, it is transformed into a new Q position, Q', and this is used to analyse how the motion appears on the observer's retina. This can be done for a grid of points within the observer's field of vision and can be plotted on a 3D graph to show how this changes over time. To get results representative of the actual scenario of a helicopter in hover, it is worth finding out what a realistic motion of a helicopter will look like. This involves looking at the dynamics of a helicopter and mapping out a pilot's control inputs to a pitching angle and a forward velocity. This is elaborated upon in more

depth in section 4.2.

The control input simulated for this is sinusoidal and is applied to the system for a total of four seconds. The exact form of the input is given by Equation 3.6

$$Input = \frac{-1}{100} * \sin\left(\frac{3}{2}\pi t\right) \tag{3.6}$$

This input was chosen after many iterations such that the resulting pitch angle and velocity were high enough for there to be a visible change in the flow, but not so high that it is no longer representative of a helicopter in a low-speed hover. The control input can be seen in Figure 3.2a, while the resulting behaviour of θ and u can be seen in Figure 3.2b and Figure 3.2c respectively:

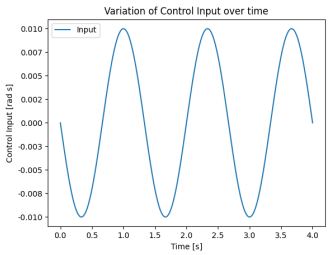

(a) Figure showing the control input applied to the helicopter dynamics

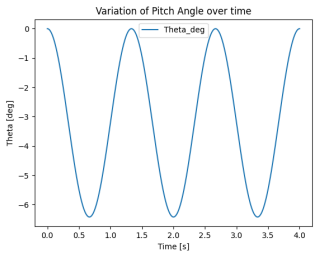

(b) Figure showing the pitch angle, θ, resulting from the control input

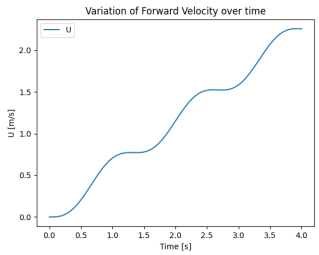

(c) Figure showing the forward velocity, u, resulting from the pitch angle

Figure 3.2: Figure showing the motion used for the analysis

The flow that an observer would see for this particular motion, is visualised for a few of the time-stamps in Figure 3.3:

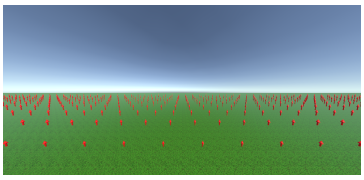

(a) Figure showing the flow at t = 0.5 [s], u = 0.2 [m/s], θ = -5 [$^\circ$] and $\dot{\theta}$ = -1.25 [$^\circ$/s]

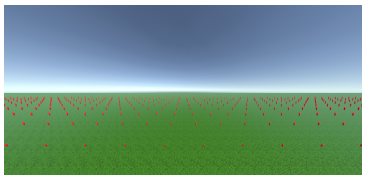

(b) Figure showing the flow at t = 1.0 [s], u = 0.69 [m/s], θ = -2.8 [$^\circ$] and $\dot{\theta}$ = 1.43 [$^\circ$/s]

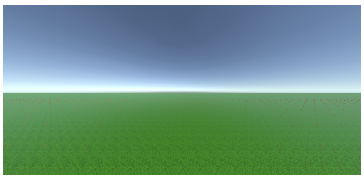

(c) Figure showing the flow at t = 1.5 [s], u = 0.77 [m/s], θ = -1.1 [$^\circ$] and $\dot{\theta}$ = -0.78 [$^\circ$/s]

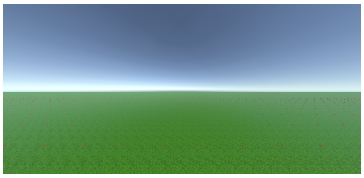

(d) Figure showing the flow at t = 2.5 [s], u = 1.49 [m/s], θ = -1.1 [$^\circ$] and $\dot{\theta}$ = 1.25 [$^\circ$/s]

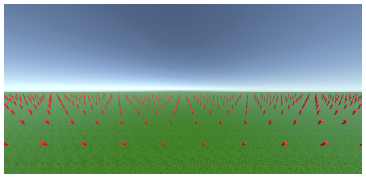

(e) Figure showing the flow at t = 3.5 [s], u = 2.03 [m/s], θ = -5 [$^\circ$] and $\dot{\theta}$ = 0.77 [$^\circ$/s]

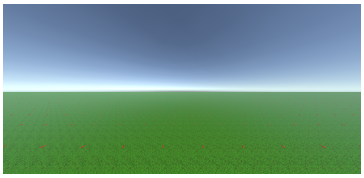

(f) Figure showing the flow at t = 4 [s], u = 2.21 [m/s], θ = 0 [$^\circ$] and $\dot{\theta}$ = 0.34 [$^\circ$/s]

Figure 3.3: Figure showing the flow for the example movement

For the sake of clarity, the full sized images of this motion are shown in Appendix B (Figure B.1 - B.6). As can be seen from Figure 3.3a and Figure 3.3f (or from Figure B.1 and Figure B.6), the flow vectors for the pitching motion are more pronounced than those for the forward motion. This is in part due to the fact that the velocity itself is relatively small for this motion and, unless the participants control the system perfectly, will be higher and more visible for the experiments and in the real world. The combination of the vectors for both motions can be seen in Figure 3.3e (or Figure B.5) and it can be seen that the flow due to the pitching motion can be more easily discerned from the images, as compared to the forward motion.

To analytically analyse the effect of these flow vectors, one can look at the change in the Azimuth and Elevation angles that occurs due to the helicopter's motion. The Azimuth and Elevation angles can

be calculated using Equation 3.7 and Equation 3.8, respectively:

$$Az = \arctan \frac{y}{x} \tag{3.7}$$

$$Ele = \arccos \frac{z}{|P|} \tag{3.8}$$

The two angles can be differentiated with respect to the pitch, θ and the distance moved, $u * dt$. Calculating the partial derivative with respect to distance instead of velocity ensures that the results are independent of the time-step chosen. The partial derivative of the azimuth angle with respect to the distance moved is given by Equation 3.9:

$$\frac{\partial Az}{\partial (udt)} = \frac{y}{D^2 + y^2} \tag{3.9}$$

where

$$D = x \cos\theta + z \sin\theta - udt \tag{3.10}$$

The partial derivative with respect to θ is given by Equation 3.11:

$$\frac{\partial Az}{\partial \theta} = \frac{yx \sin\theta - yz \cos\theta}{D^2 + y^2} \tag{3.11}$$

For the elevation angle, the partial derivative with respect to the distance moved is given by Equation 3.12:

$$\frac{\partial Ele}{\partial (udt)} = \frac{-2x \cos\theta - 2z \sin\theta + 2udt}{2\sqrt{P_x^2 + y^2} \cdot \left[C + \frac{P_x^2 + y^2}{C}\right]} \tag{3.12}$$

where

$$C = -x \sin\theta + z \cos\theta \tag{3.13}$$

and

$$\begin{aligned} P_x^2 = {} & x^2 \cos^2\theta + z^2 \sin^2\theta + 2xz \cos\theta \sin\theta \\ & - 2uxdt \cos\theta - 2uzdt \sin\theta + u^2 dt^2 \end{aligned} \tag{3.14}$$

The partial derivative with respect to θ is given by Equation 3.15:

$$\frac{\partial Ele}{\partial \theta} = \frac{B}{2\sqrt{P_x^2 + y^2} \cdot \left[C + \frac{P_x^2 + y^2}{C}\right]} \tag{3.15}$$

with

$$B = -x^2 \sin(2\theta) + z^2 \sin(2\theta) + 2xz \cos(2\theta) + 24xdt \sin\theta - 2uzdt \cos\theta \tag{3.16}$$

As can be seen from the equations, the partial derivatives are dependant on the position of the object, the speed and the pitch angle of the observer. To analyse the behaviour of these derivatives thus, one has to fix a few of these variables and analyse how the behaviour changes due to the remaining variables. For this analysis, much like the flow vectors, the speed and pitch angle were determined by the example motion shown in Figure 3.2. The z-coordinate of the position was chosen to be -5 [m] as it is believed that the points an observer would see on the ground would be the most informative [29]. The remaining variables are thus, the x and y-coordinates of the position. Since the goal is to see the effect of FoV on these quantities, the x and y-coordinates corresponding to a specific FoV can be used. However, for any FoV, one can have an infinite number of x and y-coordinates. Thus it was decided to calculate the value of the partial derivatives for a set of x and y-coordinates (that correspond to one particular FoV) and take their average value. This value can be thought of as the value of the partial derivative for this particular FoV over the whole range of x and y-coordinates.
As an example, for a chosen FoV of 140 [°], a list of x-coordinates ranging from 1 [m] to 10[m] was created. Then, the corresponding y-coordinate was calculated using Equation 3.17:

$$y = x \tan(70) \tag{3.17}$$

These x and y-coordinates, along with the rest of the fixed variables, were input into Equation 3.9, Equation 3.11, Equation 3.12 and Equation 3.15, and the trend was plotted. This can be seen in Figure 3.4:

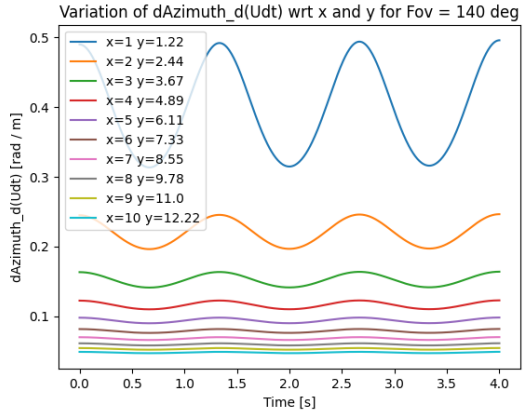

(a) Figure showing the variation of $\frac{\partial Az}{\partial(udt)}$ with x and y-coordinates

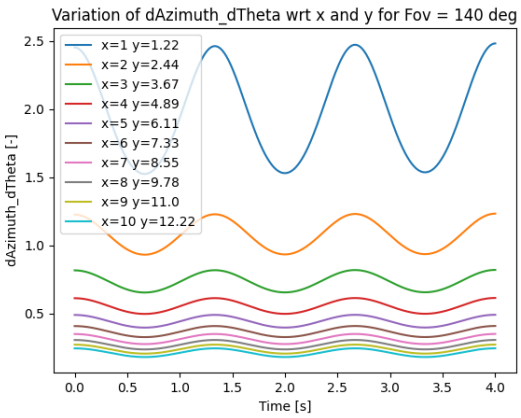

(b) Figure showing the variation of $\frac{\partial Az}{\partial\theta}$ with x and y-coordinates

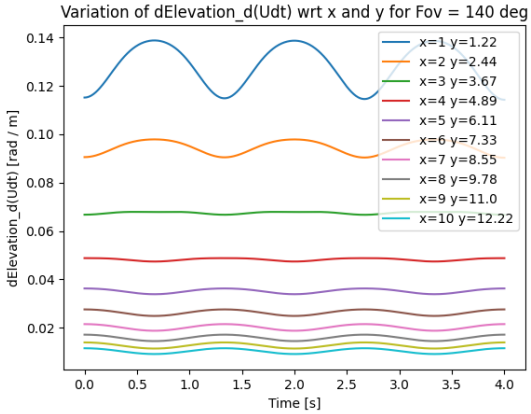

(c) Figure showing the variation of $\frac{\partial Ele}{\partial(udt)}$ with x and y-coordinates

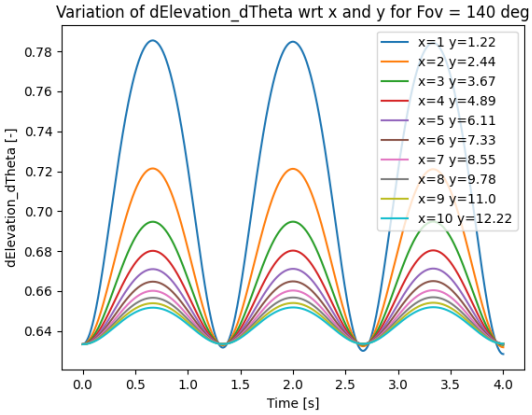

(d) Figure showing the variation of $\frac{\partial Ele}{\partial\theta}$ with x and y-coordinates

Figure 3.4: Figure showing the variation of the partial derivatives of the Azimuth and Elevation angles with x and y-coordinates

As can be seen in Figure 3.4 , the value of the partial derivatives goes to zero as the distance between the observer and the object increases. As such, if one was to average the values of the partial derivatives for all the positions, the main contribution to the final value would be from the positions closest to the observer. Since the contributions of these points are what the observer will actually be able to notice or perceive, their values can be considered a good representation of what the ”flow” is like for any particular viewing angle. Therefore, going forward, whenever the value of a partial derivative of a particular angle is mentioned, the reader can assume that this means that the value is the average value of all points that lie on that viewing angle, with the points closest to the observer having the most effect.

The procedure stated above can then be done for a wide range of FoV values to see how the partial derivatives change for points that are on the edge of the particular FoV. This is visualised in Figure 3.5:

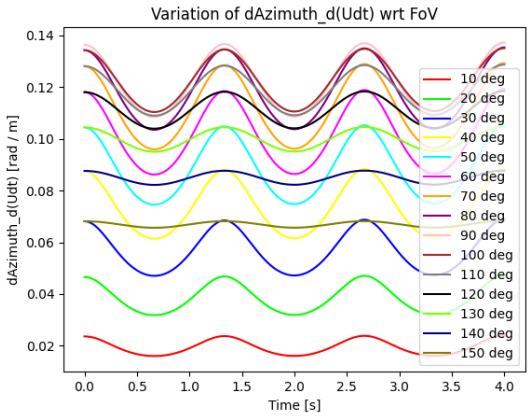

(a) Figure showing the variation of $\frac{\partial Az}{\partial(udt)}$ with FoV

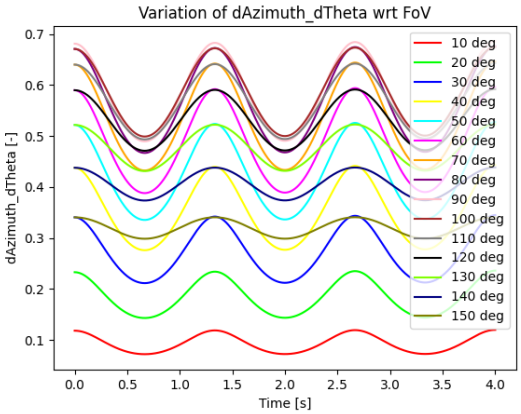

(b) Figure showing the variation of $\frac{\partial Az}{\partial \theta}$ with FoV

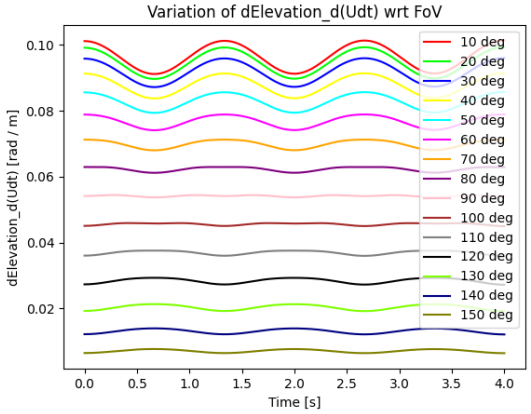

(c) Figure showing the variation of $\frac{\partial Ele}{\partial(udt)}$ with FoV

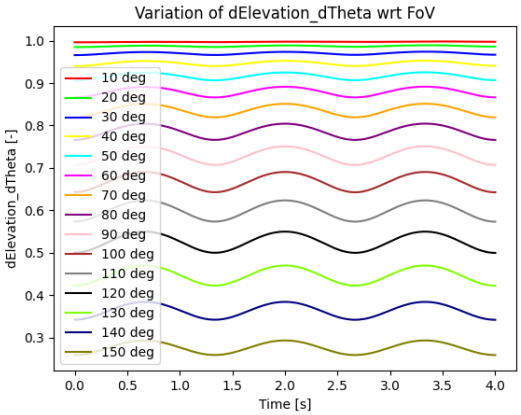

(d) Figure showing the variation of $\frac{\partial Ele}{\partial \theta}$ with FoV

Figure 3.5: Figure showing the variation of the partial derivatives of the Azimuth and the Elevation angles with FoV

As can be seen from Figure 3.5a and Figure 3.5b, the values of the partial derivatives for the Azimuth angle on the edge of the pilot's vision increases as the FoV increases up to 90 [°]. After this however, the value of the partial derivative starts to decrease. This is in stark contrast to the value of the partial derivatives for the Elevation angle, which decrease as the FoV increases. This trend is visualised in Figure 3.6:

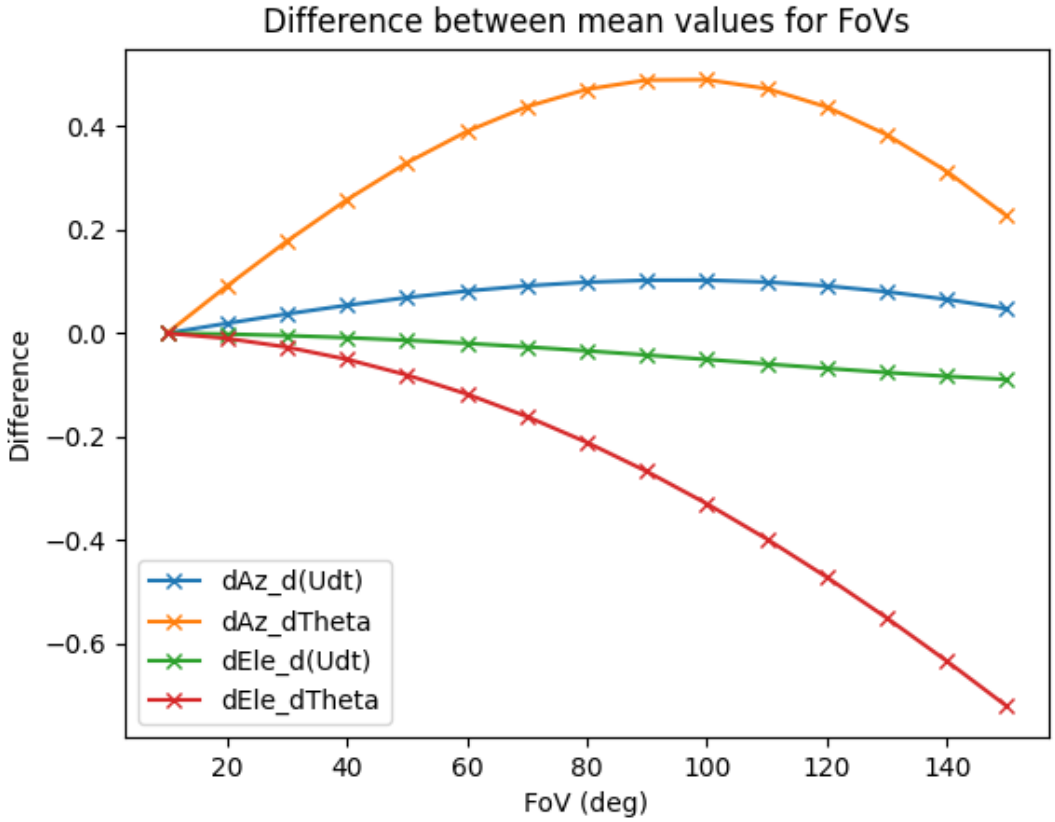

Figure 3.6: Figure showing the behaviour of the partial derivatives with respect to FoV

Figure 3.6 plots the difference between the values obtained for a particular FoV and the first value (i.e. the value for $FoV = 10[°]$). The results from Figure 3.5a, Figure 3.5b and Figure 3.6 seem to suggest that the point with the most movement in the azimuth direction, is at a horizontal viewing angle of around 90 $[°]$ from the observer. As the FoV decreases, this point would get clipped out and the next most informative point would then be on the edge of the observer's FoV. For the most informative point in terms of the elevation angle, the analysis seems to suggest that this exists right in front of the observer (i.e. at a horizontal viewing angle of 0 [°]).

To confirm these observations, one can do a grid search to find where the points with the greatest value of the derivatives are. The grid search consisted of creating points at an x-distance of between 1 [m] and 10 [m] from the observer, with 0.1 [m] increments between them. The height of the points (i.e. the z-coordinate) was set to -5 [m] which indicates that the observer is hovering 5 [m] off the ground and is looking at the ground. The y-coordinates of the points are then simply those that are visible to the observer for the particular FoV. The number of points for each FoV tested are shown in Table 3.1:

Angle [°]	Number of Points
10	386
20	749
30	1125
40	1519
50	1935
60	2390
70	2894
80	3461
90	4147
100	4902
110	5866
120	7111
130	8798
140	11267
150	15289

Table 3.1: Table showing the number of points tested for each FoV

For each of these points, the values of the four derivatives were calculated and the point with the highest value was chosen as the most informative point for that derivative. This point was expressed as a horizontal viewing angle from the observer's eye. The results for the best viewing angle to discern $\frac{\partial Az}{\partial(udt))}$ and $\frac{\partial Az}{\partial \theta}$ are shown in Figure 3.7:

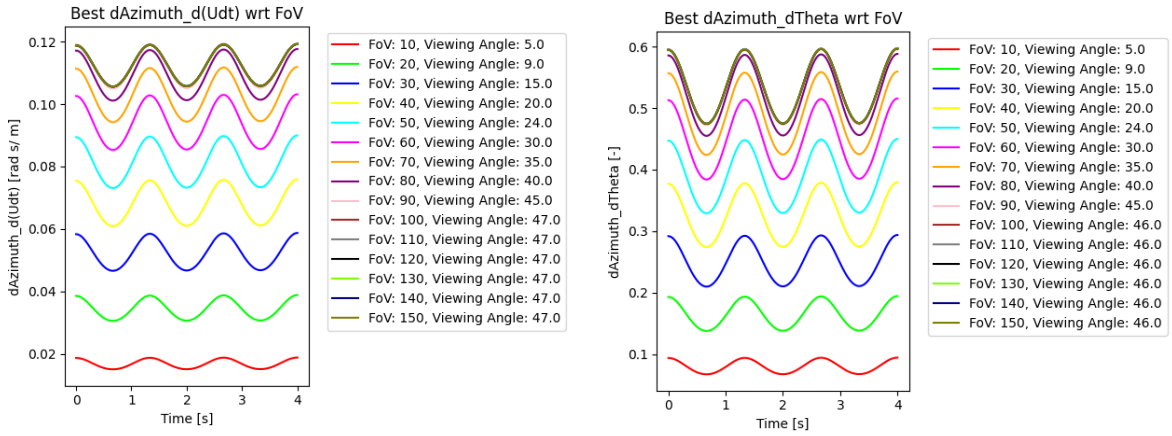

(a) Figure showing the variation of the highest value $\frac{\partial Az}{\partial(udt)}$ for the different FoVs

(b) Figure showing the variation of the highest value $\frac{\partial Az}{\partial \theta}$ for the different FoVs

Figure 3.7: Figure showing the variation of the highest value of partial derivatives of the Azimuth angle for the different FoVs

The viewing angles in Figure 3.7a and Figure 3.7b represent the angle from the centre of the pilot's vision, their right hand side. So, an angle of 10 [°] means the point is at a 10 [°] angle to the right of the pilot's view. It is worth noting that a point at the same angle on the left hand side will also have the same value of the derivatives so it does not matter which side of the pilot's view is analysed. As can be seen from Figure 3.7, the best viewing angle to observe the change in azimuth angles due to the motion seem to lie on the edge of the pilot's FoV, for FoVs smaller than 90 [°]. For FoVs equal to and larger than 90 [°], the best point is found at a horizontal viewing angle of around 45-47 [°] left or right of the observer. This implies that the most informative point for the change in azimuth angle is located at around 45 [°] and thus, as the FoV becomes smaller, this point would get clipped out of view and the pilot would start losing information about the motion being carried out.

The results for the derivatives of the Elevation angle are given in Figure 3.8:

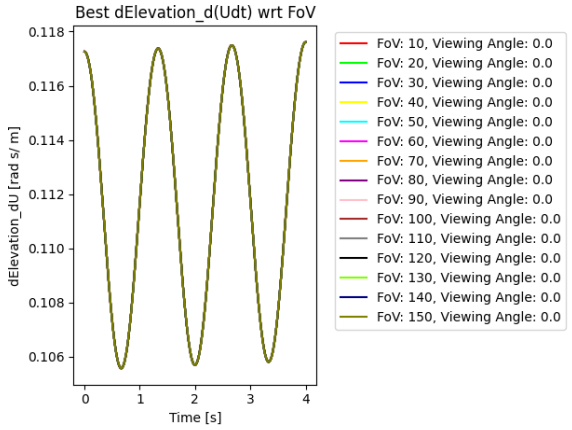

(a) Figure showing the variation of the highest value $\frac{\partial Ele}{\partial(udt)}$ for the different FoVs

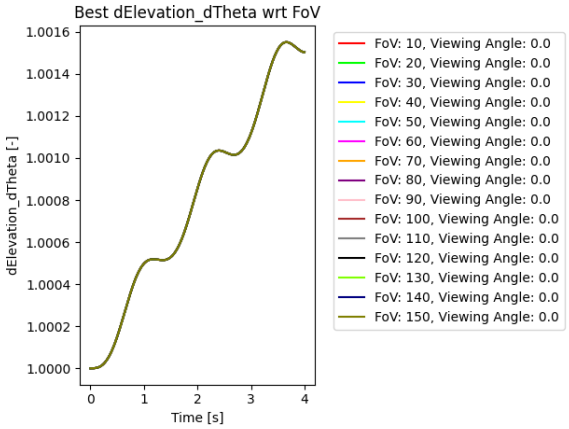

(b) Figure showing the variation of the highest value $\frac{\partial Ele}{\partial \theta}$ for the different FoVs

Figure 3.8: Figure showing the variation of the highest value of partial derivatives of the Elevation angle for the different FoVs

Figure 3.8a and Figure 3.8b seem to confirm the conclusions of the numerical analysis that the most informative point for detecting changes in the elevation angle, is indeed found right in front of the pilot.

These results can be used to draw the following conclusions:

1. As the FoV decreases from 90 [°], the pilot's perception of how the azimuth angle changes would worsen. As the FoV increases beyond 90 [°], the pilot's perception of how the azimuth angle changes would remain unaffected.
2. Changing FoV has no impact on how the pilot perceives the change in elevation angles.

As Figure 3.7 show, the change in azimuth angles due to the distance moved is greater than that for a change in pitch, while the opposite is true for the change in elevation angles. This means that for a motion where there is both pitch and forward translation, one will perceive a change in both azimuth and elevation angles and so, they are likely to be affected by any changes in FoV as per the first conclusion above). Conversely, if there is only pitching motion, then the pilot will perceive mostly elevation angle changes and they may not be affected by changing FoVs. The biggest question mark with all these observations however is the level of impact it will have on the pilot perception. While the numbers conclude that, e.g., the change in azimuth angle with respect to forward motion is 10 times larger for an FoV of 90 [°] as compared to an FoV of 10 [°], it is still unknown if that will result in a large change in performance for the pilot. That makes the experiments even more important, as they will help to contextualise the impact of the values of these partial derivatives on what the pilot can actually perceive.
Keeping all of this in mind, the following hypotheses have been formulated:

1. **H1:** If a helicopter has both pitching and forward motion, decreasing the FoV to below 90 [°] should lower a pilot's performance significantly.
2. **H2:** If a helicopter has both pitching and forward motion, increasing the FoV to above 90 [°] should have no significant effects on a pilot's performance
3. **H3**: If a helicopter has only pitching motion, changing the FoV should have no significant effect on a pilot's performance.

This page is intentionally left blank.

4

Experiment Methodology

The goal of this chapter is to detail all the important aspects of the experiments that will be done to test the hypotheses created in Chapter 3. The basic information about the experiment can be found in section 4.1 while details about the dynamics of the helicopter in the simulation can be found in section 4.2. Information about the forcing function is presented in section 4.3 and, lastly, information about the setup of the experimental equipment is found in section 4.4.

4.1. Experiment Basics

Following on from the conclusions of Chapter 3, the three hypotheses need to be proven or dis-proven based on a series of practical experiments. Since the analysis focuses only on the pitching and forward velocity of the helicopter, the experiments should be set up, such that these are the only two degrees-of-freedom allowed. Additionally, since hypothesis **H3** concerns only the pitching motion, one set of experimental conditions should have only one degree-of-freedom i.e. just the pitching.
The first set of experimental conditions (aka the Velocity Disturbance Rejection Task) will involve pilots having to do a disturbance rejection task with changing FoVs. This means that, for each FoV tested, the pilot's job is to keep the velocity of the helicopter zero, in the presence of a forcing function. This forcing function will only affect the velocity of the helicopter. The second set of experimental conditions (aka the Pitch Disturbance Rejection Task) will also be a disturbance rejection task, except this time the forcing function will affect only the pitch of the helicopter. Additionally, the velocity of the helicopter will be kept zero throughout the whole run for this task. These two sets of experimental conditions should be sufficient to prove or dis-prove the hypotheses outlined in Chapter 3.

The first thing to decide is which FoVs should be tested in the experiment phase of this project. The results of Chapter 3 show that a FoV of 90 [°] needs to be included in the experiment, and that the experiments should revolve around seeing if performance is gained or lost for FoVs that are not 90 [°]. However, the analysis did not reveal specific values of FoV larger than or smaller than 90 [°] that would be worth looking at. Therefore, it is worth looking at what FoVs were tested in previous such experiments, as is detailed in Chapter 2, and use those to build up the experiment matrix. This, of course, has to be done by keeping the limits of the Pimax 8K headset in mind and, as such, the maximum horizontal and vertical FoV that can be achieved are 140 ° and 102 ° respectively [30].

Keeping all of these factors in mind, the FoVs chosen to be tested are:

- 20 [°] : This is to see if performance does degrade drastically per the analysis of Chapter 3 and the findings of Pretto et al and Kenyon et al [10] [11]
- 30[°]: This is considered the minimum FoV needed to perceive the rotations efficiently according to the literature studied [10][11].
- 60 [°]: This is considered to be the optimal FoV needed to perceive forward velocities efficiently in literature [11].
- 90 [°]: This is per the results of Chapter 3.

- 120 [°]: Literature seems to conclude that the gain in performance is minimal between 60 [°] and 120 [°] but the analysis suggests that the performance should improve until 90 [°]. Thus, it is worth testing this FoV
- 140[°]: This is the max FoV of the Pimax in normal viewing mode and this high FoV is the unique-selling-point of the Pimax. Thus, it is worth testing to see if there is indeed any benefit to having such a large FoV.

These FoVs will be used for the Velocity Disturbance Rejection Task. For the Pitch Disturbance Rejection Task, while the same FoVs can be used, it would be more efficient to test fewer FoVs. The reason for this is two-fold; Firstly, the analysis done in Chapter 3 suggests that the performance of the pilot will remain the same for all of the listed FoVs since the most informative point will always be visible to them. Secondly, to get useful results and to get rid of errors, one would need to test each FoV at least twice, per participant. With six FoVs to test for each type of control task, each participant would have to do 24 runs in total. This can be very time-consuming and very tiring for the potential participants.
Thus, it was decided that the Pitch Disturbance Rejection Task should only have two FoVs to test; **20 [°]** and **140 [°]**. This means that, if the hypothesis is indeed correct, one should see no change in the pilot performance for the narrowest and the widest FoV and that is enough to prove the hypothesis correct. This would also then save the participants' time and energy

4.2. Model structure

The proposed structure for the Velocity Disturbance Rejection Task consists of two loops; an inner loop and an outer loop. This is a common cascade model for pilot control and is shown in Figure 4.1[29]:

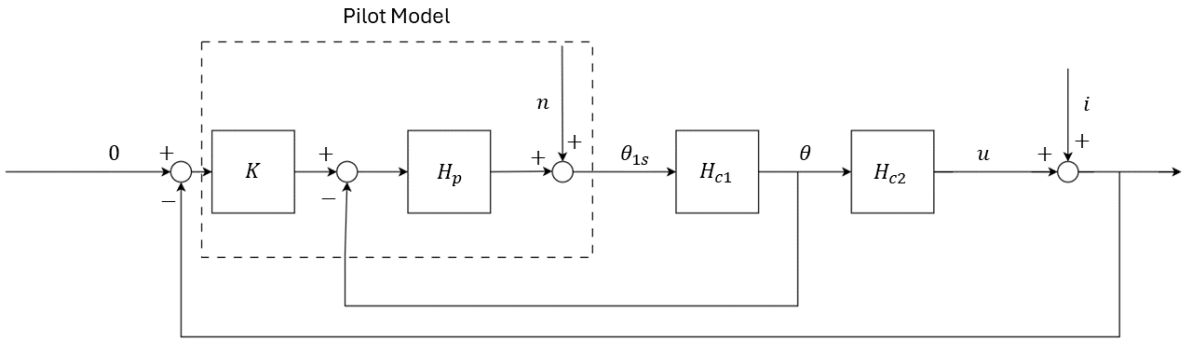

Figure 4.1: Figure showing the proposed structure for the Velocity Disturbance Rejection Task

As can be seen in Figure 4.1, the inner loop consists of the pilot changing the longitudinal cyclic input, θ_{1s} such that there is a change in the helicopter pitch angle, θ. The outer loop is then the surge velocity, u being changed due to the change in θ. This velocity is then compounded with the disturbance function, i which represents wind acting on the helicopter during its near-ground hover maneuver. The pilot model, shown in the dashed box, consists of a simple gain for the outer loop and a transfer function, H_p for the inner loop [29]. Additionally, there is also the pilot remnant, n that must be added into the pilot model. This remnant accounts for the control inputs made that are uncorrelated with any visual cues received by the pilot throughout the experiment [23].
The blocks H_{c1} and H_{c2} represent the controlled element dynamics and they can be evaluated using

the helicopter dynamics model. Starting from the general state-space system:

$$\dot{x}(t) = A\mathbf{x}(t) + B\mathbf{u}(t) \tag{4.1}$$

where

$$\begin{aligned} \mathbf{x} &= \{u, w, q, \theta, v, p, \phi, r, \psi\} \\ \mathbf{u} &= \{\theta_0, \theta_{1s}, \theta_{1c}, \theta_{0T}\} \end{aligned} \tag{4.2}$$

with the following form for the A and B matrices:

$$\mathbf{A} = \begin{bmatrix} X_u & X_w - Q_e & X_q - W_e & -g\cos\Theta_e & X_v + R_e & X_p & 0 & X_r + V_e \\ Z_u + Q_e & Z_w & Z_q + U_e & -g\cos\Phi_e\sin\Theta_e & Z_v - P_e & Z_p - V_e & -g\sin\Phi_e\cos\Theta_e & Z_r \\ M_u & M_w & M_q & 0 & M_v & \begin{matrix} M_p - 2P_e I_{xz} I_{yy} \\ -R_e\left(I_{xx} - I_{zz}\right) I_{yy} \end{matrix} & 0 & \begin{matrix} M_r + 2R_e I_{xz} I_{yy} \\ -P_e\left(I_{xx} - I_{zz}\right) I_{yy} \end{matrix} \\ 0 & 0 & \cos\Phi_e & 0 & 0 & 0 & -\Omega_a\cos\Theta_e & \sin\Phi_e \\ Y_u - R_e & Y_w + P_e & Y_q & -g\sin\Phi_e\sin\Theta_e & Y_v & Y_p + W_e & -g\cos\Phi_e\cos\Theta_e & Y_r + U_e \\ L'_u & L'_w & L'_q + k_1 P_e - k_2 R_e & 0 & L'_v & L'_p + k_1 Q_e & 0 & L'_r + k_2 Q_e \\ 0 & 0 & \sin\Phi_e\tan\Theta_e & \Omega_a\sec\Theta_e & 0 & 1 & 0 & \cos\Phi_e\tan\sin\Theta_e \\ N'_u & N'_w & N'_q - k_1 R_e - k_3 P_e & 0 & N'_v & N'_p + k_3 Q_e & 0 & N'_r + k_1 Q_e \end{bmatrix} \tag{4.3}$$

$$\mathbf{B} = \begin{bmatrix} X_{\theta_0} & X_{\theta_{1s}} & X_{\theta_{1c}} & X_{\theta_{0T}} \\ Z_{\theta_0} & Z_{\theta_{1s}} & Z_{\theta_{1c}} & Z_{\theta_{0T}} \\ M_{\theta_0} & M_{\theta_{1s}} & M_{\theta_{1c}} & M_{\theta_{0T}} \\ 0 & 0 & 0 & 0 \\ Y_{\theta_0} & Y_{\theta_{1s}} & Y_{\theta_{1c}} & Y_{\theta_{0T}} \\ L'_{\theta_0} & L'_{\theta_{1s}} & L'_{\theta_{1c}} & L'_{\theta_{0T}} \\ 0 & 0 & 0 & 0 \\ N'_{\theta_0} & N_{\theta_{1s}} & N'_{\theta_{1c}} & N'_{\theta_{0T}} \end{bmatrix} \tag{4.4}$$

One has to reduce them such that they represent the helicopter during hover and are expressed in terms of the relevant control input (i.e. θ_{1s}). For hover, the translational (U_e, V_e, W_e) and angular (P_e, Q_e, R_e) velocities are equal to 0. Furthermore, since the analysis is only for a system with two degrees of freedom (pitch and surge), the height is kept fixed. Lastly, the small angle approximation is used for the attitude angles. All of this results in the following longitudinal state equation for the helicopter response to a cyclic pitch input from a trimmed hover:

$$\begin{bmatrix} \dot{u} \\ \dot{w} \\ \dot{q} \\ \dot{\theta} \end{bmatrix} = \begin{bmatrix} X_u & X_w & X_q & -g \\ Z_u & Z_w & Z_q & -g\Theta_e \\ M_u & M_w & M_q & 0 \\ 0 & 0 & 1 & 0 \end{bmatrix} \begin{bmatrix} u \\ w \\ q \\ \theta \end{bmatrix} + \begin{bmatrix} X_{\theta_{1s}} \\ Z_{\theta_{1s}} \\ M_{\theta_{1s}} \\ 0 \end{bmatrix} [\theta_{1s}] \tag{4.5}$$

To derive the relevant equations for the controlled element dynamics, two further assumptions must be made. Firstly, since the height is fixed throughout the experiment and the fact that the contribution of the vertical velocity to the longitudinal motion is minimal, the second row of Equation 4.5 can be assumed to be zero. Secondly, it is assumed that the contribution of $X_q q$ is significantly smaller than that of $X_u u$, so $X_q q$ is set to zero. What this means in practical terms is that the forward acceleration caused by the pitch rate is much smaller than the forward acceleration caused by the surge velocity and thus, it can be ignored completely [28]. Using these assumptions, one can derive the following equations of motion:

$$\begin{aligned} \dot{u} - X_u u + g\theta &= X_{\theta_{1s}}\theta_{1s} \\ \dot{q} - M_u u - M_q q &= M_{\theta_{1s}}\theta_{1s} \\ \dot{\theta} &= q \end{aligned} \tag{4.6}$$

The first part of the controlled element dynamics to analyse is the relation between θ_{1s} and θ. This is done by assuming the surge velocity to be 0 for hover:

$$\begin{aligned} u &= 0 \\ \dot{q} - M_q q &= M_{\theta_{1s}}\theta_{1s} \\ \dot{\theta} &= q \end{aligned} \tag{4.7}$$

substituting the third equation into the second gives:

$$\ddot{\theta} - M_q\dot{\theta} = M_{\theta_{1s}}\theta_{1s} \tag{4.8}$$

Taking the Laplace transform of this and rearranging shows the form of H_{c1}:

$$\frac{\Theta(s)}{\Theta_{1s}(s)} = H_{c1} = \frac{M_{\theta_{1s}}}{s\,(s - M_q)} \tag{4.9}$$

The moment derivatives $M_{\theta_{1s}}$ and M_q represent how the pitching moment changes as a result of the longitudinal cyclic input and pitch rate respectively. Using data for the DRA (RAE) research Lynx helicopter, illustrated in Figure 4.2, the values of the derivatives are found to be **26.4** [$1/s^2$] for $M_{\theta_{1s}}$ and **-1.8955** [1/s] for M_q respectively [28].

Figure 4.2: Figure showing the DRA (RAE) research Lynx Helicopter [31]

The reason why this particular helicopter is chosen is due to the fact that it has been used extensively for flight tests by the British Royal Airforce (RAF) and the National Aeronautics and Space Administration (NASA), and has been used to calibrate agility standards of its successors [28]. This means that this helicopter is well suited for this research.
As is evident from Equation 4.9, the pilot will need to control a double integrator system for the inner loop. As McRuer et al have shown, this is quite a challenge for highly trained pilots and, since it is expected that the participants for the experiments for this project will not be highly trained pilots, it will be exceptionally difficult for the potential test subjects of this project [20]. Thus, it was decided to simplify the model to an integrator to facilitate the participants, i.e.

$$\frac{\Theta(s)}{\Theta_{1s}(s)} = H_{c1} = \frac{M_{\theta_{1s}}}{s} \tag{4.10}$$

To derive the relationship between θ and u, i.e. H_{c2}, one needs to use the first equation of Equation 4.6. Here, θ_{1s} will be substituted such that it is expressed in terms of θ and this will be done by analysing the steady state behaviour of Equation 4.9. This serves as a nice balance between the simplified version of H_{c1} used here and the actual behaviour of the system. Using the Final Value Theorem, the steady state behaviour of H_{c1} is found to be:

$$\frac{\Theta(s)}{\Theta_{1s}(s)}ss = H_{c1_{ss}} = \frac{-M_{\theta_{1s}}}{M_q} \tag{4.11}$$

Substituting this into the first equation in Equation 4.6 and taking the Laplace transform gives:

$$sU(s) - X_uU(s) + g\Theta(s) = \frac{-X_{\theta_{1s}}M_q}{M_{\theta_{1s}}}\Theta(s) \tag{4.12}$$

Rearranging this gives the form of H_{c2}:

$$\frac{U(s)}{\Theta(s)} = \frac{\frac{-X_{\theta_{1s}} M_q}{M_{\theta_{1s}}} - g}{s - X_u} \tag{4.13}$$

The values of $X_{\theta_{1s}}$ and X_u are **-9.280** $[m/s^2 rad]$ and **-0.02** [1/s] respectively [28]. The helicopter's position can then be calculated by integrating the velocity.
The values and units of all the model parameters are summarised in Table 4.1

Table 4.1: Table showing the parameters of the helicopter model

Parameter	Value	Unit
$M_{\theta_{1s}}$	26.40	$1/s^2$
M_q	-1.896	1/s
$X_{\theta_{1s}}$	-9.280	$m/s^2 rad$
X_u	-0.020	1/s

For the Pitch Disturbance Rejection Task, since there is only one degree-of-freedom, the structure will only contain one loop. This is illustrated in Figure 4.3:

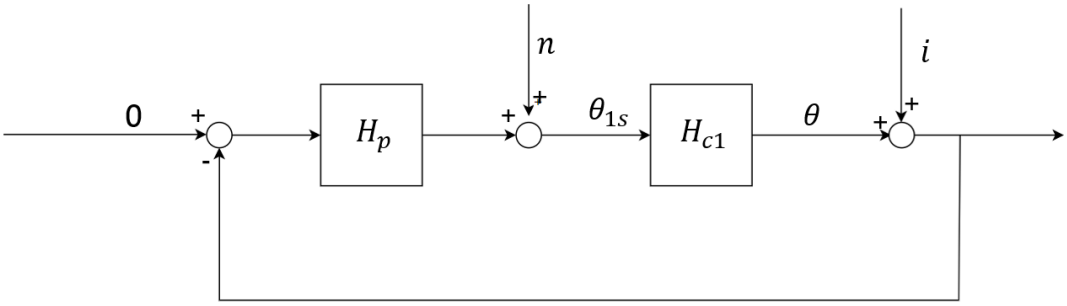

Figure 4.3: Figure showing the proposed structure for the Pitch Disturbance Rejection Task

The dynamics of H_{c1} are identical to those in Equation 4.10

4.3. Forcing Function

The forcing function is applied to the dynamics of the helicopter model to simulate the disturbance that the pilot has to correct. It has to appear random to the pilot such that the pilot is not able to predict the behaviour of the signal. If the pilot were to accurately predict what the signal is doing, they would change their behaviour to anticipate the signal and thus, they would no longer be doing a compensatory tracking task [14]. Additionally, the forcing function has to be repeatable such that identical tasks can be performed repeatedly. In this case, the disturbance acting on the helicopter is simulating the turbulence that the helicopter would experience due to its low altitude and proximity to other objects. Such turbulence consists of sharp "gusts" being dispersed throughout the course of the flight as a result of the wakes generated by the helicopter interacting with the ground and nearby objects.
To model such turbulence, the forcing function can be generated according to Equation 4.14:

$$f(t) = \sum_{k=1}^{N_t} A_t(k) \sin\left(\omega_t(k)t + \phi_t(k)\right) \tag{4.14}$$

As can be seen from Equation 4.14, the forcing function is a sum of N_t sinusoids with $A_t(k)$, $\omega_t(k)$ and $\phi_t(k)$ being the amplitude, frequency and phase of the kth sinusoid [32]. The frequencies of the

sinusoids, ω_t, have to be in a certain range such that pilot is constantly exhibiting closed loop control [14]. If the frequency is too high, the pilot will not have enough time to change the position or attitude significantly and will thus, ignore the disturbances. If the frequency is too low, then the pilot will not be sufficiently challenged. One method of choosing ω_t is to find the measurement time base frequency which is given by:

$$\omega_m = \frac{2\pi}{T_m} \tag{4.15}$$

where T_m is the measurement time of one experimental run. For this experiment, the measurement time was 120 [s]. The frequency of the sinusoids can then be integer multiples of ω_m i.e [32] [33]:

$$\omega_t(k) = n_k \omega_m \tag{4.16}$$

Lastly, the values of a particular ω_t must not be a harmonic frequency of another ω_t [34].
The amplitude of the sinusoids, A_t, should be large enough to displace the helicopter significantly but it should not be too large that the pilot needs very large control inputs (which would violate the linear approximation of the helicopter dynamics) [14]. For this, one can simply use a shelf for the amplitudes, where signals with a frequency higher than the bandwidth frequency have one-tenth the power of those lower than the bandwidth [34].
The final variable to determine is the phase of the sinusoids, ϕ_t. This can be done by creating a random set of phases and choosing those that result in the forcing function signal having a probability closest to a Gaussian distribution [33]. The phases chosen should be such that the final signal does not have any excessive peaks of velocity (for the velocity forcing function) and pitch angle (for the pitch forcing function). For this project, the relevant parameters of Equation 4.14 for the velocity and pitch forcing functions are given by Table 4.2 and Table 4.3 respectively:

Table 4.2: Table showing the values of the parameters for the velocity forcing function

n_k	$\omega_t(k)$ [rad/s]	$A_t(k)$ [m/s]	$\phi_t(k)$ [rad]
3	0.15708	1	-1.57658
7	0.36652	1	5.66384
11	0.57596	1	2.91532
17	0.89012	0.1	1.23978
23	1.20428	0.1	-4.32260
37	1.93732	0.1	-4.32290
51	2.67035	0.1	-5.55329
73	3.82227	0.1	4.60151
103	5.39307	0.1	1.27065
139	7.27802	0.1	2.61472

Table 4.3: Table showing the values of the parameters for the pitch forcing function

n_k	$\omega_t(k)$ [rad/s]	$A_t(k)$ [°]	$\phi_t(k)$ [rad]
2	0.10472	5	-1.04273
5	0.26179	5	2.768679
11	0.57596	5	-6.281748
23	1.20428	0.5	-2.483962
37	1.93732	0.5	-4.438996
51	2.67035	0.5	-5.122824
71	3.71756	0.5	-3.942570
83	4.34587	0.5	-1.940741
97	5.078908	0.5	-1.297258
137	7.173303	0.5	0.487785

The Velocity and Pitch forcing functions are visualised in Figure 4.4a and Figure 4.4b respectively:

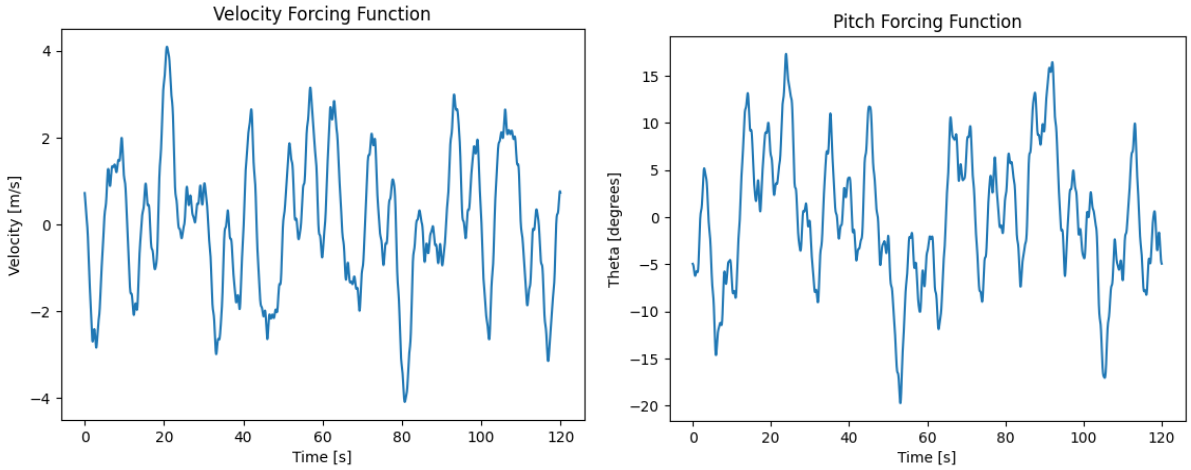

(a) Figure showing the Velocity forcing function

(b) Figure showing the Pitch forcing function

Figure 4.4: Figure showing the Velocity and Pitch Forcing Functions

4.4. Experimental setup

The experimental setup and method detailed in this section were all presented before the TU Delft Human Research Ethics Committee (HREC) to ensure that the experiments were done in an ethical manner. The experiment application, under application number 4423, was approved by the HREC on the 15th of July 2024.

The experiment consists of participants using a joystick to control the pitch of the helicopter simulation to correct against the disturbance forcing function. The simulation itself was made in Unity and consists of a first-person view of a large, unending grass field. This field consists of a repeating grass texture that is used to provide the visual flow which is used by the participants to judge their velocity. A screenshot from the simulation is shown in Figure 4.5a:

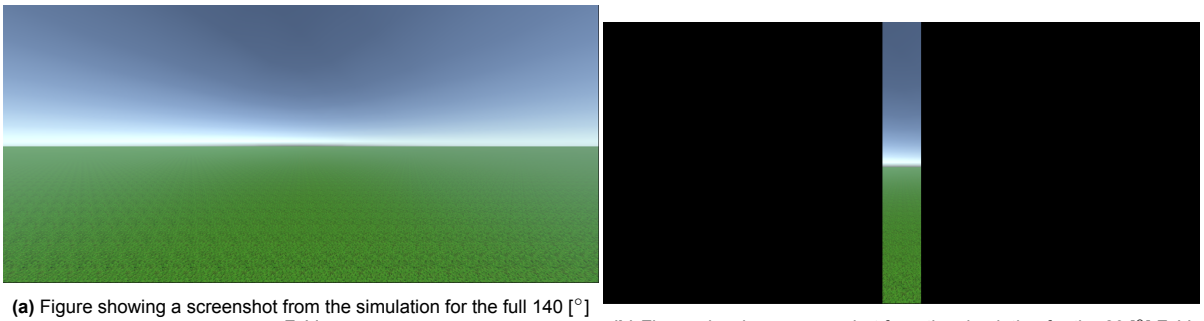

(a) Figure showing a screenshot from the simulation for the full 140 [°] FoV

(b) Figure showing a screenshot from the simulation for the 20 [°] FoV

Figure 4.5: Figure showing two screenshots from the simulation; one for and FoV of 140 [°] and one for an FoV of [°]

Figure 4.5b shows the view for the 20 [°] FoV condition. As stated previously, the FoV was changed by adding black bars to the peripheries of the Camera object in Unity to block off the scenery that would not be visible from the chosen FoV. For the Pitch Disturbance Rejection Task, the participants were also shown a reticle and a horizon line that allowed them to judge how their pitch changed. This is shown in Figure 4.6

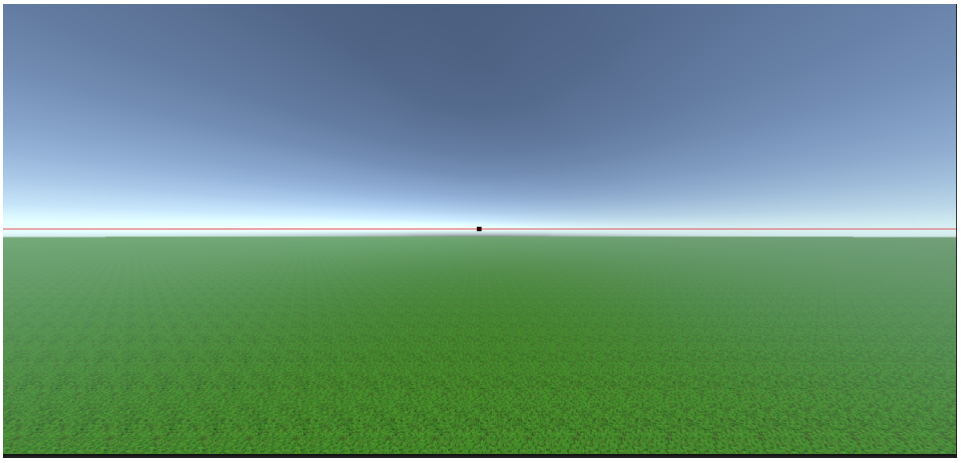

Figure 4.6: Figure showing the pitch indicator reticle and the horizon line used for the pitch disturbance rejection task

Note, the reticle and the horizon line shown in Figure 4.6 look very small in this view, but are actually bigger when viewed through the VR headset. The simulation is viewed through the Pimax 8KX VR headset. The tracking for the headset is done using two Valve Index Base Stations which allow all the VR software to know exactly what the orientation and position of the headset is. Both these components are pictured in Figure 4.7a and Figure 4.7b:

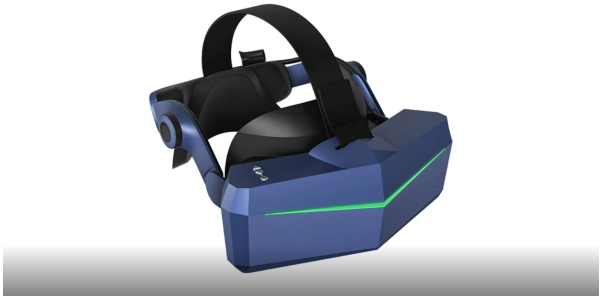

(a) Figure showing the Pimax 8KX VR headset [35]

(b) Figure showing the base station used to track the VR headset [36]

Figure 4.7: Figure showing the Pimax 8KX VR headset and the accompanying base station

It is worth pointing out that the experiment was set up such that, if the participant moved their head, then the scenery would not move with them. Instead, their view would remain as them looking forward, with the grass and the horizon of Figure 4.5a. This was done to ensure that there would be no non-linearities in what each individual participant was seeing, which aims to simplify the analysis done. If there was head tracking, i.e. the scene moved as their head did, then it would be possible to enter a situation where some participants are not doing the same experiment as the others.
Before the experiment had begun, participants were allowed to spend some time adjusting the VR headset such that it sat comfortably on their heads and they had a good, comfortable view of the simulation visuals. Then, they were allowed to move the helicopter in the simulation with the joystick, just so they could get a feel of the dynamics. This was done such that the participants could get used to how sensitive the joystick was and how much they needed to pitch to get a certain velocity. Afterwards, the participants did a test run to get an idea of what the full experiment would be like. They were allowed to repeat the test runs multiple times until they were confident enough to begin the actual experiments. During the experiments, the participants would complete the disturbance rejection task for one of the FoVs and then, when it ends, they were shown an 11-point MIsery SCale (MISC). This was done to ensure that the participants were not suffering from any adverse effects which are common for VR headsets, like motion-sickness or excessive eye strain [37]. The scale that showed up in the simulation is shown in Figure 4.8

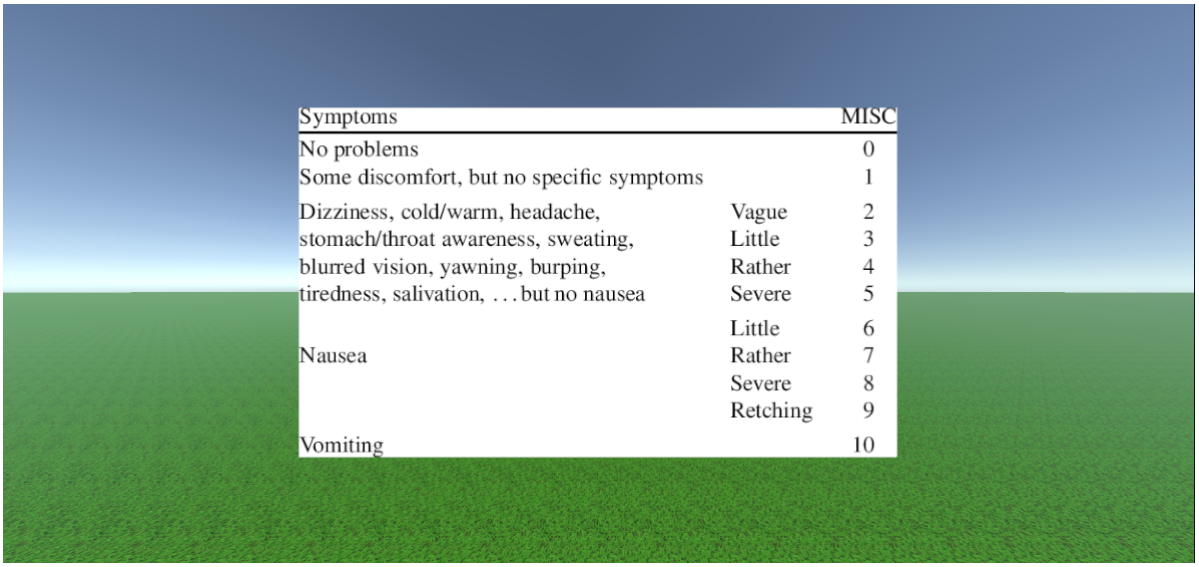

Figure 4.8: Figure showing the MISC scale as the participants would have seen it in the simulation [37]

The numbers on the right of the scale correspond to the symptoms on the left. If a participant indicated that the MISC score was anywhere in the 'nausea' category, the entire experiment would be immediately terminated and the necessary actions would be taken to get them feeling better. If this happens, the participant would no longer participate in the experiment. The procedure for this is explained in more detail in Appendix C

Since there are eight different conditions to test (six FoVs for the Velocity Disturbance Rejection Task and two for the Pitch Disturbance Rejection) and each condition is tested twice, the experiment was split up into four blocks. Each block consisted of four runs after which, the participant took the headset off and took a break for about five minutes. Of course they were free to take the headset off at any point and take a break if they felt like it. The repeat run of each FoV was carried out immediately after the first run so each block consisted of testing two FoV conditions twice. This simplified the experimental procedure but it does mean that there may be some training effects present in the final results. Since each FoV was only tested twice, it is assumed that the participants would not have had enough runs for the training effects to kick in but nonetheless, the presence of any training effects was checked for in the final results in Chapter 5. Additionally, since there are eight conditions to test, a minimum of eight participants were needed to ensure that order effects were not present within the experiment.

Each run consisted of a 30 [s] lead in time, followed by a 120 [s] measurement time. During each run, the participants' control inputs, the helicopter's velocity, the helicopter's pitch and the value of the forcing function at that time was being recorded by Unity. This data was then exported to be used for the analysis. Additionally, the participants were asked to indicate which part of the screen their vision was focused on. They were also asked to give general comments about how hard or easy they found the task to be, compared to the previously tested condition. After the experiment had concluded, participants were asked to give feedback on general aspects of the experiment, as well as how challenging they found the task overall.

This page is intentionally left blank.

5

Results and Discussion

In the end, thirteen people completed the full experiment and their data is used to draw up the conclusions. To accept or reject the hypotheses, one needs to analyse the results of the experiment to see if there is indeed any performance changes across the different testing conditions. The analysis done has a subjective and an objective component. The subjective analysis relies on using the comments gathered during the experiment to get an idea of what FoV the participants thought was the most suitable. Additionally, the participants' comments about where on the screen they were looking to get the visual cues, were used to try and understand how their behaviour changed for the different FoVs. The objective analysis was done by using the velocity and pitch data gathered in Unity to get an idea of how the pilot error changed with time. This was used as a measure of the pilot performance. Data on the pilot error for all the FoVs was then used to do a one-way Analysis of Variance (ANOVA) test and see if there was some significant difference in pilot performance for the different FoVs. If any significant difference was found, a post-hoc analysis would be done to see between which FoVs, the differences were found.

5.1. Subjective Results

Much like the objective results, the subjective results will be split into those for the velocity disturbance rejection task and the pitch disturbance rejection task. For the pitch disturbance rejection task, the participants claimed that they felt very little difference between the 20 [°] and 140 [°] FoV. The participants' attention was focused entirely on the reticle (shown in Figure 4.6) and the horizon line . This meant that they had no reason to look at the sides of the screen and thus, clipping those out of their view did not seem to affect the participants' behaviour. However, the participants did say that the 140 [°] view did feel more comfortable since the view looked normal and complete.

For the velocity disturbance rejection task, the participants stated that they were mostly focused on the ground texture slightly to the right of the middle of the screen. They claimed that they used this to get an idea of their velocity and would often look up at the horizon to get an idea of their pitch. This trend was present for every participant and for every FoV they tested. As the FoV increased, most participants stated that they found the view more comfortable, yet they found the system harder to control. The participants claim that they felt like they were moving faster for any given input when the FoV was larger hence they felt like the velocity was much harder to bring to zero. A few participants did express the opposite opinion though, where they stated that the higher FoVs were more distracting, due to extra activity in their peripheral vision, and thus it felt harder to focus on the task. These participants however were in the minority. Lastly, the participants stated that, when they pitched up, the ground was harder to see and they often had to pitch down again immediately afterwards. This meant that they found it harder to track parts of the forcing function that forced them to pitch up

5.2. Objective Results

As stated before, each participant tested every condition twice. The output data for each run, for the velocity disturbance rejection task, consisted of the time traces of the forcing function velocity, the

velocity induced due to control inputs and the overall velocity of the helicopter. The forcing function and control input velocity were used to get a visual indication of how the run had gone for the participant, and was used merely as a debugging tool to ensure no errors had occurred in the data-logging procedure. The overall velocity of the helicopter was used to get the Root-Mean Squared Error (RMSE), as shown in Equation 5.1

$$RMSE = \sqrt{\sum_{i=1}^{n} \frac{(0 - v_i)^2}{n}} \tag{5.1}$$

where v_i is the overall velocity at each time-step and n is the number of data-samples. Note, that the RMSE values for each run of a particular FoV condition was averaged to get the overall RMSE value for that FoV, for that participant. For the pitch disturbance rejection task, the output data was the forcing function pitch, the pitch induced by the control inputs and the total pitch angle. Again, the RMSE was used as the performance metric for this type of task. The mean RMSE values are then used to do an ANOVA analysis to see if there were any significant differences between the mean RMSE values for each FoV. If there are significant differences, then a post-hoc analysis can be done to see between which FoVs, the difference lies.
The general trend for the participants can be seen in the boxplots for the two tasks, which is shown in Figure 5.1

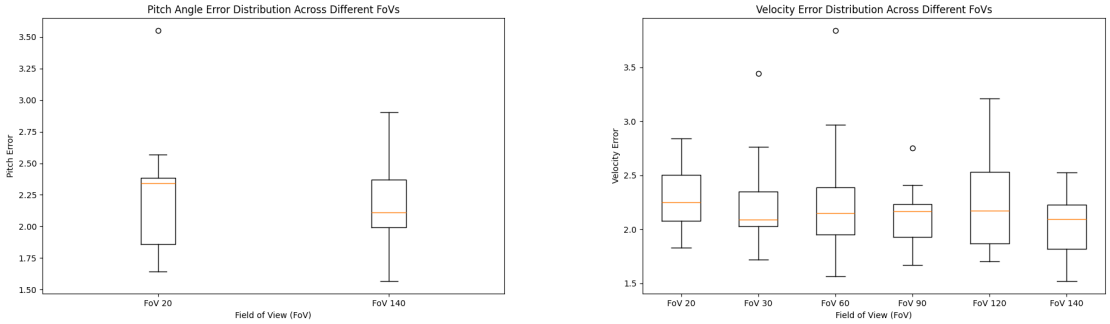

(a) Figure showing the boxplot for the pitch disturbance rejection task for all participants

(b) Figure showing the boxplot for the velocity disturbance rejection task for all participants

Figure 5.1: Figure showing the boxplots for the Pitch and velocity disturbance rejection tasks

As can be seen from Figure 5.1a, there does not seem to be much of a difference in performance for the two FoVs across all the participants. For the velocity disturbance rejection task, there does not seem to be a general trend either in performance across the FoVs for the participants. This can be backed up by looking at the results of the ANOVA analysis which are shown in Table 5.1

	Pitch Disturbance Rejection	Velocity Disturbance Rejection
df	5,7	5,7
F-statistic	0.2595	0.7879
p-value	0.6151	0.5617

Table 5.1: Table showing the results of the one-way ANOVA analysis for the two disturbance rejection tasks

5.3. Discussion

Based on the subjective results for the pitch disturbance rejection task, one can clearly see that the results match the theory outlined in Chapter 3. Because the participants were looking exclusively at the pitch indicator, they were already getting the maximum amount of feedback they could get for how the pitch was changing. As shown by the visual model of Chapter 3, the maximum amount of feedback on how the points in the world move is shown in the middle of the screen. The ANOVA analysis has a p-value that is greater than 0.05 which means that the results fail to reject the null hypothesis that there was a statistical difference between the pilot performance for the FoVs. Based on this data, it would

be unreasonable to conclude that changing FoV is likely to have an impact on pilot performance for the pitch disturbance rejection task. Despite this, participants did say that the wider FoV view felt more comfortable, despite the fact that it did not impact performance. This is consistent with the research done by Podzus et al, where they found that the pilots found the larger FoV of the Pimax headset much better than the Varjo headset [6]. This was despite the fact that the pilots found the outer areas of the Pimax's FoV rather blurry. Therefore, one can conclude that, in this context, the presence of a wider FoV had no greater impact than simply providing a more 'natural' and 'comfortable view of the world. This is especially true considering that the alternate view, the 20 [°] FoV, consisted of mostly a black screen with a small view in the centre.
Analysing the subjective results for the velocity disturbance rejection task, one can see some minor correlation between the theory of the visual model and the reality. As said previously in section 5.1, the participants felt like they were moving faster as they progressed from a smaller FoV to a larger FoV. This can be linked to the fact that, in general, the change in the azimuth angles with respect to pitch angle and the distance moved is generally larger for points on the peripheries. Additionally, just the fact that the observers are getting feedback from more points within in their vision as the FoV increases can also lead to this perception of faster motion. Additionally, while it would be useful to know between which FoVs this perception was the strongest, there was no clear consensus when all the subjective comments of the participants was analysed.
Unfortunately, the general trend for the velocity disturbance rejection task that was expected based on the hypotheses could not be proven with the objective results. As can be seen from Table 5.1 and Figure 5.1b, there is no significant trend between the RMSE and the FoV of the participants. This can be explained with the fact that, for any given input, the participant is seeing more feedback due to the pitch angle rather than velocity. To show this, the output of one experiment run was analysed. This was done for one of the participants whose results were deemed to not be outliers. Their run for the velocity disturbance rejection task for an FoV of 140 [°] is shown in Figure 5.2:

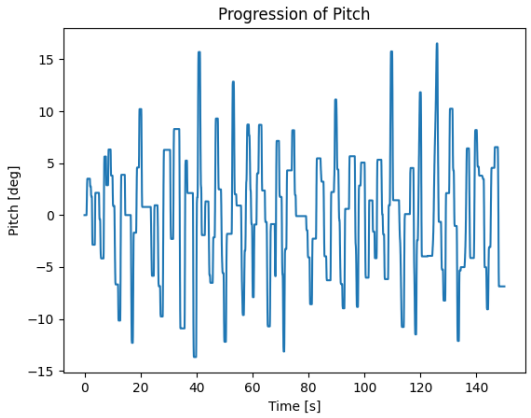

(a) Figure showing the variation of the helicopter pitch for the participant's run

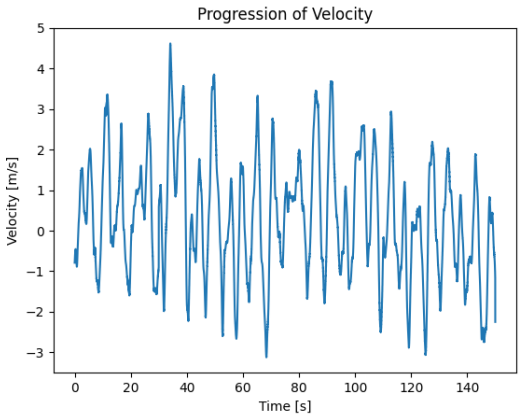

(b) Figure showing the variation of the helicopter velocity for the participant's run

Figure 5.2: Figure showing the variation of the participant's pitch angle and velocity for the chosen run

For this motion, the flow vectors were plotted for t = 35[s] to see how the flow looked for the pitch and the forward motion. This moment in time was chosen for the analysis, because at this moment, the helicopter had both a sufficiently high pitch and velocity such that the flow vectors for both pitch and velocity could be seen and compared. The actual flow resulting from both motions is shown in Figure 5.3a, the flow resulting from only the pitch is shown in Figure 5.3b and the flow resulting from only the velocity is shown in Figure 5.3c:

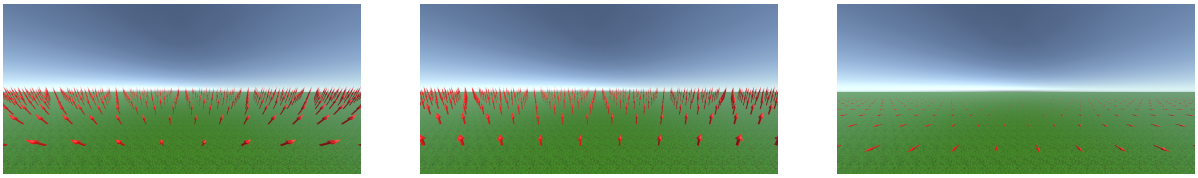

(a) Figure showing the flow for the participant's run at t = 35 [s], u = 2.64 [m/s], θ = -11 [$^\circ$] and $\dot{\theta}$ = 9.2 [$^\circ$/s]

(b) Figure showing the flow for the participant's run at t = 35 [s], u = 0.0 [m/s], θ = -11 [$^\circ$] and $\dot{\theta}$ = 9.2 [$^\circ$/s]

(c) Figure showing the flow for the participant's run at t = 35 [s], u = 2.64 [m/s], θ = 0 [$^\circ$] and $\dot{\theta}$ = 0 [$^\circ$/s]

Figure 5.3: Figure showing the flow for the participant's run

The full sized images are once again shown in Appendix B (Figure B.7 - B.9). As can be seen from Figure 5.3a, the flow is dominated mostly by the pitch rather than the forward motion. The forward motion is indeed easier to perceive towards the peripheries of the view, but it is still eclipsed by the flow due to pitch. Additionally, when one considers the flow shown in Figure 5.3c, it can be seen that the difference in the flow in the centre of the screen and the flow towards the edges of the screen, is not so easily discernible. This would lead to the conclusion that the participant is not getting significantly more information about their forward motion, and thus velocity, from their peripheries as compared to the centre of their vision. This is backed up by the comments made by some the participants. They claimed that the presence of a grass texture was enough of a velocity feedback that they did not feel like they needed to shift their gaze anywhere else to try and get more information about their velocity. Based on the pitch and velocity, the values of the partial derivatives of the Azimuth and Elevation angles can be calculated. The value of these derivatives with respect to θ will give an indication of how much of the motion seen was due to the change in pitch, and the derivatives with respect to (udt) will show that with respect to the forward motion. These values can be calculated for two separate viewing angles; where the participant should theoretically have been looking and where they were actually looking. The first set of derivatives was calculated for where the participant should have been looking i.e. **45 [$^\circ$] to the left or right**. Much like Figure 3.5, the values for the partial derivatives were calculated for all visible points that lie on this viewing angle, and their values were averaged. The results are shown in Figure 5.4b

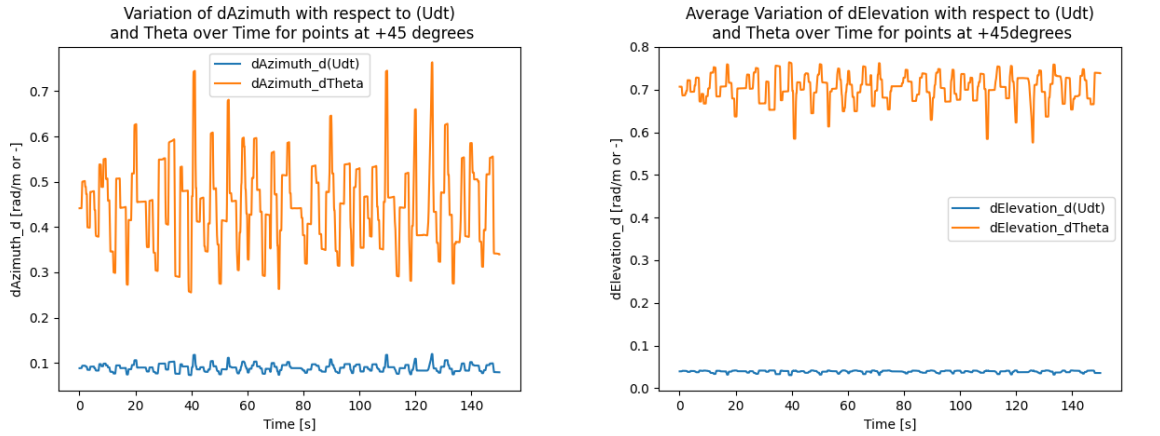

(a) Figure showing the value of the partial derivative of the Azimuth angle w.r.t θ and (udt) at an angle of 45 [$^\circ$]

(b) Figure showing the value of the partial derivative of the Elevation angle w.r.t θ and (udt) at an angle of 45 [$^\circ$]

Figure 5.4: Figure showing the value of the partial derivative of the Azimuth and Elevation angles w.r.t θ and (udt) at an angle of 45 [$^\circ$]

As can be seen from Figure 5.4a and Figure 5.4b, the magnitude of the movement caused due to the pitch angle is always magnitudes greater than that caused by the forward motion. This means that at every point on this viewing angle, the observer is likely just seeing more pitch movement than they are forward velocity movement. This is even more clear when one analyses the viewing angle where the participants were actually looking. This angle can be located from the subjective comments where all participants stated that, for the majority of the time, their gaze was focused solely on the ground texture

in front, and slightly to the right of them. Now since the participants' comments could not be used to pinpoint the exact viewing angle where their gaze was fixed, one needs to make a few assumptions. In general, the participants stated that they were always looking at the same general place regardless of the viewing angle; on the ground and slightly to the right. Since this did not change, even for the smallest FoVs, one can assume that this was at a viewing angle <= 10 [°] to the right. Therefore, one can analyse the ground points at a viewing angle of **7.5 [°] to the right** which means that the effective FoV analysed is 15 [°]. For this, the behaviour of the partial derivatives can be seen in Figure 5.5

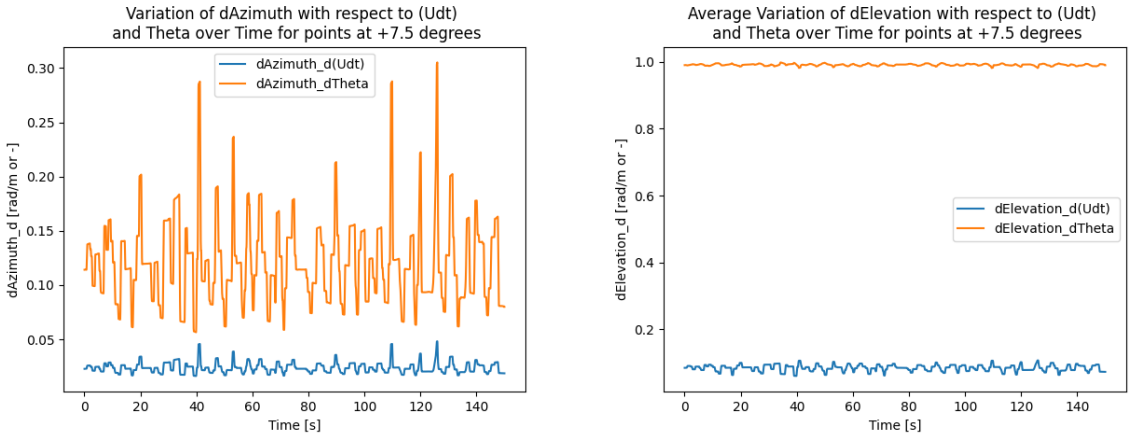

(a) Figure showing the value of the partial derivative of the Azimuth angle w.r.t θ and (udt) at an angle of 7.5 [°]

(b) Figure showing the value of the partial derivative of the Elevation angle w.r.t θ and (udt) at an angle of 7.5 [°]

Figure 5.5: Figure showing the value of the partial derivative of the Azimuth and Elevation angles w.r.t θ and (udt) at an angle of 7.5 [°]

Once again, as is shown by Figure 5.5, the values of the derivatives with respect to the pitch always remain higher. This means that even for this view, the observer sees more change due to pitch than the forward motion. Additionally, the fact that the values of the derivatives with respect to (udt) are so small means that, as the viewing angle changes from 7.5 [°] to 45 [°], the observer will find it hard to perceive any change in the value of $\frac{\partial Az}{\partial(udt)}$ or $\frac{\partial Ele}{\partial(udt)}$. This is further backed up by the lack of difference in visual flow, seen in Figure 5.3c, in the centre and the peripheries of the screen. Compare this to the value of $\frac{\partial Ele}{\partial\theta}$ for the two views, and it can seen in Figure 5.5b that the change in elevation angle with respect to pitch is always around 1. This means that the change in elevation angle perfectly matches the changes in pitch and this gives accurate information to the observer about how their pitch is indeed changing. It can thus be theorised that the reason why the participants were looking so close to the centre of the screen, was to get better feedback for how their pitch changed since the perceived feedback for their forward motion stays relatively the same throughout their vision. This means that the participant can get enough information about their velocity and motion from the centre of the screen, instead of looking at the peripheries (or at a viewing angle of 45 [°] right or left). Based on all of this, one can not accept Hypotheses **H1** and **H2**.

The last factor to consider in the experiments, is the potential training effect that could have crept in. This is an effect whereby the participants may end up getting better at doing the tasks, the longer the experiment goes on as they are getting more and more practice. This means that, the participants' performance may be better for the final few conditions tested and this may have no relation with what the condition was. To avoid this, an experiment matrix was created which ensured that each participant did the experiments in a unique order to the participants before them. This matrix is shown and explained in Appendix D. However, some participants did mention that they felt like they were getting better the more runs they did so it is still worth checking if this effect did in fact impact the results. To do this, the participants' run data was organised by run order and an ANOVA analysis was done to see if there was a significant difference between the runs done at the start of the experiment and the runs done at the end. The run-order performance and the boxplot for this, are shown in Figure 5.6a and Figure 5.6b respectively:

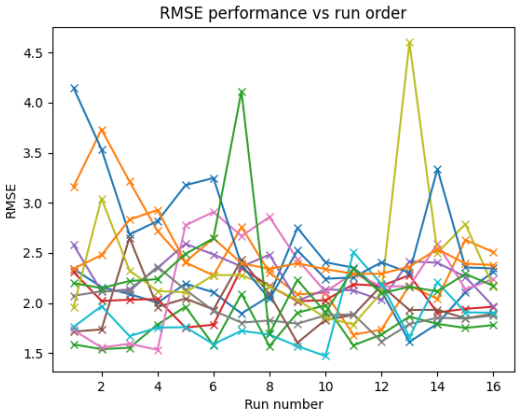

(a) Figure showing the RMSE with respect to the run order for all the participants

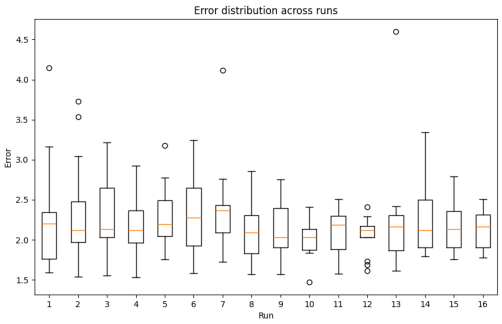

(b) Figure showing the boxplot for the run-order data for the participants

Figure 5.6: Figure showing the run order data and the boxplot for this run order data for all the participants

The ANOVA results show an F-statistic value of **0.6774** and a p-value of **0.8048**. Based on this and Figure 5.6b, it can be concluded that there is no significant trend between the run order and performance.

5.4. Recommendations

Based on the work done so far, one can outline a few recommendations that can help future researchers obtain more insight into the subject. The broad set of recommendations revolve around the idea that future experiments should be done to a higher fidelity than the one carried out in this project. The main aspect of this would be allowing more degrees-of-freedom in the helicopter, such that the pilot can control the pitch, yaw and roll of the helicopter. The reason why this might produce better results has to do with information found by previous researchers, and information given by a few of the participants of this experiment. Chung et al, during their research, asked pilots why they preferred a wider FoV when flying and the pilots stated that a wider FoV helped improve their perception of roll attitude control and longitudinal velocity [7]. This sentiment was backed up by a couple of the experiment participants, who have had some flight experience in either real helicopters or in helicopter simulators. They stated that, in a normal helicopter with six degrees-of-freedom, they would have used their peripheral vision to decouple their pitch rate from their forward velocity. In this experiment, with the simplified dynamics, that is no longer a factor and so, all they really need to see how fast they are going is any part of the ground texture. Therefore, it is recommend that any further experiments conducted allow for more degrees-of-freedom. Of course, this would require the participants to be trained pilots, or those with some flight experience, but this also opens up the opportunity to use some of the advanced subjective testing techniques mentioned in Chapter 2.

The second recommendation is to make use of the head-tracking provided by VR headsets such that the scenery of the simulation moves as the participant moves their head. As stated previously, in this experiment, the participants could only see the scenery present directly in front of them, no matter where they were looking. This was done to ensure that there were no non-linearities with the experiment setup and every participant was essentially doing the same experiment. However, as the subjective comments of the participants revealed, there were some issues associated with this setup. Firstly, whenever participants pitched up, they would often lose sight of the ground texture. In a normal setup with head tracking active, a participant would simply tilt their head downwards and regain sight of the ground, but this was not possible here. As a result, the participants would often pitch back down immediately afterwards to try and regain sight of the ground, making their tracking performance worse whenever they had to correct for a positive velocity disturbance. Additionally, some participants found it uncomfortable and disorientating whenever they moved their head, with the VR headset on, and the scenery did not move. Fortunately, this was mitigated if they kept their head very still throughout the entire run, but that was not always comfortable or natural for them to do. That is why it is recommended to enable head tracking for any future experiments on a similar topic.

The next recommendation is about understanding if the conclusions reached for the velocity disturbance rejection task are going to always be reached, or if they are a product of the experimental conditions used in this project. As was stated in section 5.3, the changes in velocity were completely drowned out by the changes in the pitch, which had a significant effect on the pilots' behaviour. This could have been a result of the fact that large changes in pitch were needed to obtain a change in velocity, which is a direct result of the dynamics of the helicopter and the velocity forcing function used. This means that if, for example, the forcing function or the helicopter dynamics were different, the pitch would no longer drown out the velocity feedback. Thus, it is worth investigating in the future if changing the experimental conditions, i.e. the dynamics or the forcing function, would result in pitch feedback not drowning out the velocity feedback, or if this will always be the case regardless of the experimental conditions. That would go a long way in further understanding the effect of FoV on a pilot's behaviour

The final recommendation has to do with the analysis done in Chapter 3. As was mentioned previously, the analysis focused on finding the most salient point in the view, and analysing what happens when this gets clipped out. However, one aspect that this analysis does not take into account is the simple fact that, as the FoV gets wider, the observer is getting information from a greater number of points. Indeed, this can be seen in Table 3.1, where the number of visible points on the ground increases drastically as the FoV increases. While the analysis of Chapter 3 shows that all of these points are not necessarily providing the *most* amount of feedback, it does not factor in the fact that they are still providing *some* feedback. Therefore, it is worth investigating in the future, how the increased number of points factors into the feedback one gets from the visual scene, and how it can be used to predict pilot performance.

This page is intentionally left blank.

6

Conclusion

The research objective for this thesis was to investigate how using VR headsets to perform visual cueing can affect the performance of helicopter pilots flying a helicopter simulation. While previous research has done a good job of documenting what changes in a pilot's perception and performance when they use VR headsets in the simulations, one large research gap still exists. This is, namely, an explanation of why these changes occur. Since VR headsets have a 360 [$^\circ$] Field of Regard (FoR) as compared to standard projection systems, they can mitigate any FoV restrictions that standard projection systems impose on a simulation. If these restrictions cause a large effect on the pilot performance, then VR headsets can be considered to be an upgrade from standard projection systems in this regard. That is why the scope of the research was narrowed to focus on how changing FoV can impact pilot performance. Previous research done into this topic revealed that restricting a pilot's FoV has a generally negative impact on their performance. As FoV is reduced, pilots see less activity in their peripheral vision, which can lead to them underestimating their forward velocity. This leads to them having a harder time in controlling their velocity and position, which can be an extreme detriment in near-ground hover manoeuvres where position and velocity control is crucial. This restricted FoV can also start clipping out key features in the out-of-window scene which forces pilots to rely on their instruments more than the out-of-window cues in such manoeuvres. This makes pilots uncomfortable since they are trained to rely more on the out-of-window cues for near-ground manoeuvres. All of this results in the pilots' effective time delay increasing, and performance worsening.
Armed with this knowledge, one can now look into developing a visual model that tries to investigate what is special about the cues in the peripheral vision. This can attempt to explain why losing peripheral vision view leads to pilots underestimating their speed and just generally having worse performance. To this end, four research questions were formulated. These, along with their answers as a result of this thesis, are outlined below:

1. **What manoeuvre is most impacted by changing Field of View (FoV)?**: A manoeuvre that requires precise position and velocity control such as a near-ground hover with disturbances.
2. **What is the predicted pilot behaviour for the critical manoeuvre with changing FoV?**: The pilots will look towards the centre of the screen to get feedback about their pitch, and at the edge of the available FoV to get velocity feedback. For FoVs greater than 90 [$^\circ$], pilots will look at an angle of $\pm 45[^\circ]$ to get velocity feedback.
3. **What is the actual pilot behaviour for the critical manoeuvre with changing FoV?**: The pilots continued to look at the ground, slightly right of the centre of the screen regardless of the FoV.
4. **What is the overall effect of changing FoV on pilot performance?**: Making the FoV smaller made the view less comfortable for the pilots but had no significant effect on performance.
5. **What strategies do pilots employ to overcome adverse effects of changing FoV?**: Since they did not feel any significant effect on their performance, the pilots did not need to change their strategy for any of the FoVs.

Based on the literature studied, it was apparent that the motion that would be most impacted by changes in FoV would be the forward/backward motion of the helicopter. As this motion is induced by the pilot

by pitching up or down, the visual model and subsequent experiments were done for a system with two degrees-of-freedom; Pitch and Surge. To build up the visual model, the two important features of the visual scene to analyse were the changes in the Azimuth and Elevation Angles of the points in the scene. By calculating how these angles would change for a given motion, one can predict what type of feedback the pilot is getting. This would then be used to try and find the most salient viewing angle, i.e the horizontal angle at which the pilot can look to get the maximum amount of feedback on how the azimuth and elevation angles change. It was found that, for the elevation angle, this was at a viewing angle of **0 [$^\circ$]** (i.e. right in front of the observer) and for the azimuth angle, this was at a viewing angle of **45 [$^\circ$]** left or right of the observer. Based on these observations, the following hypotheses were formulated and tested in the experiment phase:

1. **H1:** If a helicopter has both pitching and forward motion, decreasing the FoV below 90 [$^\circ$] should lower a pilot's performance significantly.
2. **H2:** If a helicopter has both pitching and forward motion, increasing the FoV above 90 [$^\circ$] should have no significant effects on a pilot's performance
3. **H3**: If a helicopter has only pitching motion, changing the FoV should have no significant effect on a pilot's performance.

The experiments done consisted of participants doing two types of tasks; A velocity disturbance rejection task (with six different FoVs) and a pitch disturbance rejection task (with two different FoVs). They took control of a two degree-of-freedom helicopter model and did the tasks while a Pimax 8K-X VR headset was used to do the visual cueing. The pilots' outputs were used to calculate the Root-Mean-Squared-Errors (RMSE) and a one-way ANOVA analysis was done to see if there was any significant trend in the performance with respect to FoV.
With thirteen participants in total doing the experiments, the results of the ANOVA analysis were as follows. For the pitch disturbance rejection task, the F-statistic had a value of **0.2595** and a p-value of **0.6151**, and for the velocity disturbance rejection task, the F-statistic had a value of **0.7879** and a p-value of **0.5617**. Based on this, no significant trend can be proven to exist between FoV and pilot performance for both types of Disturbance Rejection Tasks. For the pitch disturbance rejection task, the participants' subjective comments showed that for both FoVs, their gaze was fixed on the pitch indicator reticle in the middle of the screen. The wider FoV did feel a bit more comfortable to them, but they stated that they did not feel like their performance was affected in any way. This is consistent with the results of the visual model which stated that they should be getting the most feedback from the centre of the screen, and thus would focus on that area the most.

For the velocity disturbance rejection task, the participants stated that their gaze was always on the ground texture found towards the centre of the screen. This is a departure from what was predicted since the predictions said that they would look at the edge of their vision cone, until an FoV of 90 [$^\circ$], i.e at a viewing angle of $\pm 45[^\circ]$. For FoVs greater than this, they would keep looking at a viewing angle 45 [$^\circ$] to the right or left of them. They did state that a wider FoV, in general, felt more comfortable and natural to look at. To rationalise the results, the run of one of the participants was analysed and the flow, as would be seen by them, was plotted. Additionally, the values of the change in azimuth and elevation angles with respect to pitch and forward motion were calculated. The flow showed that the pilot's view was mostly dominated by the flow generated due to the pitch rather than the forward motion and that, while the flow due to forward motion was indeed larger in the peripheries, it was hard to see a noticeable difference in the flow due to forward motion at different parts of the screen. Analysing the changes in azimuth and elevation angles showed that the values of the changes due to pitch were always magnitudes higher than the changes due to the forward motion. Additionally, the value of $\frac{\partial Ele}{\partial \theta}$ was around 1.0 for a viewing angle of ± 7.5 [$^\circ$] and it only decreased as the viewing angle increased. All of this, along with the knowledge gained from the subjective comments of the participants, leads to the conclusion that the pilots were seeing more pitch than forward motion and their perception of pitch degraded as they shifted their gaze from the centre of the screen. Therefore, participants chose to continue looking at the centre of the screen regardless of the FoV and only needed a small piece of grass texture to determine their velocity.

The goal of this thesis was to try and find a link between the FoV and the pilot performance, and it was chosen that this would be done by looking at how losing information in your peripheries affects

the performance. Based on the research questions stated above, this goal was accomplished to a satisfactory level. The visual model made, showed that the pilot was at the risk of losing the feedback of the most salient point, when it comes to velocity feedback, if their FoV was reduced by a significant degree. The biggest question mark surrounding the visual model however, was the idea that even if this point gets clipped out, how much would this actually impact pilot perception. In the end, the results showed that the answer to that question is that the pilot perception remains somewhat the same. Regardless, the experiments and the visual model are an excellent starting point for future researchers, and the following recommendations can certainly help them learn more in this field. The first among them, is the idea that such experiments should be re-done, but with a higher fidelity when it comes to the degrees-of-freedom of the helicopter. Previous research, and comments made by some of the participants who had significant flight experience, show that peripheral vision may be crucial for pilots to decouple different modes of motion and rotation in a helicopter. This means that, for any experiment that wishes to investigate impact of peripheral vision on flight, the helicopter model and subsequent experimental task done with it, must allow for multiple degrees-of-freedom in translation and rotation. Secondly, it could be that the results obtained for the velocity disturbance rejection tasks were dependant on the experimental conditions used, and that if those conditions were different, the same results would not be achieved. It is thus recommended to change up factors such as the helicopter model or velocity forcing function to ascertain if the results are indeed dependant on the experimental conditions Furthermore, any experiments involving VR headsets should enable head tracking on the headsets. This was disabled in this project to simplify the analysis, but enabling it offers a more in-depth look into the impact of VR headsets and offers a more comfortable experience to the pilots. Last, but not least, any visual model that aims to achieve the same goals as this thesis, should try and account for how the number of visible points can affect pilot perception. In the analysis done for this thesis, the fact that as FoV increases, the pilots just see more points and get feedback from more points, was not really taken into account. Therefore, it is recommended that future visual models try and incorporate this factor into their analysis.

References

[1] Adam T Biggs, Daniel J Geyer, Valarie M Schroeder, F Eric Robinson, and John L Bradley. “Adapting virtual reality and augmented reality systems for naval aviation training”. In: *Naval medical research unit dayton wright-patterson AFB United States* (2018).

[2] Yasemin Çetin, Erdal Yılmaz, and Yasemin Yardımcı Çetin. “Evaluation of visual cues of three-dimensional virtual environments for helicopter simulators”. In: *The Journal of Defense Modeling and Simulation* 9.4 (2012), pp. 347–360.

[3] Eric D Ragan, Ajith Sowndararajan, Regis Kopper, and Doug A Bowman. “The effects of higher levels of immersion on procedure memorization performance and implications for educational virtual environments”. In: *Presence: Teleoperators and Virtual Environments* 19.6 (2010), pp. 527–543.

[4] RA Hess and W Siwakosit. “Assessment of flight simulator fidelity in multiaxis tasks including visual cue quality”. In: *Journal of aircraft* 38.4 (2001), pp. 607–614.

[5] Ronald A Hess. “Application of a model-based flight director design technique to a longitudinal hover task”. In: *Journal of Aircraft* 14.3 (1977), pp. 265–271.

[6] Philipp Podzus, Jur Crijnen, Michael Jones, Stefan van’t Hoff, and Paul Breed. “Evaluation of Simulator Cueing Fidelity for Rotorcraft Certification by Simulation”. In: *78th Annual Vertical Flight Society Forum and Technology Display, FORUM 2022*. 2022.

[7] William Chung, Barbara Sweet, Mary Kaiser, and Emily Lewis. “Visual Cueing Effects Investigation for a Hovering Task”. In: *AIAA Modeling and Simulation Technologies Conference and Exhibit*. 2003, p. 5524.

[8] Sheldon Baron, Roy Lancraft, and Greg Zacharias. “Pilot/vehicle model analysis of visual and motion cue requirements in flight simulation”. In: *NASA contract report* (1980).

[9] Adolph Atencio Jr. *Fidelity Assessment of a UH-60A Simulation on the NASA Ames Vertical Motion Simulator.pdf*. English. Tech. rep. California, USA: NASA, 1993, p. 324.

[10] Robert V Kenyon and Edward W Kneller. “The effects of field of view size on the control of roll motion”. In: *IEEE transactions on systems, man, and cybernetics* 23.1 (1993), pp. 183–193.

[11] Paolo Pretto, Maelle Ogier, Heinrich H Bülthoff, and J-P Bresciani. “Influence of the size of the field of view on motion perception”. In: *Computers & Graphics* 33.2 (2009), pp. 139–146.

[12] HB-L Duh, JW Lin, Robert V Kenyon, Donald E Parker, and Thomas A Furness. “Effects of field of view on balance in an immersive environment”. In: *Proceedings IEEE Virtual Reality 2001*. IEEE. 2001, pp. 235–240.

[13] Roger H Hoh. *The effects of degraded visual cueing and divided attention on obstruction avoidance in rotorcraft*. US Federal Aviation Administration, Research and Development Service, 1990.

[14] Helen Marie Baker. “An investigation of pilot modelling for helicopter handling qualities analysis”. PhD thesis. University of Liverpool, 2010.

[15] Laura Iseler. “Piloted Simulator Investigation of Category A Civil Rotorcraft Terminal Area Cockpit Displays”. In: *Journal of the American Helicopter Society* 43.3 (1998), pp. 185–194.

[16] Fabian Erazo, Sion Jennings, Kris Ellis, and Jason Etele. “Effects of Hover Symbology Display Scaling on Performance and Workload”. In: *Journal of the American Helicopter Society* 66.2 (2021), pp. 1–14.

[17] Jongki Moon, Jean Charles Domercant, and Dimitri Mavris. “A simplified approach to assessment of mission success for helicopter landing on a ship”. In: *International Journal of Control, Automation and Systems* 13 (2015), pp. 680–688.

[18] Edward N Bachelder and Duane McRuer. “Perception-based synthetic cueing for night vision device rotorcraft hover operations”. In: *Helmet-and Head-Mounted Displays VII*. Vol. 4711. SPIE. 2002, pp. 377–388.

[19] WA Memon, Mark D White, Gareth D Padfield, N Cameron, and Linghai Lu. “Helicopter Handling Qualities: A study in pilot control compensation”. In: *The Aeronautical Journal* 126.1295 (2022), pp. 152–186.

[20] Duane McRuer and Ezra Krendel. “Mathematical Models of Human Pilot Behavior”. In: *AGARDograph* (Jan. 1974), p. 83.

[21] Francesca Roncolini, Giuseppe Quaranta, et al. “Virtual pilot: a review of the human pilot’s mathematical modeling techniques”. In: *11th ECCOMAS Thematic Conference on Multibody Dynamics 2023*. 2023, pp. 1–14.

[22] Daan Marinus Pool, Peter MT Zaal, Herman J Damveld, Marinus Maria van Paassen, and Max Mulder. “A Cybernetic Approach to Assess Flight Simulator Motion Fidelity”. In: *IFAC Proceedings Volumes* 43.13 (2010), pp. 380–385.

[23] D.M. Pool and P.M.T. Zaal. “A Cybernetic Approach to Assess the Training of Manual Control Skills”. en. In: *IFAC-PapersOnLine* 49.19 (2016), pp. 343–348. ISSN: 24058963. DOI: 10.1016/j.ifacol.2016.10.588. URL: https://linkinghub.elsevier.com/retrieve/pii/S2405896316321796 (visited on 02/20/2024).

[24] P. M. T. Zaal, D. M. Pool, Q. P. Chu, M. M. Van Paassen, M. Mulder, and J. A. Mulder. “Modeling Human Multimodal Perception and Control Using Genetic Maximum Likelihood Estimation”. en. In: *Journal of Guidance, Control, and Dynamics* 32.4 (July 2009), pp. 1089–1099. ISSN: 0731-5090, 1533-3884. DOI: 10.2514/1.42843. URL: https://arc.aiaa.org/doi/10.2514/1.42843 (visited on 02/28/2024).

[25] Marinus M. Van Paassen and Max Mulder. “Identification of Human Control Behavior”. In: *International Encyclopedia of Ergonomics and Human Factors*. Jan. 2006, pp. 400–407. ISBN: ISBN 041530430X.

[26] George E Cooper and Robert P Harper. *The use of pilot rating in the evaluation of aircraft handling qualities*. National Aeronautics and Space Administration, 1969.

[27] A.H. Roscoe, G.A. Ellis, Royal Aerospace Establishment (Great Britain), and Great Britain Ministry of Defence Procurement Executive. *A Subjective Rating Scale for Assessing Pilot Workload in Flight: A Decade of Practical Use*. Technical report (Royal Aerospace Establishment (Great Britain)). Procurement Executive, Ministry of Defence, 1990. URL: https://books.google.nl/books?id=0_eJXwAACAAJ.

[28] Gareth D Padfield. *Helicopter flight dynamics: the theory and application of flying qualities and simulation modelling*. John Wiley & Sons, 2008.

[29] Max Mulder and JA Mulder. “Cybernetic analysis of perspective flight-path display dimensions”. In: *Journal of Guidance, Control, and Dynamics* 28.3 (2005), pp. 398–411.

[30] Richard Musil. *HMD Geometry Database*. en. Dec. 2023. URL: https://risa2000.github.io/hmdgdb/ (visited on 04/22/2024).

[31] *Appendix 4B The Three Case Helicopters: Lynx, Bo105 and Puma | Helicopters & Aircrafts*. en-US. URL: http://heli-air.net/2016/03/26/appendix-4b-the-three-case-helicopters-lynx-bo105-and-puma/ (visited on 08/25/2024).

[32] Peter MT Zaal, Daan M Pool, Jaap de Bruin, Max Mulder, and Marinus M van Paassen. “Use of pitch and heave motion cues in a pitch control task”. In: *Journal of Guidance, Control, and Dynamics* 32.2 (2009), pp. 366–377.

[33] Tjeerd Groot, Herman Damveld, M Mulder, and M Van Paassen. “Effects of aeroelasticity on the pilot’s psychomotor behavior”. In: *AIAA atmospheric flight mechanics conference and exhibit*. 2006, p. 6494.

[34] Enviromental Ergonomics. “International encyclopedia of ergonomics and human factors”. In: (2001).

[35] *Pimax "8K" X Update Enables 90Hz Refresh Rate With Max Resolution on GeForce 30-series GPUs*. URL: https://www.roadtovr.com/pimax-8k-x-90hz-refresh-rate-native-mode-firmware/ (visited on 05/28/2024).

[36] *Valve Index Base 3D Model - TurboSquid 1670059*. en. URL: https://www.turbosquid.com/3d-models/valve-index-base-3d-model-1670059 (visited on 05/28/2024).

[37] Jelte E Bos. "Less sickness with more motion and/or mental distraction". In: *Journal of Vestibular Research* 25.1 (2015), pp. 23–33.

[38] Max Mulder. *Cybernetics of tunnel-in-the-sky displays*. Delft University Press Delft, 1999.

A

Alternate Visual Model

This chapter details the steps taken to create an alternate version of the visual model, as compared to Chapter 3. The information regarding the setup of the model is shown in section A.1. The results for the model are outlined in section A.2 and the steps taken for, and the results of, the sensitivity analysis are shown in section A.3. lastly, the discussion of the results obtained is shown in section A.4.

A.1. Background

The goal of this chapter is to create a visual model to try and predict how pilot behaviour will change as the FoV is changed. The literature study has shown that pilot performance does degrades but the goal is to try and find if the exact nature and extent of the degradation can be predicted. As the FoV decreases, it can be intuited that the pilot's perception of velocity also decreases. Duh et al and Pretto et al found out that this was due to the fact that there is less motion in the pilot's peripheries which degrades their immersion and performance [11][12]. To this end, one can try and quantify how this velocity perception degradation occurs by looking at how perspective projection occurs. This is outlined in Figure A.1:

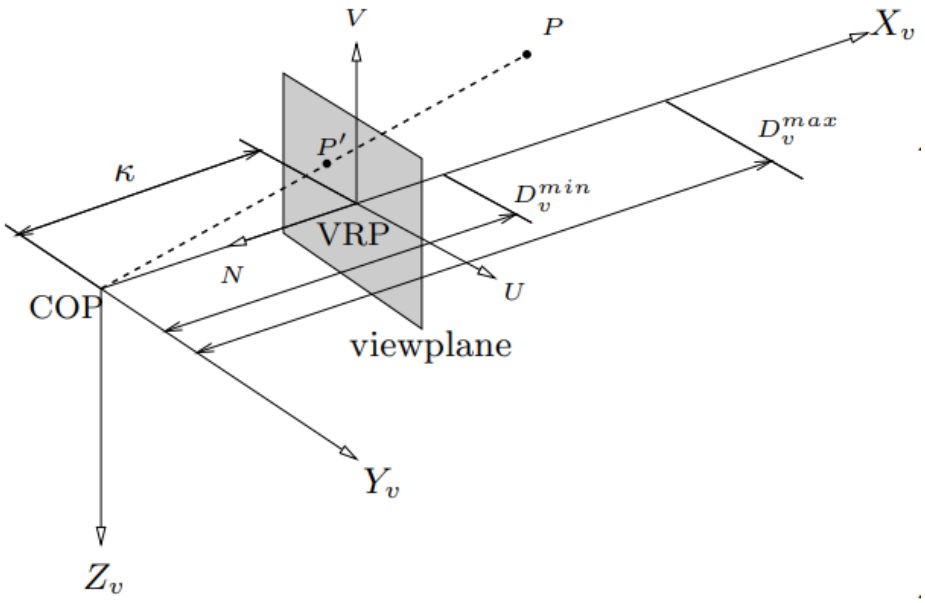

Figure A.1: Figure showing the perspective projection method [38]

The HSC and VSC are the horizontal and vertical screen size, and HGFOV and VGFOV are the

horizontal and vertical FoV. The COP is the Centre of Projection with X_v, Y_v and Z_v being the viewing axis. A point P is projected onto the viewplane at position, P'. The viewplane has the vertical axis, V and horizontal axis, U. The viewplane is a distance κ away from the COP. D_v^{min} and D_v^{max} are the minimum and maximum viewing distances and they represent the front and back planes of the viewing frustum. That means that any point not within these two planes gets clipped out.
κ can be calculated using [38]:

$$\kappa = \frac{HSC}{2\tan(HGFOV/2)} = \frac{VSC}{2\tan(VGFOV/2)} \tag{A.1}$$

Using this, the position P' of an object, P in the viewing plane can be given by [38]:

$$\begin{aligned} u_p &= \kappa \left(\frac{y_p^v}{x_p^v} \right) \\ v_p &= -\kappa \left(\frac{z_p^v}{x_p^v} \right) \end{aligned} \tag{A.2}$$

where x_p^v, y_p^v and z_p^v are the x, y and z coordinates of point P in the Viewing axis. Do note we assume the Viewing axis to be aligned with the helicopter Body axis. These positions can be calculated using [38]:

$$\underline{x}_p^v = [x_p^v, y_p^v, z_p^v] = R_X(\phi) R_Y(\theta) R_Z(\psi) \cdot \left(\underline{x}_p^w - \underline{x}_{COP}^w \right), \tag{A.3}$$

where $\underline{x}_p^w$ are the coordinates of point P in the World axis and $\underline{x}_{COP}^w$ are the coordinates of the COP in the World axis. The orthogonal rotation matrices $R_X(\phi)$, $R_Y(\theta)$ and $R_Z(\psi)$ are given by [38]:

$$\underbrace{\begin{pmatrix} 1 & 0 & 0 \\ 0 & \cos\phi & \sin\phi \\ 0 & -\sin\phi & \cos\phi \end{pmatrix}}_{R_X} \underbrace{\begin{pmatrix} \cos\theta & 0 & -\sin\theta \\ 0 & 1 & 0 \\ \sin\theta & 0 & \cos\theta \end{pmatrix}}_{R_Y} \underbrace{\begin{pmatrix} \cos\psi & \sin\psi & 0 \\ -\sin\psi & \cos\psi & 0 \\ 0 & 0 & 1 \end{pmatrix}}_{R_Z} \tag{A.4}$$

with θ being the pitch angle, ϕ being the roll angle and ψ being the yaw angle.
All of this can be used to then see how the velocity of P in the viewing plane changes for a discrete motion. This is done using the image field equations [38]:

$$\begin{aligned} \dot{u}_p &= \underbrace{\left(-\kappa v^b + u_p u^b\right)/x_p^b}_{\dot{u}_p^T} + \underbrace{\left(-\kappa^2 r^b - \kappa v_p p^b - u_p v_p q^b - u_p^2 r^b\right)/\kappa}_{\dot{u}_p^R}; \\ \dot{v}_p &= \underbrace{\left(+\kappa w^b + v_p u^b\right)/x_p^b}_{\dot{v}_p^T} + \underbrace{\left(-\kappa^2 q^b + \kappa u_p p^b - u_p v_p r^b - v_p^2 q^b\right)/\kappa}_{\dot{v}_p^R}. \end{aligned} \tag{A.5}$$

The image field equations allow the calculation of the velocity of point P on the viewplane by taking into account the helicopter's body velocity in all three axes (u^b,v^b and w^b) and its attitude rates (p^b, q^b and r^b). Additionally, it can be seen that the velocity components of point P are split into translational components ($\dot{u}_p^T$ and $\dot{v}_p^T$) and rotational components ($\dot{u}_p^R$ and $\dot{v}_p^R$)

The goal of this analysis is to try and find a point in the world that offers the maximum amount of forward velocity information to the pilot. It is assumed that, if such a point exists and is dependent of the FoV, then when the FoV is lowered, this point would get clipped out of the view. This means that the pilot would no longer see the most salient point of the environment and would need to shift their gaze to the next-most salient point. Presumably, this would result in the pilot getting feedback of their velocity being much smaller and could be the reason for why people tend to underestimate their velocity as FoV shrinks, as per the findings of Pretto et al and others [11][12].
To quantify how much velocity feedback the pilot is getting, it was decided that the key parameter to analyse would be the ratio of the velocity of point P on the viewing plane (i.e. the on-screen velocity) and the actual velocity of the observer (or helicopter). Thus, the greater the ratio, the greater the velocity feedback. The reason why the ratio was chosen as a metric instead of the on-screen velocity

is because it allows one to normalise velocity and allow for comparison between the values obtained for different observer velocities and attitude rates. Lastly, this can also be useful in providing some key FoVs that can be used for the experiment phase.
The first step in this analysis is to simplify Equation A.5. As shown in Chapter 2, the performance of the pilot degrades the most as FoV changes for forward translational motion. As such, it is worth analysing cases where the helicopter would move forward and backwards to see if the point of maximum feedback does exist. However, since helicopters must change their pitch to change their forward velocity, it is also worth considering the impact of the pitching motion. Thus, for this analysis, the helicopter motion to investigate involves only forward velocity, u^b and pitch (which results in a pitch rate, q^b). This means that one can remove the other velocity and attitude rate terms from Equation A.5 to give:

$$\begin{aligned} \dot{u}_p &= \underbrace{\frac{u_p u^b}{x_p^b}}_{\dot{u}_p^T} + \underbrace{\frac{-u_p v_p q^b}{\kappa}}_{\dot{u}_p^R} \\ \dot{v}_p &= \underbrace{\frac{v_p u^b}{x_p^b}}_{\dot{v}_p^T} + \underbrace{\frac{-\kappa^2 q^b - v_p^2 q^b}{\kappa}}_{\dot{v}_p^R}. \end{aligned} \tag{A.6}$$

The ratio of on-screen velocity to actual velocity, henceforth called Δ is given by:

$$\Delta = \frac{\sqrt{(\dot{u}_p^T)^2 + (\dot{v}_p^T)^2}}{u^b} + \frac{\sqrt{(\dot{u}_p^R)^2 + (\dot{v}_p^R)^2}}{\sqrt{(q z_p^v)^2 + (q x_p^v)^2}} \tag{A.7}$$

As can be seen in Equation A.7, the ratio is calculated by first getting the magnitude of the velocities caused by the translations and rotations, and then dividing by the corresponding motion that caused the velocities. For the rotational components, the divisor is the magnitude of the cross product between the rotational rate of the helicopter in all three axis, and the 3D-coordinates of the position $\underline{x}_p^v$. This is done because the numerator of the expression is linear velocity in [m/s] while the pitch rate is an angular velocity in [rad/s]. Thus, the angular velocity needs to be converted to a linear velocity. Since there is only rotation in one axis, the cross product is given by:

$$\begin{aligned} &\vec{v} = \vec{\omega} \times \vec{r} \\ &\vec{v} = \begin{pmatrix} 0 \\ q \\ 0 \end{pmatrix} \times \begin{pmatrix} x \\ y \\ z \end{pmatrix} = \begin{vmatrix} \hat{i} & \hat{j} & \hat{k} \\ 0 & q & 0 \\ x & y & z \end{vmatrix} \\ &\vec{v} = \hat{i}(q \cdot z - 0) - \hat{j}(0 \cdot z - 0 \cdot x) + \hat{k}(0 \cdot y - q \cdot x) = \begin{pmatrix} qz \\ 0 \\ -qx \end{pmatrix} \end{aligned} \tag{A.8}$$

It is now apparent that $\dot{u}_p$ and $\dot{v}_p$ are affected by changes in two main categories:

- **Changes in FoV:** This can either mean a change in the value of κ as per Equation A.1 or can mean keeping κ the same and simply making the view frustum smaller.
- **Change in helicopter motion:** This means that u^b and q^b change

Therefore, one can analyse what the affect is on the ratio of on-screen velocity to helicopter body velocity of these two categories. The individual conditions to analyse are:

1. Change the FoV in Equation A.1 to change the value of κ
2. Use the same value of κ for all FoVs but analyse only the positions of P that would be visible for this FoV.
3. Analyse the change in on-screen velocity for 1 Degree-of-Freedom (DOF) by only changing u^b
4. Analyse the change in on-screen velocity for 1 DOF by only changing q^b
5. Analyse the change in on-screen velocity for 2 DOF by changing both u^b and q^b

The difference between the first and second condition is simply the fact that the first condition takes into account the projection effects of changing FoV, while the second condition ignores the projection effects and simply focuses on the changes in how much can be seen with changing FoVs. This is highlighted by the examples shown in Figure A.2:

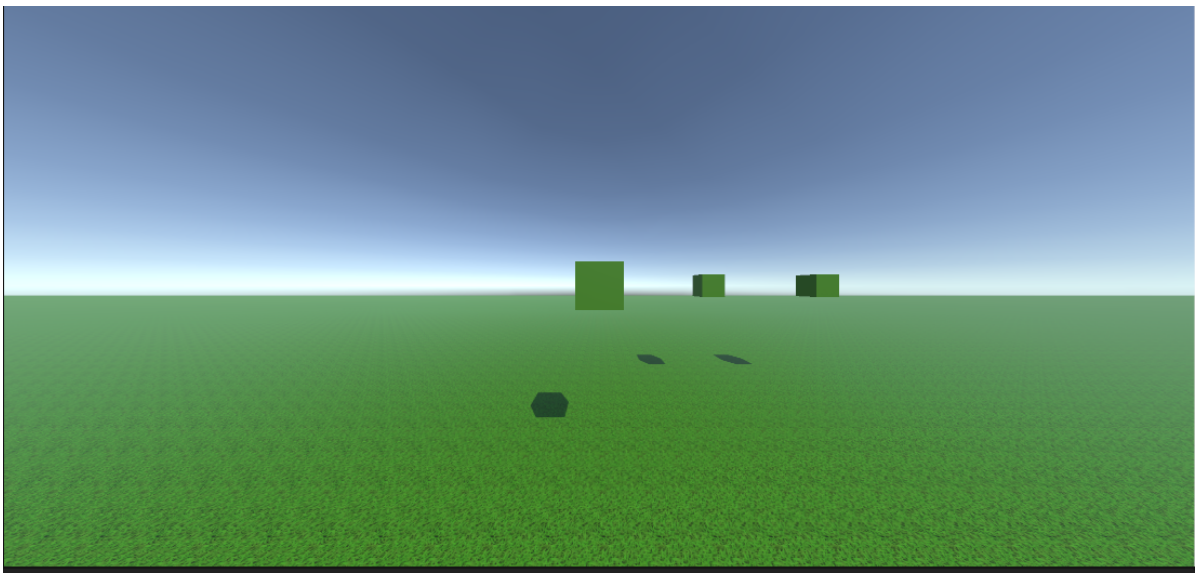

(a) Figure showing an example of a view with an FoV of 140 [°]

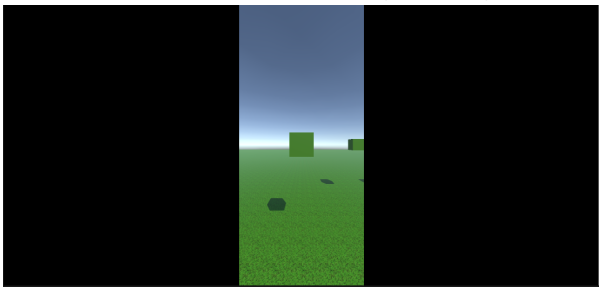

(b) Figure showing the view with an FoV of 60 [°] with no projection effects

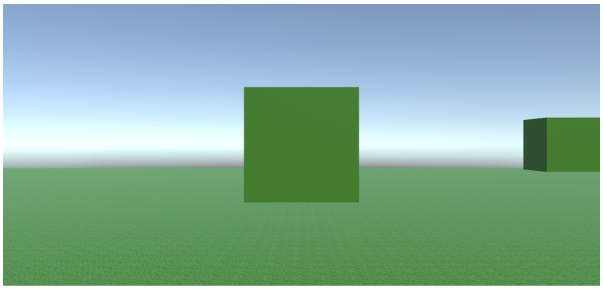

(c) Figure showing the view with an FoV of 60 [°] with projection effects

Figure A.2: Figure showing the difference in projection effects and no projection effects on the view

The standard view with an FoV of 140 [°] can be seen in Figure A.2a. If one was to restrict the FoV by keeping κ constant (no projection effects), then the view would look like Figure A.2b. As is apparent, some parts of the scenery get clipped out but the objects seem to be at the same distance as before. Conversely, if projection effects were taken into account, like in Figure A.2c, then the objects appear much closer than they actually are.
Since the changes in on-screen velocity can only be analysed if the helicopter is moving, there are six cases to analyse which can be seen in Table A.1:

Table A.1: Table showing the six cases to analyse

	κ **is constant**	κ **changes**
1 DOF (u^b**)**	Case 1	Case 4
1 DOF (q^b**)**	Case 2	Case 5
2 DOF	Case 3	Case 6

For each of the cases, seven FoVs were tested: **20**, **40**, **60**, **80**, **100**, **120** and **140** $[deg]$. For each case, the values of D_v^{min} and D_v^{max} were set to **1** [m] and **10** [m] respectively and a list of X_v values in this range (in increments of 0.1 [m]) were generated. Using these values and each of the FoVs, a full

list of Y_v and Z_v values were generated which resulted in all possible permutations of coordinates for a point P within the view frustum for each FoV. The number of possible positions to analyse for each FoV is shown in Table A.2:

Table A.2: Table showing the number of positions to analyse for each FoV

FoV [deg]	Number of positions
20	74401
40	150677
60	237039
80	343186
100	485900
120	704947
140	116708

For each case, the value of the ratio of on-screen velocity and actual velocity was calculated for all the possible positions and the postion which gave the highest ratio was chosen. The horizontal and vertical viewing angle (VA_H and VA_V) for this optimal position was then calculated, based on Equation A.9, to see where in the pilot's FoV this was located:

$$\begin{aligned} VA_H &= 2\arctan\frac{Y_{optimal}}{X_{optimal}} \\ VA_V &= 2\arctan\frac{Z_{optimal}}{X_{optimal}} \end{aligned} \tag{A.9}$$

The values of the free variables in Equation A.6 for each of the cases are presented in Table A.3:

Table A.3: Table showing the values of the parameters used for each Case

Case	u^b [m/s]	θ [deg]	q^b [rad/s]	HSC [m]	κ [m]
1	**2**	0	0	0.4878	0.088
2	0	**-5**	**-0.087**	0.4878	0.088
3	**2**	**-5**	**-0.087**	0.4878	0.088
4	**2**	0	0	0.4878	**Variable**
5	0	**-5**	**-0.087**	0.4878	**Variable**
6	**2**	**-5**	**-0.087**	0.4878	**Variable**

The value of κ for the first three cases is calculated using the horizontal screen size and the horizontal FoV. The reason this was done is because the end goal is to do experiments to accept or reject any hypotheses this analysis presents. The experiments will be done using a Pimax 8KX VR headset that has a maximum horizontal FoV of 140 [°] and a maximum vertical FoV of 100 [°] [35]. Additionally, the vertical FoV does not change when one changes the FoV settings on the actual headset which is why it was decided that, for this analysis and the experiments, κ will be calculated using the horizontal screen size of the Pimax (**0.4878** [m]) and the max horizontal FoV (140 [°]). Lastly, the different positions generated in Table A.2 were generated by looking at the view frustums achieved with a vertical FoV of 100 [°] and the horizontal FoVs given in the table.
The values of u^b and θ used in the analysis were chosen such that they would be representative of a helicopter in a hover scenario. In such a scenario, a helicopter pilot would apply small pitch angles onto the helicopter to keep it steady which would result in small velocities. However, the velocity and pitch angle should still be large enough such that there is a noticeable change in the on-screen velocities so it was decided to use the aforementioned values.

A.2. Results

This section outlines the results gathered from this analysis. The results for a constant κ are outlined in subsection A.2.1 while the results for a variable value of κ are shown in subsection A.2.2.

A.2.1. Constant κ

For the first of the three cases where κ was kept constant, the results can be seen in Table A.4:

Table A.4: Table showing the optimal position, the horizontal and vertical viewing angle of this position and the value of Δ for each FoV for Case 1

FoV [deg]	Optimal Position (x,y,z) [m]	Horizontal Viewing angle [deg]	Vertical Viewing Angle [deg]	Δ
20	(1.20, 0.2, -1.45)	18.92	100.7	0.0174
40	(1.10, 0.4, -1.35)	39.97	101.6	0.041
60	(1.0, 0.5, -1.15)	53.13	97.93	0.063
80	(1.0, 0.8, -1.15)	77.32	97.93	0.10
100	(1.0, 1.1, -1.15)	95.45	97.93	0.14
120	(1.0, 1.70, -1.15)	119.1	97.93	0.21
140	(1.0, 2.7, -1.15)	139.3	97.93	0.34

The results can also be visualised in Figure A.3a and Figure A.3b:

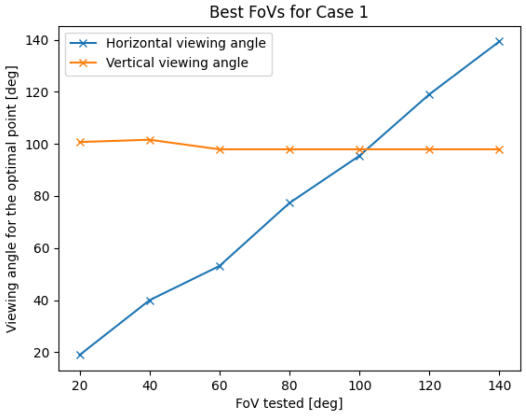

(a) Figure showing the viewing angles of the optimal positions for every FoV for Case 1

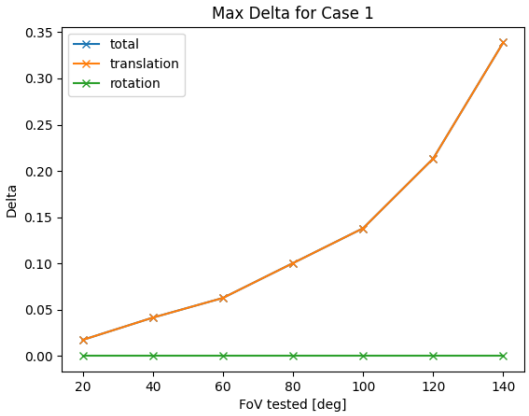

(b) Figure showing the max value of Δ for each FoV for Case 1

Figure A.3: Figure showing the viewing angle for the optimal positions and the max Δ for each FoV for Case 1

As the figures show, the best horizontal viewing angle for each of the FoVs tends to be right on the edge of the FoV. This can be explained when one considers the fact that this position corresponds to the maximum possible y-coordinate in the view frustum. As can be seen by Equation A.2, the value of u_p increases as y_p^v increases. This higher u_p then accounts for a greater value of $\dot{u_p}$ (as seen by Equation A.6) which results in a higher Δ. Keeping in mind that the Z Viewing axis is defined as positive downwards, the same logic applies to why Δ increases for a decreasing z_p^v. Lastly, this is also why the most optimal position is one with the lowest possible X-coordinate. These findings are consistent with the findings from the literature study which suggested that, for forward motion, the most flow can be seen in the peripheries of one's vision. The value of total Δ, shown in Figure A.3b, also increases for each FoV suggesting that the bigger the FoV, the more flow can be seen. As one would expect, the Δ provided by the rotational components is zero since there was no rotation occurring.

For Case 2, the results can be seen in Table A.5

Table A.5: Table showing the optimal position, the horizontal and vertical viewing angle of this position and the value of Δ for each FoV for Case 2

FoV [deg]	Optimal Position (x,y,z) [m]	Horizontal Viewing angle [deg]	Vertical Viewing Angle [deg]	Δ
20	(1.0, 0.1, -0.05)	11.42	5.607	0.089
40	(1.0, 0.3, -0.05)	33.39	5.607	0.097
60	(1.0, 0.5, -0.05)	53.13	5.607	0.113
80	(1.0, 0.8, -0.05)	77.32	5.607	0.157
100	(1.1, 1.3, -0.15)	95.52	15.42	0.226
120	(1.0, 1.7, -0.15)	119.1	16.94	0.43
140	(1.0, 2.7, -0.15)	139.4	16.94	1.00

The results are visualised in Figure A.4a and Figure A.4b:

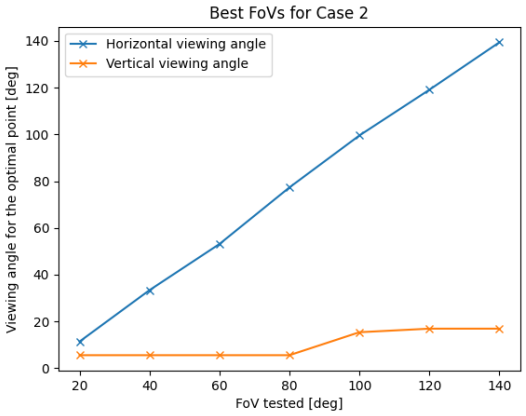

(a) Figure showing the viewing angles of the optimal positions for every FoV for Case 2

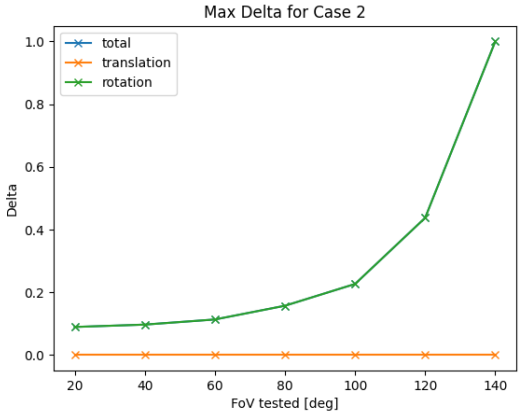

(b) Figure showing the max value of Δ for each FoV for Case 2

Figure A.4: Figure showing the viewing angle for the optimal positions and the max Δ for each FoV for Case 2

Much like Case 1, the most optimal horizontal viewing angle continues to be on the edge of the corresponding FoV. However, the most optimal vertical FoV is now significantly lower. The reason for this comes down to the value of the Z-coordinate for the most optimal position. As can be seen in Equation A.2 and Equation A.6, a more negative value of z_p^v should result in a higher value of v_p and of the on-screen velocities $\dot{u_p}$ and $\dot{v_p}$, which still remains true. However, the difference between Case 1 and 2 is the fact that the rotational component of Δ (i.e. the right expression in Equation A.7) dictates the final value for all coordinates. Therefore, large values of z_p^v mean a larger denominator in Equation A.7 which results in a lower overall value of Δ. Since there is no y_p^v term in the denominator of Equation A.7, the most optimal value of y_p^v is still one which results in the largest value of u_p, which remains to be the largest value of y_p^v for that FoV.

The results for the third and final case for a constant κ can be seen in Table A.6 and are visualised in Figure A.5a and Figure A.5b:

Table A.6: Table showing the optimal position, the horizontal and vertical viewing angle of this position and the value of Δ for each FoV for Case 3

FoV [deg]	Optimal Position (x,y,z) [m]	Horizontal Viewing angle [deg]	Vertical Viewing Angle [deg]	Δ
20	(1.0, 0.1,-0.049)	11.42	5.607	0.102
40	(1.0, 0.30,-0.049)	33.39	5.607	0.135
60	(1.0, 0.5, -0.15)	53.13	16.95	0.178
80	(1.0, 0.8, -0.25)	77.32	27.96	0.261
100	(1.0, 1.1, -0.25)	95.45	27.96	0.369
120	(1.0, 1.7,-0.25)	119.1	27.96	0.660
140	(1.0, 2.7, -0.25)	139.3	27.96	1.35

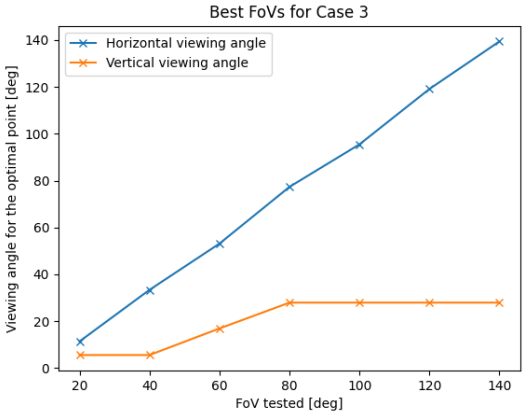

(a) Figure showing the viewing angles of the optimal positions for every FoV for Case 3

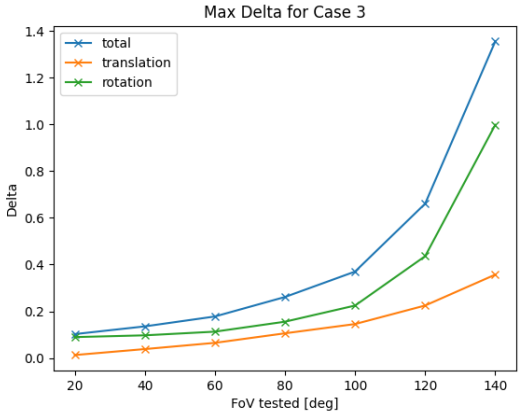

(b) Figure showing the max value of Δ for each FoV for Case 3

Figure A.5: Figure showing the viewing angle for the optimal positions and the max Δ for each FoV for Case 3

As can be expected, the results of Case 3 shadow the results of the previous two cases. Once again, the best Horizontal angle to get the most information, seems to be on the edge of the FoV. This was true for both previous cases and is, thus, true for this one as well. For the vertical viewing angle, there was a mismatch between the optimal value for Case 1 and Case 2. For Case 3, it seems that the results for Case 2 are more prevalent for the optimal vertical viewing angle. This can be explained by looking at the impact of the rotational component and translational component of Δ, shown in Figure A.5b. The value of Δ caused by the rotation is greater than that for the translational component and that means, for each of the possible positions of P, the movement in the vertical viewing axis, v_p, is dominated by the rotational movement. Thus, the optimal Z-coordinate (which is what is used to calculate the optimal vertical viewing angle as per Equation A.9) is one that is optimal in rotation. Of course, the translational component does also have a contribution, which is why the optimal vertical viewing angles for Case 3 are higher than those for Case 2, but since the rotational component dominates this balance, they are not as high as those for Case 1.

A.2.2. Variable κ

For the first of the variable κ cases, the results are presented in Table A.7

Table A.7: Table showing the optimal position, the horizontal and vertical viewing angle of this position and the value of Δ for each FoV for Case 4

FoV [deg]	Optimal Position (x,y,z) [m]	Horizontal Viewing angle [deg]	Vertical Viewing Angle [deg]	Δ
20	(1.2, 0.2, -1.45)	18.92	100.7	0.272
40	(1.1, 0.4, -1.35)	39.96	101.6	0.313
60	(1.0, 0.5, -1.15)	53.13	97.93	0.299
80	(1.0, 0.8, -1.15)	77.32	97.93	0.329
100	(1.0, 1.1, -1.15)	95.45	97.93	0.319
120	(1.0, 1.75,-1.15)	119.1	97.93	0.338
140	(1.0, 2.7, -1.15)	139.4	97.93	0.338

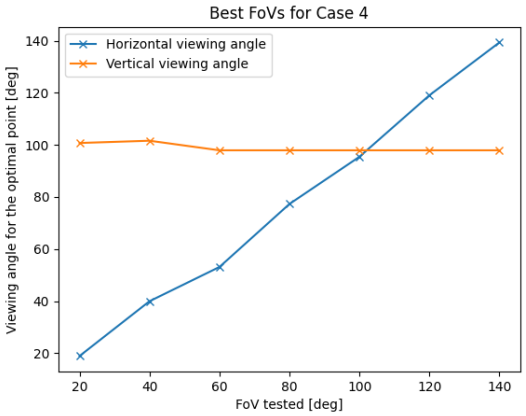

(a) Figure showing the viewing angles of the optimal positions for every FoV for Case 4

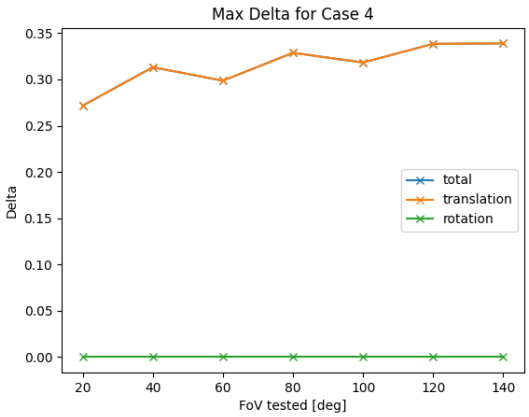

(b) Figure showing the max value of Δ for each FoV for Case 4

Figure A.6: Figure showing the viewing angle for the optimal positions and the max Δ for each FoV for Case 4

As can be seen from the results, the optimal viewing angles in both the horizontal and vertical case are the exact same as those for Case 1, but the values of Δ are significantly higher and show a different pattern. As the FoV increases, the change in κ is shown in:

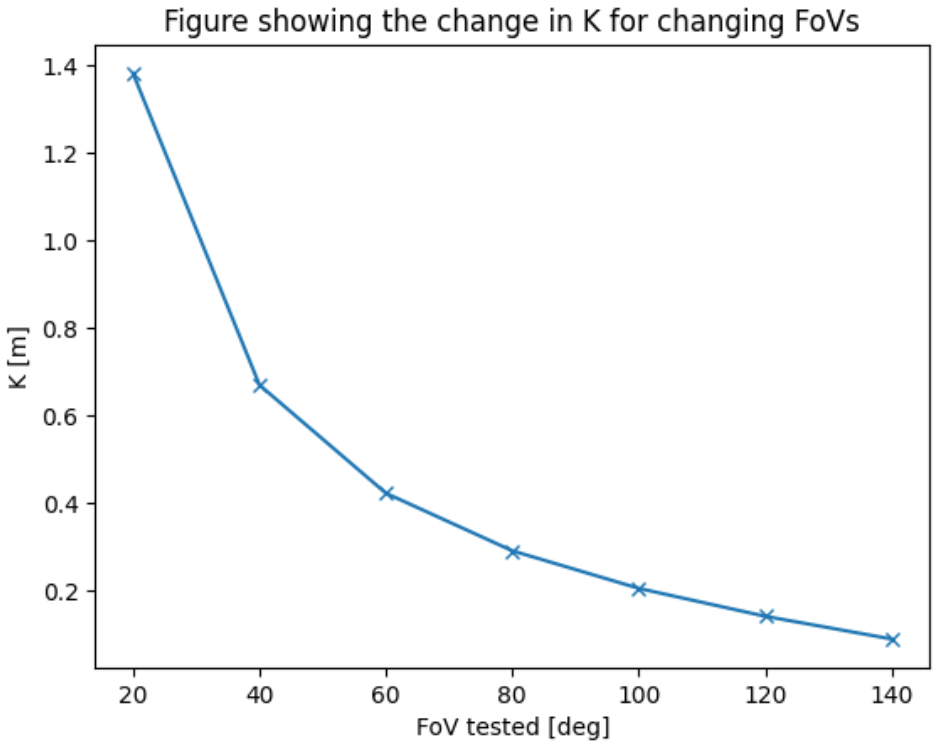

Figure A.7: Figure showing the change in κ for changing FoVs

The values for κ are shown in Table A.8:

Table A.8: Table showing the values of κ as FoV increases

Angle [deg]	κ [m]
20	1.38
40	0.66
60	0.42
80	0.29
100	0.20
120	0.14
140	0.088

As the FoV increases, the value of κ decreases tangentially. This also changes the value of u_p and v_p non-linearly since, in this case, the value of those two terms is dependant on the product of κ and the position coordinates of the point. Combining these effects in the final equation to calculate Δ seems to output the result that the ratio of on-screen velocity to actual velocity remains constant for all FoVs. If this is true, then this implies that there is very little feedback lost as FoV is decreased.

The results for Case 5 are outlined in Table A.9 and visualised in Figure A.8a and Figure A.8b:

Table A.9: Table showing the optimal position, the horizontal and vertical viewing angle of this position and the value of Δ for each FoV for Case 5

FoV [deg]	Optimal Position (x,y,z) [m]	Horizontal Viewing angle [deg]	Vertical Viewing Angle [deg]	Δ
20	(1.0, 0.1,-0.049)	11.42	5.607	1.39
40	(1.0, 0.3,-0.045)	33.39	5.607	0.733
60	(1.0, 0.5, -0.045)	53.13	5.607	0.539
80	(1.0, 0.8, -0.045)	77.32	5.607	0.515
100	(1.1, 1.3, -0.15)	99.53	15.43	0.522
120	(1.0, 1.7;-0.15)	119.07	16.95	0.694
140	(1.0, 2.7, -0.15)	139.35	16.95	1.00

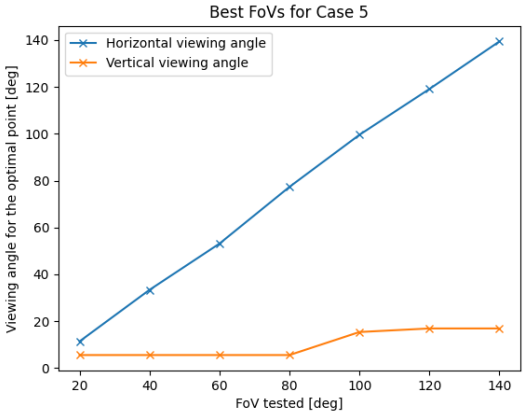

(a) Figure showing the viewing angles of the optimal positions for every FoV for Case 5

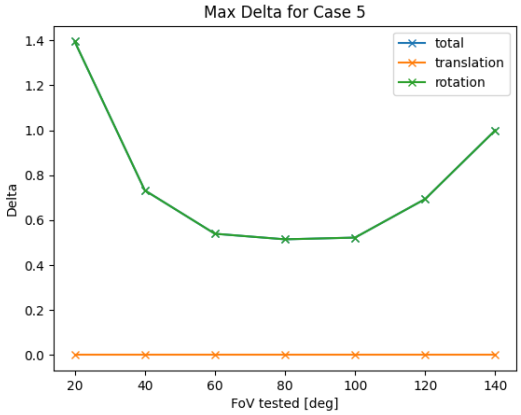

(b) Figure showing the max value of Δ for each FoV for Case 5

Figure A.8: Figure showing the viewing angle for the optimal positions and the max Δ for each FoV for Case 5

The results for this case, in terms of the optimal viewing angles, are the same as those for the previous cases. However, the values and behaviour of Δ is significantly different from any previous case. The analysis suggests that the greatest amount of feedback is received from the lowest FoV, and that the feedback gained plateaus and then rises again. Mathematically, this can be explained with the idea that the rotational component of $\dot{u_p}$ and $\dot{v_p}$ have a non-linear relationship with κ. This combines with the non-linearities which results from the multiplication of a variable κ and variable position coordinates to create a highly non-linear relationship.
In practical terms it can be explained when one considers the projection effects that arise due to a variable κ. For small FoVs, the observer feels as if they've "zoomed in" on the view, which means that the movements they observe are exaggerated. This can account for the high value of Δ for the lower FoVs. However, this does not account for why the values increase again after 100 [°].

Finally, the results for Case 6 are outlined in Table A.10 and visualised in Figure A.9a and Figure A.9b

Table A.10: Table showing the optimal position, the horizontal and vertical viewing angle of this position and the value of Δ for each FoV for Case 6

FoV [deg]	Optimal Position (x,y,z) [m]	Horizontal Viewing angle [deg]	Vertical Viewing Angle [deg]	Δ
20	(1.0, 0.1,-0.049)	11.42	5.607	1.59
40	(1.0, 0.3,-0.045)	33.40	5.607	1.02
60	(1.0, 0.5, -0.15)	53.13	16.94	0.846
80	(1.0, 0.8, -0.25)	77.32	27.96	0.855
100	(1.0, 1.1, -0.25)	95.45	27.96	0.853
120	(1.0, 1.7,-0.25)	119.1	27.96	1.05
140	(1.0, 2.7, -0.25)	139.3	27.96	1.35

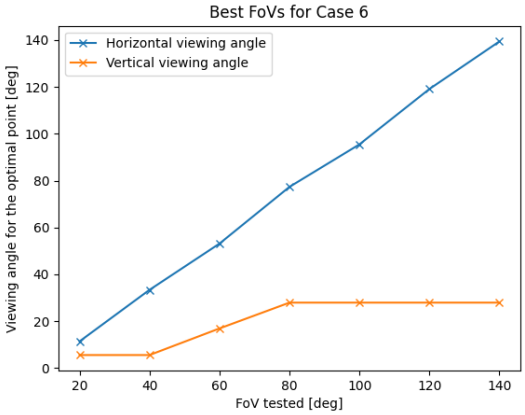

(a) Figure showing the viewing angles of the optimal positions for every FoV for Case 6

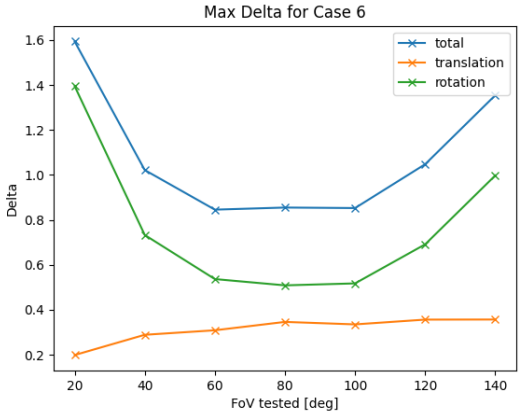

(b) Figure showing the max value of Δ for each FoV for Case 6

Figure A.9: Figure showing the viewing angle for the optimal positions and the max Δ for each FoV for Case 6

As one would expect, the results for Case 6 follow the same pattern as those for Case 3. The final values of Δ are simply the sum of the rotational and translational components of Δ which can be seen in Case 4 and Case 5. As mentioned previously, the rotational components have a stronger influence on the final value than the translational components.

A.3. Sensitivity Analysis

To test if the velocities and pitch angles used to do the analysis have any impact on the optimal viewing angles or the Δ values, a sensitivity analysis was done. This involved:

- **For Case 1 and 4**: The velocity, u^b was varied from 1 [m/s] to 6 [m/s]
- **For Case 3 and 5**: The pitch angle, θ was varied from -6 [°] to -1 [°]
- **For Case 3 and 6**: Each combination of the previously mentioned velocities and pitch angles were used.

For each of these sensitivity cases, the best horizontal viewing angle, the best vertical viewing angle and the maximum value of Δ for all positions was calculated. The best horizontal viewing angles for each cases are shown in Figure A.10:

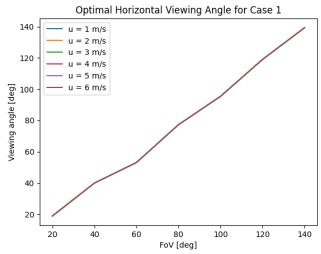

(a) Figure showing the optimal horizontal viewing angle for Case 1

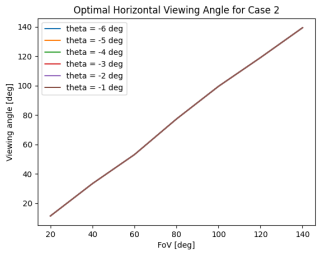

(b) Figure showing the optimal horizontal viewing angle for Case 2

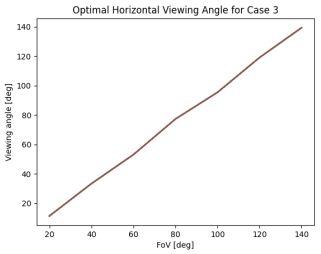

(c) Figure showing the optimal horizontal viewing angle for Case 3

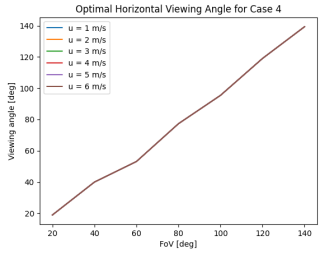

(d) Figure showing the optimal horizontal viewing angle for Case 4

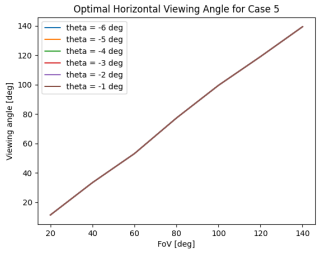

(e) Figure showing the optimal horizontal viewing angle for Case 5

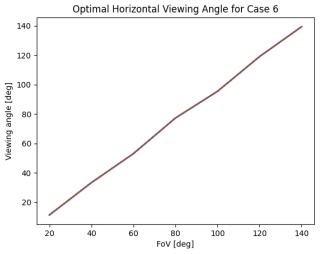

(f) Figure showing the optimal horizontal viewing angle for Case 6

Figure A.10: Figure showing the optimal horizontal viewing angle for all six Cases

As can be seen in Figure A.10, the optimal horizontal viewing angles for all combinations tend to stay on the edge of a pilot's FoV. This seems to suggest that the most amount of feedback for such low speeds and small pitching motions will be gotten from the peripheries of one's vision.
A similar trend can be seen for the optimal vertical viewing angles shown in:

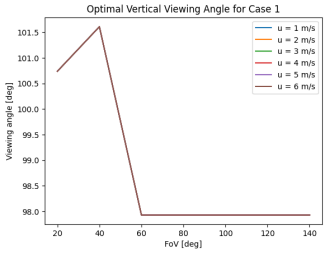

(a) Figure showing the optimal vertical viewing angle for Case 1

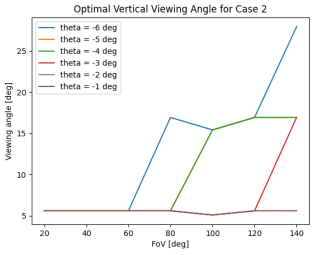

(b) Figure showing the optimal vertical viewing angle for Case 2

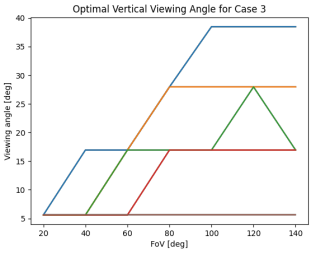

(c) Figure showing the optimal vertical viewing angle for Case 3

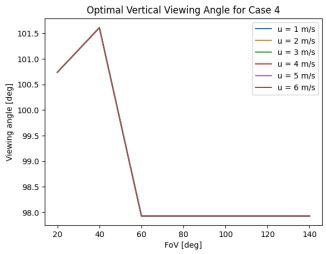

(d) Figure showing the optimal vertical viewing angle for Case 4

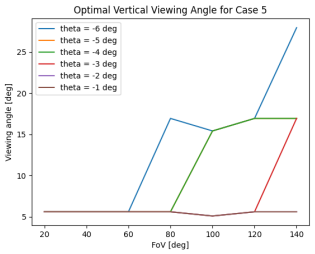

(e) Figure showing the optimal vertical viewing angle for Case 5

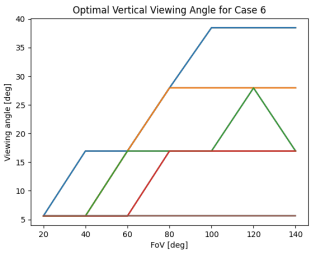

(f) Figure showing the optimal vertical viewing angle for Case 6

Figure A.11: Figure showing the optimal vertical viewing angle for all six Cases

As can be seen from Figure A.11a and Figure A.11d, the optimal vertical angle is the same for all translations within this range. However, this not the case for purely rotational motion. For Case 2 and Case 5, there are some variations in what the most optimal vertical viewing angle is and this can be down to the fact that the Δ values for some adjacent positions were very similar. That means that the

code would have chosen an adjacent position to the one for a previous sensitivity case. For Case 3 and Case 6, the conditions for which the values of the optimal viewing angle were different that the rest are shown in the legends of Figure A.11c and Figure A.11f. A similar explanation can be used to explain this deviance even though the difference in angles is very different. This can be confirmed if one looks at the trend of the maximum value of Δ for all cases as shown in Figure A.12

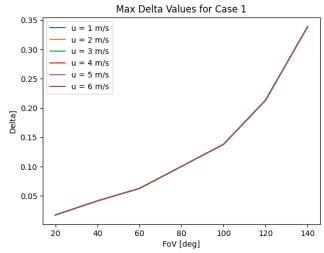

(a) Figure showing the maximum value of Δ for Case 1

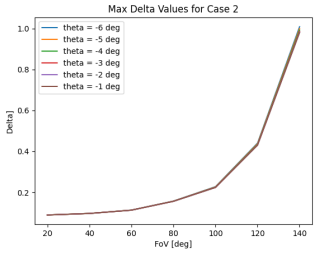

(b) Figure showing the maximum value of Δ for Case 2

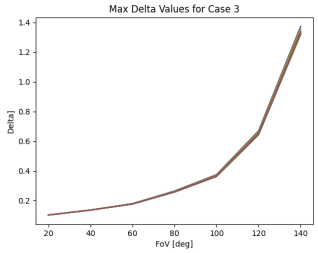

(c) Figure showing the maximum value of Δ for Case 3

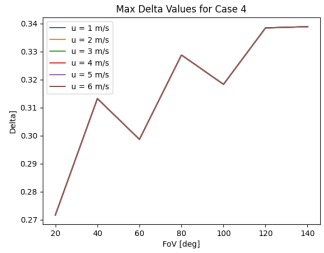

(d) Figure showing the maximum value of Δ for Case 4

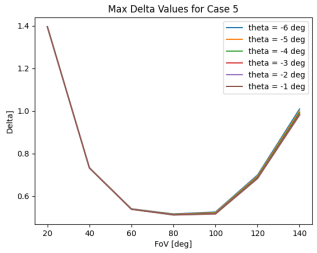

(e) Figure showing the maximum value of Δ for Case 5

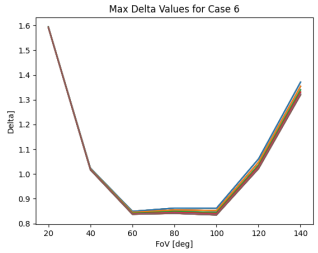

(f) Figure showing the maximum value of Δ for Case 6

Figure A.12: Figure showing the maximum value of Δ for all six Cases

As one would expect, the differences in maximum Δ for the cases with only translation or only rotation are negligible. However, even though there are visible differences for Case 3 and Case 6, the absolute values of the differences never exceed 0.1. If one was to consider this in percentage terms, then the difference in the on-screen velocity seen by the pilot for different conditions is less than 10 [%]. Additionally, the optimal vertical viewing angles are never high enough for any given FoV such that they can be clipped out , which means that the optimal point will always be in the pilot's view. This combined with the low change in Δ means that the pilot would not be missing out on any information

A.4. Discussion

The goal of this analysis was to try and find an FoV-invariant point, that provides the greatest amount of velocity feedback to the pilot. While the analysis did not successfully deliver the required point, there is still some use that can be derived from it. Firstly, the analysis shows that for a two DOF system, the greatest amount of feedback is being gathered from the peripheries of a pilot. This means that, in theory, should the FoV be lowered, the pilot would lose out on a lot of velocity feedback and their performance would worsen. Additionally, using the metric of the ratio on on-screen velocity to the actual velocity, Δ reveals that the change in feedback for each FoV is largely invariant of the motion. This means that if one analyses the percentage decrease in Δ for each FoV, then the loss in velocity feedback can potentially be quantified.
The percentage decrease, PD for each FoV can be calculated using Equation A.10:

$$PD = \frac{\Delta_{140} - \Delta_{FoV}}{\Delta 140} * 100 \tag{A.10}$$

The results for each case are shown in Table A.11:

Table A.11: Table showing the Percentage decrease for all six Cases

	Percentage decrease [%]					
FoV [deg]	Case 1	Case 2	Case 3	Case 4	Case 5	Case 6
20	94.86	91.05	92.45	19.85	-39.51	-17.68
40	87.76	90.29	90.01	7.58	26.72	24.57
60	81.48	88.66	86.88	11.87	46.03	37.57
80	70.37	84.28	80.72	2.98	48.52	36.88
100	59.26	77.34	72.69	6.08	47.75	37.05
120	37.04	56.24	51.24	0.12	30.59	22.65
140	0.00	0.00	0.00	0.00	0.00	0.00

As can be seen in Table A.11, for the cases with a fixed κ, there is a large reduction in information between the smallest and largest FoV. For Case 3, which can be considered the most realistic case, there is already a 51 [%] decrease in feedback from 140 [°] to 120 [°] . This is already the largest decrease from one FoV to another but the decrease does taper off. This may mean that the pilot may not perceive much difference as they transition from FoVs of 120 [°] to a lower one, but theoretically their performance should degrade. For the Cases with the variable κ, the percentage decreases are of a lower magnitude all across the board. Additionally, between the smallest and the largest FoVs, for Case 5 and Case 6, there is a percentage increase in the value of Δ. The percentage difference increases slightly when going from 140 [°] to 80 [°], but it then starts decreasing afterwards.

While the analysis does provide meaningful results, it is important to consider what assumptions were made to come to the conclusions. The first assumption is the idea that one can quantify the amount of feedback being received by the pilot using the velocity seen on-screen. It is assumed that, for a simple one or two degree-of-freedom motion, the more velocity the pilot sees on screen, the better their perception of speed will be which would allow them to better control the helicopter. While literature has indeed stated that, as FoV decreases and the pilot sees less, their performance degrades, it is a big assumption to make that this performance degradation will occur because the pilot is seeing lower velocity components on their screen. It may well be the case that the pilot's performance is independent of how fast the on-screen velocity is and it simply depends on the presence of on-screen velocity. This of course, is a hypothesis that can be tested during the experimentation phase.
Another major assumption made while doing the analysis was that the optimal position for each case and each FoV, remains on screen for the entirety of the motion. In a real world case, as the helicopter moves forward, all points close to the helicopter would get clipped out of view. This is mitigated slightly in the analysis by the fact that the velocity and pitch of the helicopter are kept small. This is exactly why emphasis is put on the viewing angle of the optimal points instead of their exact coordinates. For a simple visual scene that consists only of a ground and a sky, as the helicopter moves through the scene, all points on one specific viewing angle will behave the exact same way regardless of their exact coordinate. If that scene were to have distinct scenery such as trees or other objects however, then the exact coordinate of those objects plays a part in how much feedback the pilot is getting in the sense that they are now getting both position and velocity feedback. If one considers only an experiment where velocity feedback is provided, then this analysis provides good results on what can be expected.

B

Flow Visualisation

The full sized images for the flow at specific times for the example motion in Chapter 3 are shown below:

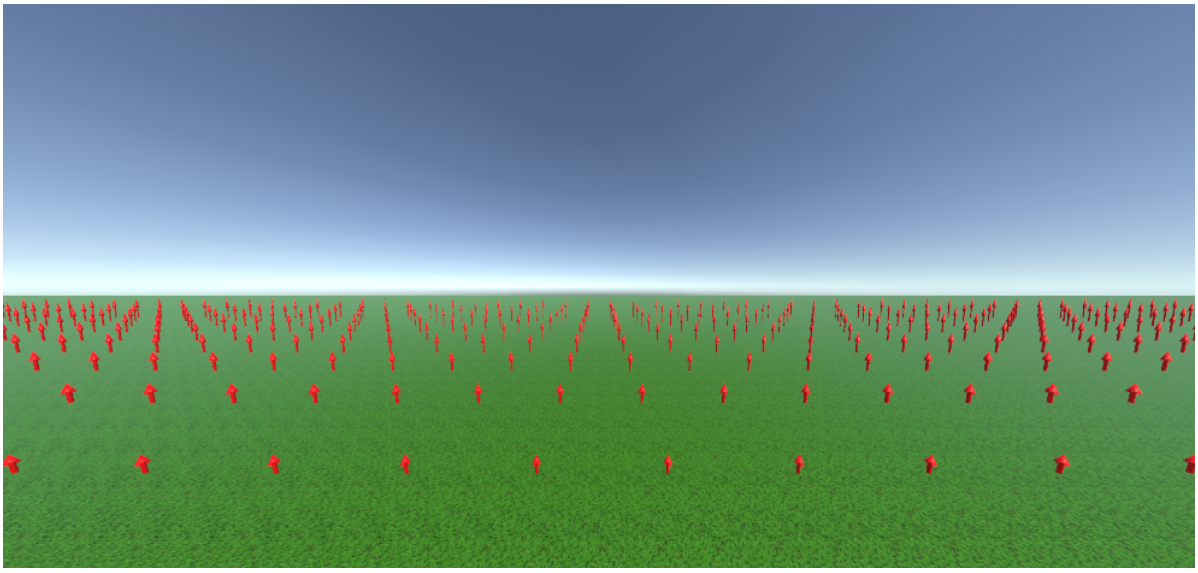

Figure B.1: Figure showing the flow at t = 0.5 [s], u = 0.2 [m/s], θ = -5 [$^\circ$] and $\dot{\theta}$ = -1.25 [$^\circ$/s]

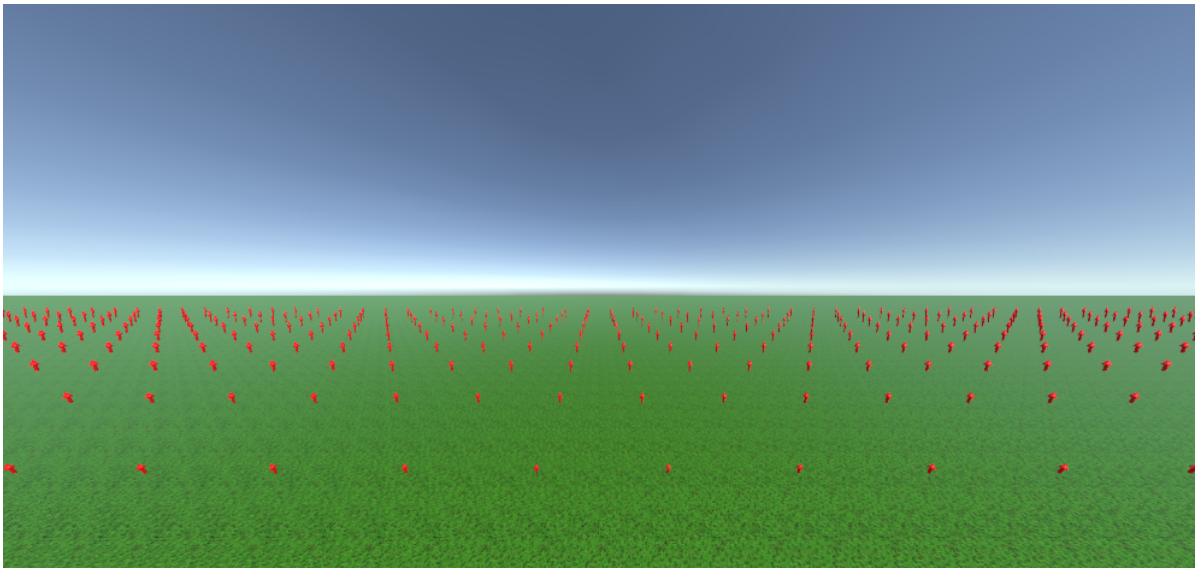

Figure B.2: Figure showing the flow at t = 1.0 [s], u = 0.69 [m/s], θ = -2.8 [$^\circ$] and $\dot{\theta}$ = 1.43 [$^\circ$/s]

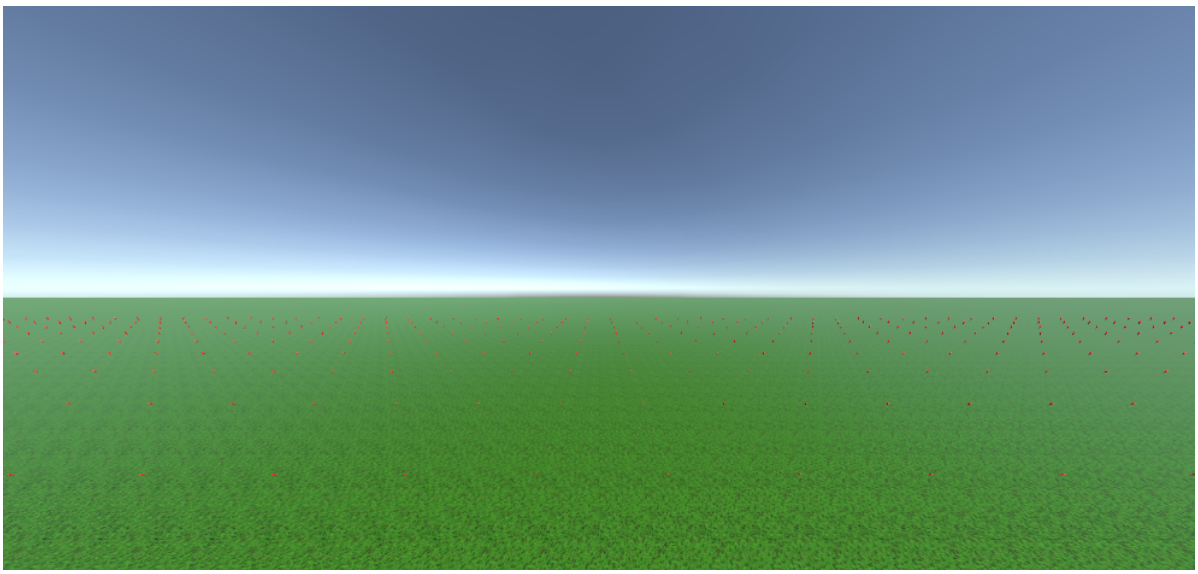

Figure B.3: Figure showing the flow at t = 1.5 [s], u = 0.77 [m/s], θ = -1.1 [$^\circ$] and $\dot{\theta}$ = -0.78 [$^\circ$/s]

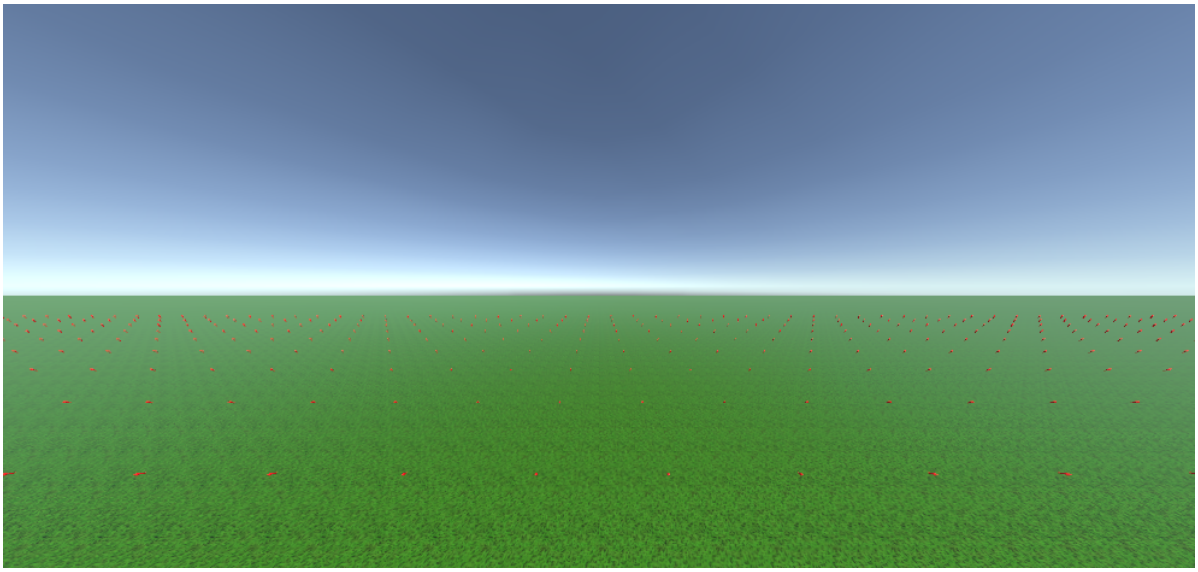

Figure B.4: Figure showing the flow at t = 2.5 [s], u = 1.49 [m/s], θ = -1.1 [°] and $\dot{\theta}$ = 1.25 [°/s]

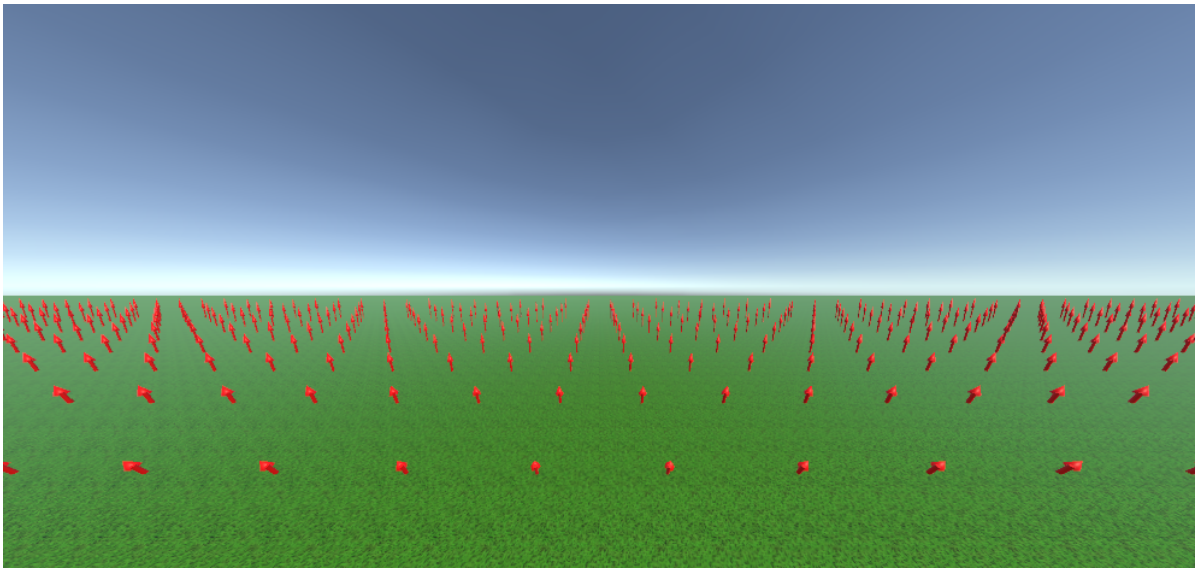

Figure B.5: Figure showing the flow at t = 3.5 [s], u = 2.03 [m/s], θ = -5 [°] and $\dot{\theta}$ = 0.77 [°/s]

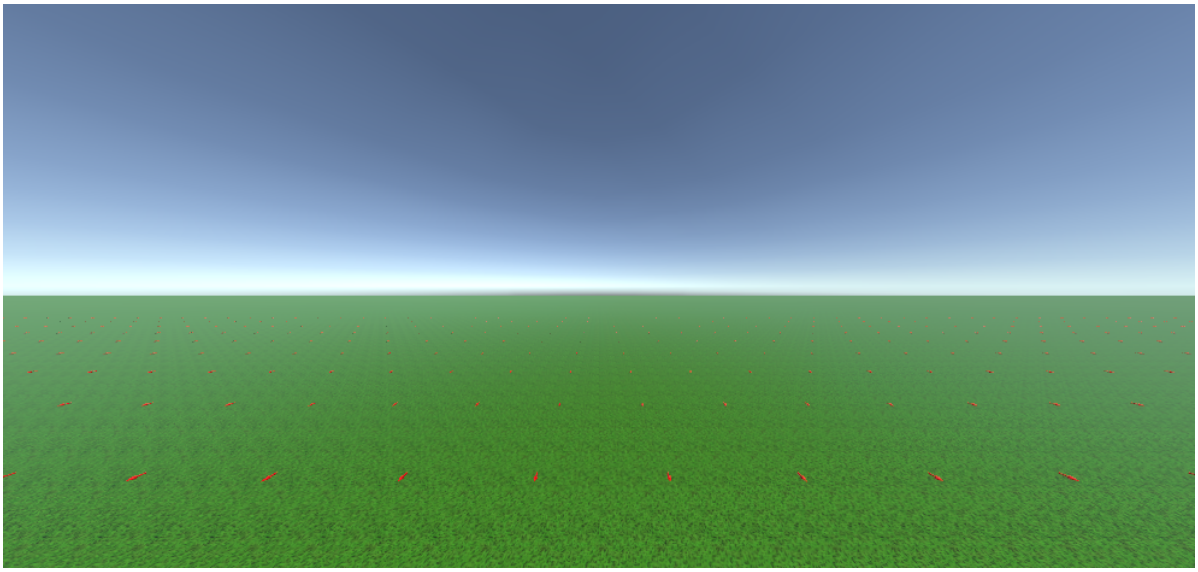

Figure B.6: Figure showing the flow at t = 4 [s], u = 2.21 [m/s], θ = 0 [°] and $\dot{\theta}$ = 0.34 [°/s]

The full sized images for the flow seen by the actual participant during their run are shown below:

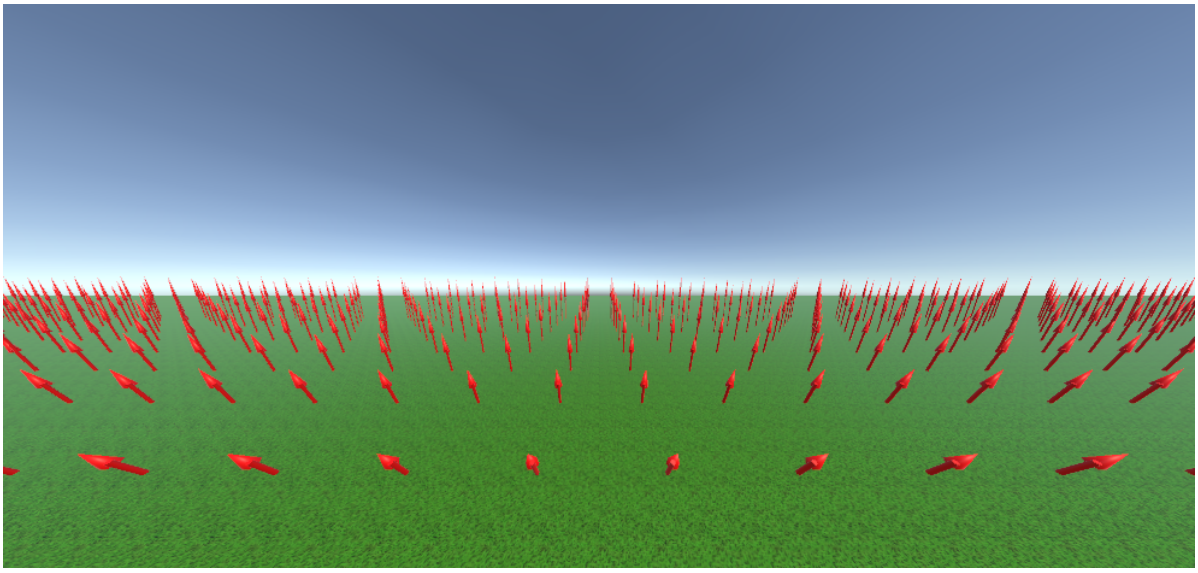

Figure B.7: Figure showing the flow for the participant's run at t = 35 [s], u = 2.64 [m/s], θ = -11 [°] and $\dot{\theta}$ = 9.1 [°/s]

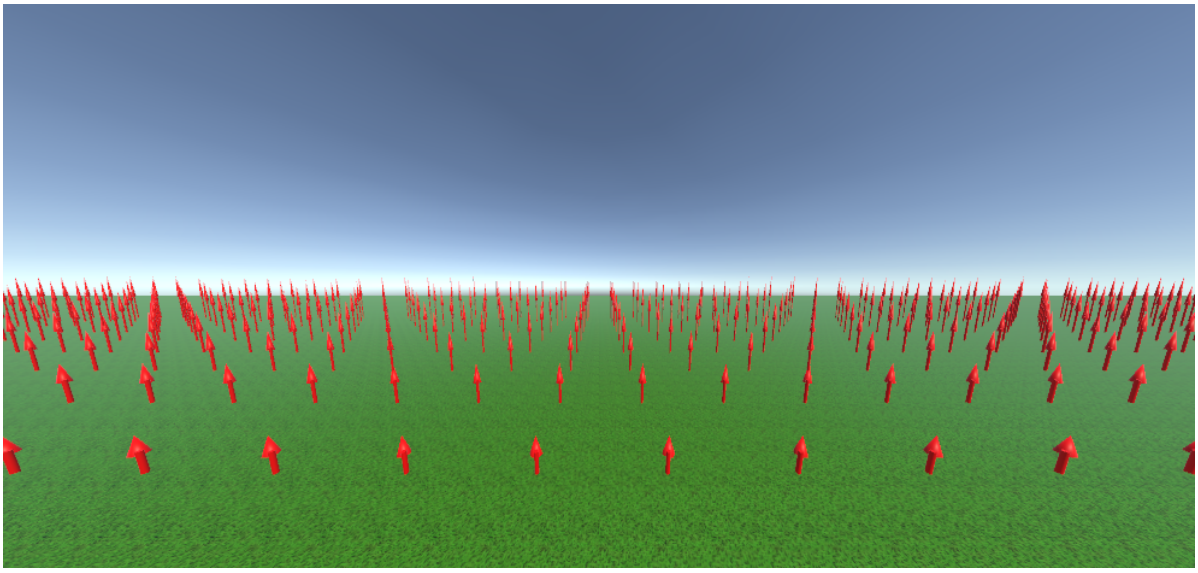

Figure B.8: Figure showing the flow for the participant's run at t = 35 [s], u = 0.0 [m/s], θ = -11 [°] and $\dot{\theta}$ = 9.1 [°/s]

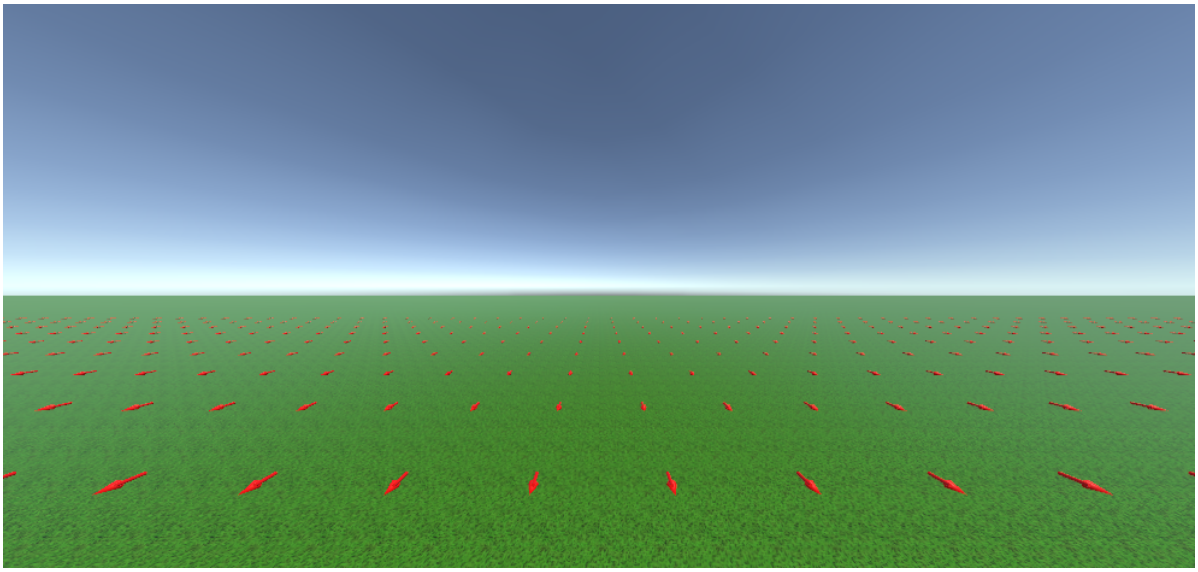

Figure B.9: Figure showing the flow for the participant's run at t = 35 [s], u = 2.64 [m/s], θ = 0 [°] and $\dot{\theta}$ = 0 [°/s]

C

Experiment Procedure

C.1. General Procedure

Each participant's experiment took around 1.5 hours, which includes the time taken for explaining the experiment and the training run. When the participant first enters the room, they are asked to take a seat so the experiment details can be explained to them. They are told that they will putting on a VR headset and using a joystick to control a simulation of a helicopter in near-ground hover. Then the two types of tasks that they will do, namely the Velocity Disturbance and Pitch Disturbance Rejection Tasks, are explained to them. Then, they are asked to sign the Informed Consent Form. During this time, the researcher can change the ID field in the Unity simulation to the ID that is designated for the participant. This allows the researchers to identify which dataset belongs to which participant. After this, the participant is asked to put the VR headset on and adjust it such that it sits comfortably on their head. They are free to change the settings of the headset such that they can see the scenery, shown in Figure 4.5a, clearly. They are then shown the MISC scale to make sure that they can read the scale properly. If not, the scale is moved closer or further away from them until they feel comfortable. This distance between the observer and the scale is then recorded in Unity, such that the scale always shows up in that exact same position. They then get to use the joystick to move the helicopter around such that they get used to the motion. This also serves to check whether or not the participants feel any adverse effects of motion sickness already.
The experiment begins with one or more training runs of the Velocity Disturbance Rejection Task with an FoV of 140 [$^\circ$]. Before the run is started, the participants are told that, during the run, the researcher will ask them the following three questions:

- Which part of the screen are their eyes mostly focused on?
- Do they feel like they are doing better for this experimental condition compared to the previous one (if applicable)?
- Do they feel more comfortable with this view compared to the previous one (if applicable)?

These questions are usually asked around the 40-50 second mark. This ensures that they have made it past the lead-in phase of the run and are fully focused and comfortable with the control strategy they are employing for the task. After the run is over, they are asked to use the MISC scale to give a rating corresponding to their condition. The name of the CSV file that contains the output of the run is then entered into the Python code (either **errorAnalysisSpeed.py** or **errorAnalysisTheta.py**), such that their RMSE can be checked. In general, if the RMSE is below 2.5 - 3.0 [$(m/s)^2$], the participants are ready to continue with the actual experimental runs. If the RMSE is higher than 3.0 [$(m/s)^2$], more training runs should be conducted.
The simulation is set up such that the entire simulation can be controlled by using certain keybinds. These are detailed in Table C.1:

Table C.1: Table showing the commands and the associated keybinds for the simulation

Command	Keybind
Start training forcing function	T
Start Velocity or Pitch forcing function	Space
Show pitch reticle and horizon line (If this is activated then pressing Space will start the Pitch Forcing Function)	P
Reset	R
Show MISC Scale	H
Change FoV to 20 degrees	Z
Change FoV to 30 degrees	X
Change FoV to 60 degrees	C
Change FoV to 90 degrees	V
Change FoV to 120 degrees	B
Change FoV to 140 degrees	N

Note that pressing **P** switches the simulation to Pitch Mode, which means that forward/backward movement is disabled and pressing **Space** will start the Pitch Forcing Function (i.e. Figure 4.4b) instead of the Velocity Forcing Function (i.e. Figure 4.4a).

The procedure for the experimental runs is as follows:

1. Use the Key Commands, shown in Table C.1, to set up the correct FoV for the run
2. Confirm with the participants if the view is correct
3. Begin the run
4. At around the 40-50 second mark, ask them the aforementioned questions and record their responses
5. When the run ends, ask them for their MISC rating and record this
6. Use the Python script to check their RMSE and the time traces of their control activity, to ensure that the data was recorded properly.
7. Repeat the previous steps for the second run for this experimental condition

Every four runs, the participant should be asked to take the headset off, such that they get a little break and their eyes can reset. At any point, if the participant wants to stop, the simulation should be immediately terminated and they should take the headset off. Depending on how severe the participants' symptoms are, the experiment should be terminated entirely or it should continue. This is explained in the next section.

C.2. Terminating Experiment Due To Motion Sickness

If at any point the participant indicates a MISC score of 6 or higher (i.e. Nausea or Vomiting), the experiment must be terminated. **UNDER NO CIRCUMSTANCE MUST THE PARTICIPANT BE ALLOWED TO CONTINUE THE EXPERIMENT!** The participant should take the headset off and sit down until they stop feeling nauseous. This can be helped by giving them fizzy drinks which induce burping and help settle the stomach. Until the participant feels good enough to stand up and walk around, they must not be allowed to leave the room. It is generally advised to wait up to an hour before the participant is allowed to drive or cycle.

D

Experiment Matrix

Since there are eight conditions to test, the minimum number of participants needed is also eight. This ensures that the results have no order effects since each participant will test the different conditions in different orders. This is why an experiment matrix is used to determine in which order a participant does the experiment. This is shown in Table D.1

Table D.1: Table showing the Experiment Matrix used to determine the order in which the participants do the experiments

	Experiment Condition							
Participant number	1	2	3	4	5	6	7	8
1	V20	V30	V60	V90	V120	V140	P20	P140
2	V30	V60	V90	V120	V140	P20	P140	V20
3	V60	V90	V120	V140	P20	P140	V20	V30
4	V90	V120	V140	P20	P140	V20	V30	V60
5	V120	V140	P20	P140	V20	V30	V60	V90
6	V140	P20	P140	V20	V30	V60	V90	V120
7	P20	P140	V20	V30	V60	V90	V120	V140
8	P140	V20	V30	V60	V90	V120	V140	P20

In Table D.1, the condition **V20** refers to a Velocity Disturbance Rejection task with an FoV of 20 [$^\circ$], **V30** refers to a Velocity Disturbance Rejection task with an FoV of 30 [$^\circ$] and so on. **P20** refers to a Pitch Disturbance Rejection Task with an FoV of 20 [$^\circ$] and so on. The table is created such that each condition appears only once per column and once per row. This ensures that nobody in the group of participants does the experiments in the same order as another. If there are more than eight participants, then the ninth participant does the order in the first column, the second does the order in the second column and so on.

E

Human Research Ethics Committee Documents

To be able to do the experiments, the potential participants had to sign an Informed Consent Form. This is shown below.

Opening Statement
You are being invited to participate in a Masters research study titled “Testing Pilot Behaviour for Helicopter flight using VR headsets”. This study is being done by Sheharyar Ali from the TU Delft The purpose of this research study is to see how a pilot’s performance changes when they are using VR headsets for visual cueing. The goal is to change the Field Of View (FoV) of the headset and test what happens to the performance of the pilot. The experiment will take you approximately *120* minutes to complete. The data will be used for a Master’s thesis researching how control behaviour is affected by such a task. We will be asking you to use a joystick to control a simulation of a helicopter and your task will be to keep the helicopter stationary in the face of a disturbance. You will do this while wearing a VR headset which will be used to show you the simulation. Please note: wearing a VR headset can cause motion sickness so please only participate if you have no previous history of motion sickness. As with any online activity the risk of a breach is always possible. To the best of our ability your answers in this study will remain confidential. We will minimize any risks by anonymising all data collected. Data such as your name and email addresses will not be published in any way and the published data will only consists of performance parameters of the participant. This data will be published with no reference to who the participant was. Your participation in this study is entirely voluntary and you can withdraw at any time. You are free to omit any questions. Should you wish to withdraw your consent to publish the data from your experiment, we will happily remove all of the requested data from storage and your results will not be published. If you have any questions or complaints, feel free to email me at

PLEASE TICK THE APPROPRIATE BOXES	Yes	No
A: GENERAL AGREEMENT – RESEARCH GOALS, PARTICPANT TASKS AND VOLUNTARY PARTICIPATION		
1. I have read and understood the study information dated _____ ,or it has been read to me. I have been able to ask questions about the study and my questions have been answered to my satisfaction.	☐	☐
2. I consent voluntarily to be a participant in this study and understand that I can refuse to answer questions and I can withdraw from the study at any time, without having to give a reason.	☐	☐
3. I understand that taking part in the study involves: • Using a VR headset and a joystick to control the simulation of a helicopter	☐	☐

PLEASE TICK THE APPROPRIATE BOXES	Yes	No
• Collecting data on how well a participant does by collecting data on control input and errors • A small discussion about how the experiment went after the experiment has finished		
4. I understand that the study will end around the end of September 2024	☐	☐
B: POTENTIAL RISKS OF PARTICIPATING (INCLUDING DATA PROTECTION)		
5. I understand that taking part in the study involves the use of VR headsets which may cause motion sickness or dizziness. I understand that these will be mitigated by: • **Doing the experiment in a well-ventilated room** • **Stopping the experiment at any point if any sign of discomfort is shown by the participant or if the participant wants to stop** • **Taking frequent breaks to let the participant rest**	☐	☐
• 6. I understand that taking part in the study also involves collecting specific personally identifiable information (PII) and associated personally identifiable research data (PIRD) with the potential risk of my identity being revealed. The PII and PIRD collected is limited to the participant's name, email address, age and gender	☐	☐
• 8. I understand that the following steps will be taken to minimise the threat of a data breach, and protect my identity in the event of such a breach	☐	☐
• Data is only accessible by the researcher, Sheharyar Ali and their supervisor, Olaf Stroosma • The data is stored in encrypted storage locations like the TU Delft Surf Drive and TU Delft One drive • The non-anonymised data will be deleted upon the completion of this study • All data can be removed at the request of the participant	☐	☐
9. I understand that personal information collected about me that can identify me, such as my name and email address, will not be shared beyond the study team.	☐	☐
10. I understand that the (identifiable) personal data I provide will be destroyed once the thesis is published at the end of September, or when I request for it to be deleted	☐	☐
C: RESEARCH PUBLICATION, DISSEMINATION AND APPLICATION		
11. I understand that after the research study the de-identified information I provide will be used for : • **Analysing the trends in pilot control behaviour for different testing conditions** • **Publishing the general trend shown by the participants in how their control behaviour changed** • **Publishing the general findings of the study in a final thesis report**	☐	☐

Signatures

_____	_____	_____
Name of participant [printed]	Signature	Date

I, as researcher, have accurately read out the information sheet to the potential participant and, to the best of my ability, ensured that the participant understands to what they are freely consenting.

Sheharyar Ali

_____	_____	_____
Researcher name [printed]	Signature	Date

Study contact details for further information:

Back to text